Austrian Journal of Technical and Natural Sciences

№ 11–12 2016
November–December

«East West» Association for Advanced Studies and Higher Education GmbH

Vienna
2016

Austrian Journal of Technical and Natural Sciences

Scientific journal

№ 11–12 2016 (November–December)

ISSN 2310-5607

Editorial office European Science Review
"East West" Association for Advanced Studies
and Higher Education GmbH, Am Gestade 1
1010 Vienna, Austria

Email: info@ew-a.org

Homepage: www.ew-a.org

Austrian Journal of Technical and Natural Sciences is an international, German/English/Russian language, peer-reviewed journal. It is published bimonthly with circulation of 1000 copies.

The decisive criterion for accepting a manuscript for publication is scientific quality. All research articles published in this journal have undergone a rigorous peer review. Based on initial screening by the editors, each paper is anonymized and reviewed by at least two anonymous referees. Recommending the articles for publishing, the reviewers confirm that in their opinion the submitted article contains important or new scientific results.

East West Association GmbH is not responsible for the stylistic content of the article. The responsibility for the stylistic content lies on an author of an article.

Instructions for authors

Full instructions for manuscript preparation and submission can be found through the "East West" Association GmbH home page at: http://www.ew-a.org.

Material disclaimer

The opinions expressed in the conference proceedings do not necessarily reflect those of the «East West» Association for Advanced Studies and Higher Education GmbH, the editor, the editorial board, or the organization to which the authors are affiliated.

East West Association GmbH is not responsible for the stylistic content of the article. The responsibility for the stylistic content lies on an author of an article.

Included to the open access repositories:

Typeset in Berling by Ziegler Buchdruckerei, Linz, Austria.
Printed by «East West» Association for Advanced Studies and Higher Education GmbH, Vienna, Austria on acid-free paper.

Section 1. Biology

DOI: http://dx.doi.org/10.20534/AJT-16-11.12-3-5

Kidirbayeva Arzygul Yuldashevna,
Karakalpak State University,
Senior scientific researcher

Mambetullaeva Svetlana Mirzamuratovna,
Karakalpak State University,
Professor at the Department of Ecology and soil science,
Nukus, Republic of Uzbekistan
E-mail: arzigull@gmail.com

Ethological aspects of the wolf (*canis lupus linneus,* 1758) in the aral sea region

Abstract: The article considers the questions of the ethology of a wolf (*Canis Lupus Linneus,* 1758) in the Aral Sea region. It has been established that the territorial movements of the wolf population at a model site play an important role in the stability of survival and population size as a behavioral reaction to the changing environment conditions.

Keywords: Aral Sea region, wolf population, ethology, movements.

The study of the animal behavior attracts attention for many reasons. The information about the behavior of animals is required to understand their ecology (peculiarities of lifestyle), which, in turn, corresponds to the development of the problem of nature protection and rational use of nature.

The behavior is one of the most important ways of active adjustment of the animals to the diversity of the environmental conditions. It ensures the survival and successful reproduction of both a separate animal unit and the species in the whole. Ethology was formed as an independent discipline in the 30ies of XX century based on zoology and theory of evolution.

Ethology (from Greek *ethos* — customs, character) is the science about *the behavior of an animal unit in the environment natural for the given species.* It was formed in the 30ies of XX century by an Austrian researcher Konrad Lorenz (1903–1989) and a Dutch biologist Nikolaas Tinbergen (1907–1988), who worked in the Great Britain his whole life. Ethology was developing in close contact with physiology, population genetics, behavioral genetics etc. [4, P. 320]. Many works of famous scientists are dedicated to animal ethology [17, P. 487; 15, P. 43; 2, P. 68; 11, P. 72; 18, P. 20–26; 9, P. 520]. Each of them presents an original narrative about the basics of the science about animal behavior. The behavior of carnivores was also covered in the works of known scientists such as P. A. Manteifel, A. N. Formozov, L. V. Krushinskiy, E. Seton, K. Lorenz, I. Tinbergen, B. Grzimek and some other authors.

Currently, vast material has been accumulated, which characterizes the behavior as the combination of different forms of adaptive activity. The behavior of animals is endlessly diverse in its forms, manifestations and mechanisms. The works of Palvaniyazov (1974) and Reimov (1978) are dedicated to the study of the ethology of a wolf in the conditions of the Aral Sea region. In this work, we made an attempt to present modern data on the study of behavioral aspects of the wolf population with regard to the changing conditions of the Aral Sea region. We studied some individual and social peculiarities of behavior of this carnivore.

Wolf (*Canis Lupus Linneus,* 1758) is a typical dweller of sand desert, plains, mountains and riparian woodlands in the Central Asia. It is most common of all carnivores in the southern part of the Aral Sea region and plays an important role in the biocoenosis of deserts (Kyzyl-Kum, Ustyurt) and riparian woodlands of this region.

Wolf is noted for a big ecological flexibility and highly developed psychic. It helps wolves successfully resist

the variety of ways of combating them. For a long time, the behavior of animals, wolves in particular, was determined from the point of view of their instincts and conditional reflexes. The presence of such form of collective survival and interaction as a pack is an important characteristics of the kind. The pack is, in fact, a family consisting of two parents and young wolves up to two-three years old [16, P. 72].

Results obtained in the course of research show that the studied population of wolves consists of animal units united in the pack, which use certain territories of native sites and single animals, not belonging to their pack, and can be noted for significant mobility.

The size of the habitual site of the wolf population in the Aral Sea region is defined by a certain landscape and varies according to different districts. The size of the territory and density of one pack depend on the food provisions, presence of shelters, degree of chasing the carnivores and location of water sources. There is a strict hierarchy in the pack. The base of the hierarchy consists of alpha-male, alpha-female, a few low rank wolves of both sex, among which, one can distinguish a beta-male, and cubs, who are beyond the hierarchy.

In the course of our researches, it was established that at the territory of the model site (f/e Aspantai-Shakaman), the packs of wolves live as family groups, the base of which consists of a couple of experienced wolves with the offspring of the current year (new arrivals), the offspring of the previous year of birth (second year) as well as one grown-up male (5–6 years old) and one old male (12–13 years old).

According to our observations, the wolves belonging to one pack-family often hunt in the common site alone or in groups of 2–4 animals. Based on our example, the researched pack-family inhabiting the model site consists of 8 animal units. Apart from wolves living in packs at certain territories, there are wandering wolves, "homeless". and non-territorial ones. These, as rule, are animal units who outgrew the age of the second year (there can be both second-year animals, new arrivals as well as old animals), who were ousted by experienced wolves and couldn't find a free site for themselves.

Based on our observations, seasonal changes in the family and territorial relations were revealed in the studied pack of wolves. One of such changes is a brooding period. The brooding period starts from the birth of wolf cubs (April) and continues throughout summer. The brooding period is followed by pack period. The pack period starts from autumn (mid-September) and continues until the first half of winter (February). During this period, the second-year wolves join the experienced wolves and new arrivals. The pack, whole or in parts, wanders throughout the family-pack site and leaves its borders only at the territory free of wolves.

The estrum among wolves is observed in the first half of January and lasts for about two weeks. The duration of pregnancy of she-wolves is 62–75 days. The mass whelping takes place from March to April. The number of cubs varies from 2 to 7 [5, P. 41–43]. During the period of estrum, the disintegration of the pack occurs. During this period (end of January, beginning of February), the new arrivals separate from the pack and live separately at same pack site. The estrum pack is formed of an experienced she-wolf in estrum and following her males — experience wolf and, usually, second-year animals, sometimes a candidate from foreign wolves. The composition of an estrum pack can be more complicated. According to our observations (f/e Aspantai-Shakaman), the estrum pack of wolves consisted of 15 animal units. After the end of estrum, the wolves, except for a couple of masters and new arrivals, left the pack site.

During the research at the model site, we tracked all daily and seasonal movements of the research pack of wolves. In total, the distance of passing through the territory of the pack site of the given population was about 200 km. Based on the results of the research, it was established that the daily movement was 82–87km at average. At the same time, sometimes the animal units of the population can violate the border of their territory and pass the river of Amudarya through "the floating bridge towards" Qongirot district. There were also cases when entire packs (11 animal units) of the Qongirot population went to the territory of the Aspantai-Shakaman population in search of prey. The wolves instinctively "mark" the borders of their territory with urine, excrement and energetic "scraping". Thus, following the track of the wolf pack of the Aspantai-Shakaman population in May 2011, we found several scrapings at every 5–6km at the intersection of the roads. In addition, a wolf left one excrement at the distance of 2–3 meters in three places. The wolf moved using motorways. In six cases, it urinated near six bushes around the road. The scrapings were located either near or at short distance (2 meters) from the urinated spot (the sizes of the biggest scrapings were 190x50 centimeters). The wolf scraped the soil with the hind legs, very energetically, removing it at the back; the soil had very big scratches from the claws.

According to the American zoologists R. Peters (1977) and D. Mitch (1970), the wolves cover their territory with network of scent marks. They mark border sites more intensively (twice more often). The bigger the pack is, the more marks they leave.

Thus, the pack characteristic and territorial movements of the wolf population at the model site (f\e Aspantai-Shakaman) play an important role in the stability of maintaining the life activity and number of the population as behavioral reaction to the changing conditions of the environment of the given kind.

References:

1. Гудолл Дж. Шимпанзе в природе: поведение. – М.: Мир, – 1992. – С. 41–43.
2. Дьюсбери Д. Поведение животных: Сравнительные аспекты. – ML: Мир, – 1981.
3. Зворыкин Н. А. Волк и борьба с ним – М.: КОИЗ, – 1936. – С. 120.
4. Зорина З. А., Полетаева И. И. Элементарное мышление животных: Учебное пособие. – М.: Аспект Пресс, – 2002. – 320 с.
5. Кидирбаева А. Ю., Мамбетуллаева С. М. Журн «Известия Дагестанского государственного педагогического университета. Серия Естественные и точные науки». – Дагестан. – 2009. – № 2 (7). – С. 41–43.
6. Корытин С. А. «Повадки диких зверей», – Москва, Агропромиздат, – 1978.
7. Крушинский Л. В. Биологические основы рассудочной деятельности. – М.: Изд-во МГУ, – 1986.
8. Кудактин А. Н. Территориальное размещение и структура популяции волка в Кавказском заповеднике /А. Н. Кудактин//Бюллетень Московского общества испытателей природы. Отделение биологии. – 19796. – Т. 84. – вып. 2. – С. 56–65.
9. Мак-фарленд Поведение животных: психобиология, этология и эволюция: пер. С англ. – М.: мир, – 1988. – 520 с.
10. Меннинг О. Поведение животных: Вводный курс. – М.: Мир, – 1982.
11. Павлов М. П. Волк. – М.: Агропромиздат, – 1990. – 350 с.
12. Палваниязов М. Хищные звери пустынь Средней Азии. – Нукус, Каракалпакстан. – 1974. – 320 с.
13. Реймов Р. Р. К вопросу изучения сложных форм поведения млекопитающих в природе/Р. Р. Реймов //Вопросы зоопсихологии, этологии и сравнительной психологии: сборник статей; под ред. К. Э. Фабри. – М.: Изд-во МГУ, – 1978.
14. Хайнд Р. Поведение животных. – М.: Мир, – 1975.
15. Шквыря М. Г. Конфликт человек-хищник на территории Украины. – К.: Принт Квик, – 2012. – 72 с.
16. Шовен Р. Поведение животных/Р. Шовен. – М.: КД «Либроком», – 2009. – 487 с.
17. Эрман Д., Парсонс П. Генетика поведения и эволюция. – М.: Мир, – 1984.
18. Mech D. The wolf: The ecology and behavior of endangered species. N. Y.: The Natur. Hist. Press Garden City, – 1970 a. – 834 p.
19. Peterson R. Wolf ecology and prey relationship on Isle Royale. US Nat. Park Serv. Sci. Monogr. Ser., – 1977, – No 71, – P. 210.

DOI: http://dx.doi.org/10.20534/AJT-16-11.12-5-8

Khurramov Alisher Shukurovich,
Associate Professor, Department of Zoology chair
E-mail: Khurramov10@mail.ru

Nazaralieva Makhfuza Pardayevna,
Termez State University, a student of the Faculty of Natural Sciences

Bobokeldiyeva Lobar Abdusamatovna,
Termez State University teacher of biology chair

Phytohelmintological research in grain in southern regions of Uzbekistan

Abstract: The article analyzes faunal complex nematodes wheat collected in 16 districts and 48 farms in Surkhandarya and Kashkadarya regions of Uzbekistan. During the study period on wheat agrocenoses 158 species of phytonematodes belonging to 3 subclasses, 8 orders and 25 families were found.

Keywords: fauna, phytonematodes, wheat, eudominants, dominants, subdominant, subrecedents.

In the Republic of Uzbekistan, wheat is one of the main agricultural crop. Analyzing the main phytohelminthological studies conducted around the globe shows that wheat fields differ quite a big variety of faunal assemblages of plant nematodes. Having analyzed literary sources should be noted that the nematode fauna of wheat and its rhizosphere soil contains more than 600 species. Analyzing the nature of nematodological studies on wheat fields it should be noted that the bulk of the work is devoted to the study of parasitic nematode species. Integrated studies covering the full range of nematode species on wheat, conducted mainly in the CIS countries and Eastern Europe. Studies in other parts of the world, where mainly studied parasitic species, which have a practical orientation [1, 225–234].

Despite the large number of works on wheat nematodes abroad, until present time comprehensive studies have not been conducted in the territory of Uzbekistan. In Uzbekistan the first time we carried out a comprehensive study in this area.

Wheat cultivation in large areas of the Republic and not a study faunal assemblage of plant nematodes were the basis for phytohelminthological research on this culture.

Material and Methods of research

Faunistic research was conducted by a conventional route method [2, 3–11]. The material phytohelminthological research were samples of wheat plants and rhizosphere soil collected in 16 districts and 48 farms in Surkhandarya and Kashkadarya regions. In each region in order to collect the material were chosen three farms. Field studies were carried out in the period from 2012 to 2015.

In the route faunal studies all 864 soil and 3438 plant samples were collected. To isolate nematodes from soil and plant organs we used a modified Infundibular method of Berman. Soil samples for the presence of cyst form nematodes we usually analyzed according to the method of Dekker [3, 221–237].

For fixing the nematode 6.4% formalin, and glycerol formulations were prepared according to the procedure of Seinchorst [4, 57–69].

In determining the species of plant nematodes accessories were used works of domestic and foreign authors, as well as phytonematodes atlas, compiled by the Institute of Parasitology, Republican Academy of Sciences, as well as we used morphometric parameters obtained by the standard formula de Mann according to Micoletzky modification [5, 16–38].

The degree of dominance of nematodes in plant and soil samples was determined by the percentage of specimens of individual species among all detected. At the same time the dominant species or eudominants are up more than 10% of the number of detected, dominants — 5,1–10%, subdominants — 2,1 5%, less than 2.1% subrecedent individuals [2, 3–11].

Results of the research

In the study period, on wheat and its rhizosphere soil we found 158 species of plant-parasitic nematodes belonging to 3 subclasses, 8 orders and 25 families.

In our material Adenophorea subclass represented by 3 orders: Enoplida, Mononchida, Dorylaimida. Enoplida order contains only one family with two rarely occurring species: *Trishistoma monohystera, Tobrilus kirjanova*. In the order of Mononchida there are two families contained one type of each. Dorylaimida order represented 6 families: Dorylaimidae, Qudsianematidae, Discolaimidae, Aporcelaimidae, Xiphinematidae, Leptonchidae, among which the most diverse in species composition is Qudsianematidae (4 species), Aporcelaimidae (4), Dorylaimidae (4). The rest of the families contain 1–2 species.

Chromadoria subclass presented 2 orders: Monhysterida, Plectida. Monhysterida order represented by one family Monhysteridae, and the other order family Plectidae. Monhysteridae family includes freshwater species: *Monhystera simplex, Geomonhystera villosa*. The family Plectidae is represented by four rarely occurring species.

Rhabditia subclass includes Rhabditida, Aphelenchida, Tylenchida orders. Rhabditida order includes 3 families: Cephalobidae, Panagrolaimidae, Rhabditidae. Among the above families of the greatest species diversity observed in the family Cephalobidae (28 species), the family Panagrolaimidae contains 14, Rhabditidae — 10 species.

Aphelenchida order represented by 4 families: Aphelenchidae, Paraphelenchidae, Aphelenchoididae, Seinuridae and 40 species, 33 of which belong to the family Aphelenchoididae, 5 — to Aphelenchidae, one by one — Paraphelenchidae and Seinuridae.

Tylenchida order includes 40 species belonging to 7 families: Tylenchidae (10 species), Dolichodoridae (4), Psilenchidae (2), Hoplolaimidae (3), Pratylenchidae (4), Neotylenchidae (5), Anguinae (12).

On a variety of species and number of individuals among the orders allocated Rhabditida, containing more than 32% of all detected species and 61% of individuals of phytonematodes. Aphelenchida and Tylenchida orders comprise 25.3% of the species, 22.6% and 14.3% of individuals nematodes. All other orders in the fauna of wheat presented rarely occurring and few species.

In the root soil of wheat dominated types (in descending order): *Panagrolaimus rigidus* (popular type), *P. subelongatus, Chiloplacus sclerovaginatus, Aphelenchoides parietinus, A.composticola, Rhabditis brevispina, Ditylenchus dipsaci, Acrobeloides nanus, A.buetshlii, Cepholobus persegnis, Pratylenchus pratensis, Bitylenchus dubius, Tylenchorhynchus brassicae,* (total 13 species). The roots of wheat dominant species are absent; to a frequently met species belong: *Aphelenchus avenae, A. parietinus, P. rigidus, D. dipsaci, Chiloplacus propinquus, Rh. brevispina, A. composticola, A. nanus, Ch. sclerovaginatus, P. subelongatus* (total 10 species).

The species composition of plant nematodes, and soil rhizosphere of wheat is significantly different from each other both in terms of species composition and on the number of individuals. In wheat rhizosphere soil it was recorded 15035 nematode species belonging to the 149 species. Of which often met *A. avenae, A. parietinus, Ch.propinquus, Ch. sclerovaginatus, P.rigidus, P. subelongatus.*

The main faunal complex nematodes rhizosphere soils constitute *P. rigidus, A. avenae, Ch. propinquus, Ch. sclerovaginatus, A.parietinus, P.subelongatus, Rh. brevispina, D. dipsaci, A. nanus, A. buetschlii, A. labiatus, C. persegnis, P. pratensis, B. dubius, T. brassicae, Eudorylaimus centrocercus, A. composticola, Helicotylenchus dihystera* etc. (all 30 species). The first 4 species belong to the mass species, among which the largest biomass form *P. rigidus* individuals that make up a third of the species found in the soil.

For the root of soil fauna is abundant species of the families Panagrolaimimidae, Cephalobidae and Aphelenchidae, in particular species *P. rigidus, Ch. propinquus*. Relatively often met *A. avenae, Ch. sclerovaginatus, P. subelongatus and A. parietinus*. By frequently encountered species belong to the types of families Rhabditidae *(Rh. Brevispina)*, Anguinidae *(D. dipsaci)*, Cephalobidae *(A. nanus, A. buetschlii, C. persegnis)*, Dolichodoridae *(T. brassicae, B. dubius)*, Pratylenchidae *(P. pratensis)*, Aphelenchoididae *(A. composticola)*. Less frequent met types *Tylenchorhynchus tener* (Dolichodoridae family), *A. labitus* (Cephalobidae family), *Panagrolaimus fuchsi* (Panagrolaimidae family), *Helicotylenchus dihystera*, (Hoplolaimidae family), *E. centrocercus* (Qudsianematidae family), *Eucephalobus oxyuroides, E. mucronatus* (Cephalobidae family), *Filenchus filiformis, Lelenchus discrepans* (Tylenchidae family), *Helicotylenchus pseudorobustus* (Hoplolaimidae family), *Pratylenchus neglectus, P. penetrans, Pratylenchoides crenicauda* (Pratylenchidae family), *Ditylenchus triformis* (Anguinidae family). From the above mentioned phytonematodes the first group of 6 species belong to the mass species and is the main background fauna nematodes rhizosphere soil of wheat. Among them, the highest frequency of occurrence of stands *P. rigidus*. The second group of phytonematodes of 9 species are dominants, the third group of phytonematodes 14 species — to subdominants, to recedents are 30 species; in particular, *Mesodorylaimus bastiani, Eudorylaimus paraobtusicaudatus, Monhystera simplex, Acrobeloides emarqinatus, Chiloplacus lentus, Panagrolaimus longicaudatus, P. multidentatus, Xylorhabditis operosa, Pelodera strongiloides, Aphelenchus cylindricaudatus, Tylenchus davainei, Psilenchus hilarulus* and others.

The root system of wheat was found 7103 species nematodes, relating to 113 species. The root system of massive species are also absent. Often found *A. avenae, A. parietinus, B. dubius, P. pratensis, A. composticola, Helicotylenchus dihystera, Ditylenchus triformis, Acrobeloides buetschlii, A. nanus, Ch. propinquus, Ch. sclerovaginatus, P. subelongatus, Rh. brevispina, Panagrolaimus multidentatus, P. mycophilus, C. persegnis, Filenchus valkanovi* and others. The species composition is dominated Aphelenchoididae family (28 species), Cephalobidae (22 species) and Panagrolaimidae (13 species).

In the wheat stalks have been identified 27 species in the amount of 1157 individuals. Mass types in the stems of wheat are also absent. Constantly we met in stems *P. rigidus, A. avenae*. The faunal complex of the stem can include other 10 species: *P. subelongatus, A. parietinus, Panagrolaimus mycophilus, P. multidentatus, Ch. propinquus, Ch. sclerovaginatus, C. persegnis, Eucephalobus oxyroides, D. dipsaci, A.composticola*. All other species are rare and not included to faunal complex.

On the leaves of 21 species were discovered 1491 individual nematodes. Here as well as in roots and stems, abundant species are absent. To constantly meet species on the leaves are *A. avenae, P. rigidus, P. multidentatus.* To the faunal complex nematodes leaves you can include other 10 species: *C. persegnis, E. oxyroides, Ch. propinquus, Ch.sclerovaginatus, P.anagrolaimus mycophilus, P. subelongatus, A. parietinus, A. composticola, Filenchus valkanovi, D. dipsaci.* The remaining 8 species are rare and are not included in the complex.

Thus, as a result of studies on the wheat we registered 13 species of phytonematodes belonging to the orders Dorylaimida and Tylenchida, families Xiphinemidae (1), Dolicholoridae (4), Hoplolaimidae (3), Pratylenchidae (4), Anguinidae (1). Nematodes of this group registered in the plant tissues. Phytoparasites are species of Xiphinema, Tylenchorhynchus, Bitylenchus, Merlinius, Helicotylenchus, Pratylenchus, Pratylenchoides, Ditylenchus genera. From the plant-parasitic nematodes in wheat and its rhizosphere were revealed the following

species: *Xiphinema. index, Tylenchorhynchus brassicae, T. tener, Bitylenchus dubius, Merlinius bogdanovi-katjkovi, Helicotylenchus dihystera, H. erythrinae, H. pseudorobustus, Pratylenchus pratensis, P. neglectus, P. penetrans, Pratylenchoides crenicauda, and Ditylenchus dipsaci.*

Discussion of research results

158 species are given in our material on fauna of wheat phytonematodes and its root soil. Discovered species belong to 3 classes, 8 orders of phytonematodes and 25 families. In the roots and rhizosphere soil of wheat the largest variety of different members of the family Aphelenchoididae (33 species), Cephalobidae (28 species). As the number of individuals in the root soil is dominated by 15 species, mass species is *P. rigidus*. In the roots of the dominant species are absent, dominated by 10 species. In the stems and leaves of phytonematodes relatively few in number.

According to the frequency of occurrence of these species can be distributed among the following groups: eudominants (6 species), dominants (9 species), subdominants (14 species), recedents (30 species) and subrecedents (99 species).

It should be noted that the above mentioned parasitic nematodes were few and serious threat to wheat is not. However, to identify the wheat fields of the complex is very pathogenic parasitic nematode species — *Pratylenchoides crenicauda, Helicotylenchus dihystera, Tylenchorhynchus brassicae, Ditylenchus dipsaci* and with a sufficiently high density of their populations, it is of particular concern, as the widespread danger of disease.

References:

1. Kiryanova E. S., Kral E. L. Plant parasitic nematodes and their control measures. Monography. – Moscow, – 1969. – T. 1. – 447 p.
2. Paramonov A. A. About some principle matters of phytohelminthology. – Moscow, – 1958. – P. 3–11.
3. Decker H. Schädliche Nematodenarten des Getreides und der Gräser. – Berlin, – 1974. – P. 221–237.
4. Seinchorst J. W. A rapid method for the transfer of nematodes from fixative to anhydrous glycerin. Nematologica, – 1959. – V. 4. – P. 57–69.
5. Micoletzky G. Die freilebenden Erd-Nematoden, mit besonderer Berucksichti-gung der Steiermark un der Bukowina, Zugleich mit einer Revision Samtlicher nicht mariner, freilebender Nematoden in Farm von esenus – Beschreibungen und Bestimmungs – Schlusseln, Arch. Naturgesch, – V. – 87, – 1922.

Section 2. Information technology

DOI: http://dx.doi.org/10.20534/AJT-16-11.12-9-13

Bukharaev Nail Dr.,
Candidate of Physics-Mathematical Sciences
Associate professor in the Department
of programming technologies.
Kazan Federal University. Russia
E-mail: boukharay@gmail.com

Altaher Ammar Wisam,
PhD Student in the Department of programming technologies
Kazan Federal University. Russia
E-mail: Smart.computing@yahoo.com

Analysis memory allocation between virtual machine as venerability for hypervisor

Abstract: In this paper we will give a complete description hypervisor concept. In addition, we will allocate the major types of it, we also give a technical description of the main elements.

Earlier the cloud computing became popular relatively recently, due to the fact that they provide sufficiently large computing power. The client should not buy expensive equipment, you just "renting" it for a certain period, the customer required. Below, we present the basic terms that describe the essence of cloud computing.

The aim of our research is to review the weakness of memory allocation types for virtual machine and how it could lead to possible attacks on the hypervisor, and also answering the question why hyper-v is important to use? We will examine the most common types of hypervisors that can be installed on an ordinary personal computer. That corresponds to the characteristics of Microsoft Hyper-V, an example of the hypervisor.

Keywords: hypervisor; cloud computing; virtualization.

Introduction

Threats subject to a system of virtual environment management, in particular, the server and client software components that enable locally or remotely control the settings of the hypervisor and virtual machines. Sami virtual machines due to the fact that its membership include system and application software, and is also quite vulnerable with solutions that are integrated into the virtual platform and aim to ensure the safety of multiple virtual machines, some of their components can be protected. The great danger is that the owner of the information, for example, just does not know about the fact of virtualization and therefore do not take into account the risks, or knows about it, but has no information about the device that virtualization — this situation can also lead to errors in the risk assessment. All this must be considered when creating a comprehensive system of protection in the case of virtualization mechanisms.

1. Hypervisor

We must now consider the internal structure of cloud computing. As follows from the description above, the cloud is a set of hardware and software. The software installed on this software should be fast enough to provide resources computer system to individual customer's request. For this purpose it was developed virtualization technology.

Virtualization is usually applied to physical hardware resources by combining multiple physical resourc-

es into shared pools from which users receive virtual resources. With virtualization, one physical resource can be made several virtual.

Moreover, virtual resources can have functions or features that are absent in the original physical resources.

The main element of cloud computing is the hypervisor. Hypervisor — a specialized operating system that is responsible for the allocation of resources. The scheme can be represented by the hypervisor Unlike conventional operating system follows.

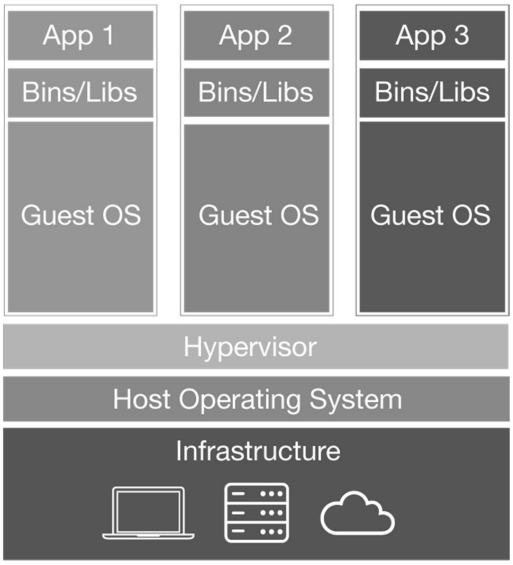

Figure 1. Organization of the virtual machine

1.1 Overview of hypervisors

There are two types of hypervisors:

- Type 1 hypervisors.
- Type 2 hypervisors.

Type 1 hypervisors run directly on the system hardware. Type 2 hypervisors run on top of the base operating system, which provides virtualization services, such as support for I/O and memory management.

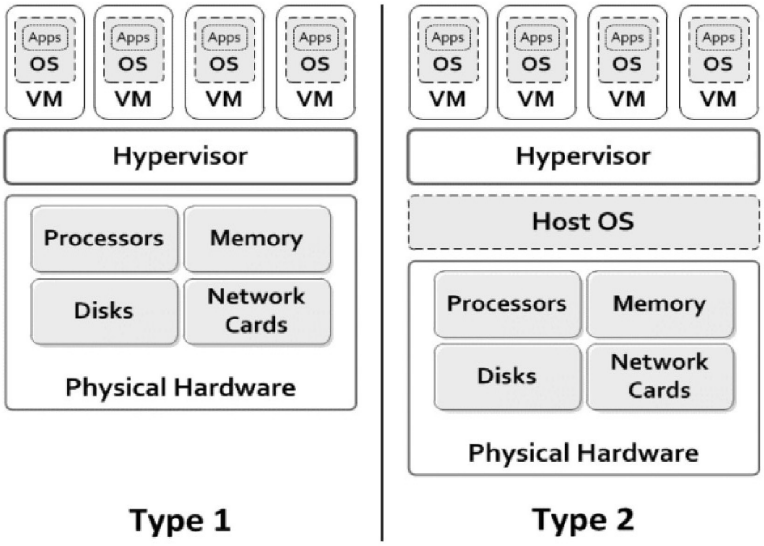

Figure 2. Types of hypervisors

1.2 Client hypervisors

Microsoft Hyper-V — referred to as hypervisors first type, that is, running a hypervisor on the "bare metal".

Hypervisors first type of technologically more complex, but also more effective in the sense that they provide a minimum overhead and maximum isolation of virtual machines. Because they have won recognition in a server environment.

Microsoft hypervisor requires a parent or root OS (also sometimes say "section"), in which he actually built. This OS, respectively, is in a special situation, in particular, even though it partly virtualized, but still has access to the graphics accelerator and other components.

1.3 Memory Management

The main objective of the virtual machine is to allocate resources for the user depending on his needs.

Particular attention here should be paid to the memory allocation. This is one of the key points in the organization's security during the use of virtual computing.

Typically, only one physical server can be used to create multiple virtual machines. There are several approaches to allocate memory.

• Sharing memory between processes "pages sharing";

• Dynamic memory allocation at runtime;

• data compression.

The problem statement

The problem statement examining memory allocation and other resources with Investigation of how this weakness lead to attacks on the hypervisor.

Memory allocation From our point of view, As the tasks using the Same Physical a memory across the virtual machines, could be a risk for security of Our the data. For how of CAN we use the Same index in Different machines in the Same way the if we Constantly reallocate the a memory Between Processes, we will of the BE Able to the read the data from another virtual machine.

For example "Memory page creation" Typically, the process of memory allocation in a virtual machine. For example, the area is allocated in the memory "pages", which manages and hypervisor. If the amount of memory is not enough for all the processes that allowed the same page multiple processes. In this case, it is determined whether there are processes running on the same data. In this case, two different memory pages are combined into one. The process also creates two pointers to the same memory. If one process modifies the data on one page, the second pointer is overwritten.

1.3.1 Separation memory

The most common is another method of memory allocation, namely the allocation of a separate address space for each process.This method is similar to the allocation of memory for each application. Thus, each user is allocated a separate physical disk space. This memory itself is abstracted from the physical media. Thus, the memory can be used in various processes.

Disadvantage this memory allocation can greatly overload the processor. It turns out that we must keep in mind not only the virtual and physical address data, but also, and more links to this memory for a virtual machine

1.3.2 Allocation

However, this method of memory allocation can not be efficient from the point of view that the hypervisor can not effectively manage such a memory allocation. For example, one virtual machine there is an overabundance of memory (memory is not used) to another machine, there is its deficit. With this memory management, in fact, it is impossible to keep track of the current memory status of each machine. In order to make the process more efficient memory allocation method called "balooning" was created or otherwise "inflation" memory. To use this method, you a must the install a memory-remapping driver on the virtual machine. With this a case, the special driver monitors the state of a memory in the virtual machines. If one's of the machines a memory Shortage Occurs, the virtual machine signals this special driver. After that the driver keeps track of memory usage in other virtual machines, and then unlocks the memory is not used in other virtual machines.

1.3.3 Chaotic exchange memory

There is another way to allocate a memory. This method assumes if one's of the virtual machines of might the BE an acute Shortage of a memory, the then there is a Chaotic Exchange of a memory pages in the Physical of layer. There are Different Approaches to the selection of a memory pages the Exchange for, Including a Chaotic Exchange. This Approach CAN load the hypervisor large enough to SLOW down and Calculation Computation process, a memory and the optimization of result not the BE CAN Achieved.

1.3.4 Memory Compression

Sharing a memory Between the virtual machines process is quite Difficult and not safe. Therefore, a memory the compression method is USED more often the. Of The hypervisor Could the compress the data of one's page in the half, and the then the put the this page on your of hard drive and the save IT. HOWEVER, this situation the in, we Obtain the Physical address to the virtual machine's a memory. Hypervisors to have the save to your pages of hard drive partitions, as with not all of the pages of twice CAN the BE compressed.

2. Proposed Solutions

As we CAN see, the Exchange of the data between the virtual machines is the Same entity with the transmission of the data on the of Internet. THUS, the virtual networks have some Inherent security Issues with a Conventional network. and this attacks "the man on the gray one's" packet sniffing and could lead to the hypervisor attack.from the point of our view the solution could be using the Hyper-V with the smart page for Packing and assigning addresses because In Microsoft Hyper-V R2 Service Pack 1, the Dynamic Memory feature uses a memory-ballooning process that is similar to VMware vSphere's. Built into Hyper-V's Integration Components is a guest kernel enlightenment that allows a VM to communicate with the host to recognize which

memory pages are (and are not) in use. As such, the host can add and remove guest memory as required. As we will define it below.

2.1 "Smart Pages"in Hyper-V

Of The Hyper-the V the hypervisor is Provided the following method of a memory allocation. Of The Fact That in the standard situation, the when a the virtual machine STARTS up closeup, the maximum size bed of a memory Allocated. a sufficiently large amount of a memory is not USED, the virtual machine can restart with a smaller memory size.

Approach has Been This added to the Windows Server 2012. This method adapts the virtual machine for a memory of a case each use. This method Ensures That there will of the BE enough a memory required for the correct operation of the machine. Of course the, this method is not convenient Because that it is necessary to restart the virtual machine, which can cause the system to crash.

Memory in the hyper-V consists of the following components:

The Startup the RAM — a parameter specifies the required a memory for the virtual machine the start. During working installation, the parameter Should to take Into account That the a memory Should BE enough to the start the virtual machine, and the amount of a memory Should BE minimized to enough a memory for OTHER virtual machines.

The RAM the Minimum -. Determines the minimum amount of the BE a memory That a must Allocated to the virtual machine a the after the virtual machine STARTS of The of value may BE the set just 32 MB from the maximum value.

The Maximum the RAM – Specifies the maximum amount of a memory That CAN the BE USED by the virtual machine. It CAN to take from a minimum of value up closeup to 1 the TB It Should BE Borne in yet Mind That the if the guest the operating system CAN only work with 32 GB of memory, and this option is set to 64 GB, the virtual machine will use a total of 32 GB.

The Memory buffer — a parameter determines how of much a memory you need to the allocate an Additional guest the operating system. Depending on the PERCENTAGE of the original a memory. With In the Hyper-the V, there are performance counters Database the calculate the Actual Primary a memory USED in applications. Then statement Performed a memory calculation you want to add.

The following formula is used to compute this parameter:

– the amount of memory to be added = how much memory you really need/(size of the buffer memory/100);

Memory weight — a method by which the Hyper-V may determine how to allocate the required memory between virtual machines.

– in the Hyper-the V the Windows Server 2012 will of the BE available through to two Mechanisms: the Generic the Routing Encapsulation and the IP Rewrite. Let Briefly examine each of Them.

2.1.1 Generic Routing Encapsulation

This approach forms GRE tunnels between the Hyper-V hosts in order to capture virtualized networks using details described in the NVGRE Draft RFC document. NVGRE can be applied across current physical network without demanding changes to physical network Switch architecture. If our firewall is blocking the GRE tunnels in the middle of the sites, we should configure firewalls to support the forwarding GRE tunnel traffic. In short, Server virtualization is very good technology that has started to gain momentum. Server virtualization is the covering of resources of server, including identity and number of separate physical servers, operating systems, processor from users of server. The virtual environments are also known as virtual private servers, guests, containers, instances and emulations. Yes, we will move forward with the implementation of virtual infrastructure because there are a lot of advantages of Hyper-V Network Virtualization over Traditional VLANs that are:

- Limited Scalability;
- Configuration complexity and cost;
- Constrained to single subnet;
- Cross-subnet live migration of Virtual machines;
- VM Portability and IP Address across premises and subnets;
- Multi-tenancy with overlapping IP address ranges.

2.1.2 IP Rewrite

Second Mechanism for Their Ideology is Somewhat simpler. Each the CA-address is Assigned a unique constraint the PA-address. For When the package leaves the virtual machine the host the Hyper-the V replaces the IP-the header packet the CA-the PA-address on the address and Sends the packet to the network a. of the Receiving the host PERFORMS to inverse the change in addresses is, and Delivers the packet. of As the algorithm Described, on each Physical the host with the Hyper-the V role a must BE configured as with the PA-in addresses is as with the CA-in addresses is USED in all the running on a Given host virtual machines using the network virtualization.

Conclusion

With In this paper, we Looked AT the internal, structure of the hypervisor. Organization of Interaction Between the parent partition, and the virtual machines. one important question found here is - a memory allocation for a the virtual machine. This "leakage" of a memory from one's the virtual machine to another leads to the "theft" of confidential data.

The second weakness of virtualization is possible vulnerabilities in data transmission between devices and processes between the virtual machines and the parent partition. This exchange of information should be hidden from prying processes hosted on the same machine. To do this, use a VPN connection between the outside of the Processes the virtual machine. HOWEVER, using the known Vulnerabilities in this transfer, we CAN the access the information circulates inside the virtual machine, and our recommendation was using the Hyper-V because of its mechanism for data transmission.

References:

1. In Virtualization the Windows 8: a built the Hyper-V – the access free: URL: http://www.ixbt.com/soft/windows-8-hyper-v.shtml
2. Of site of The Microsoft. The Description of the Hyper-V – the access free: URL: http://msdn.microsoft.com/en-us/library/cc768520(v=bts.10).aspx
3. Website Habrahabr. The Description of the Hyper-V – the access free: the URL: http://habrahabr. Of Ru / the post / 98580
4. Protocol the Description the GRE and NVGRE – the access free: URL: http://tools.ietf.org/html/draft-sridharan-virtualization-nvgre-00
5. The Microsoft Virtualization Solutions 'of The' Understanding (of Second Edition is is) / the Microsoft / 2010 g .
6. The virtualization hypervisors About. Website the IBM – the access free: URL: http://www.ibm.com/developerworks/ru/library/cl-hypervisorcompare/
7. Basil Malanin, manager Have by products for Center the Data, the Microsoft / Review, of the virtualization solutions from the Microsoft. – the TechNet
8. Morozov's from Dmitry, a specialist in solutions for the data center, the Microsoft /"the virtual and Physical Infrastructure management" – the TechNet
9. Virtualizing the vSphere, the Hyper – the V , the XenServer and Of Red Of Hat's's – free the access URL: http://www.vmgu.ru/articles/Virtualnie-mashini-doma-iv-biznese
10. The Filosofiya education: "The structures the network: Virtualization the and Adaptation the in modern society" Publisher,: Siberian Branch is of the Russian Academy of Sciences (Novosibirsk)
11. URL: https://www.business.att.com/content/whitepaper/WP_Virt_16501_v4_7-11-08.pdf
12. URL: https://www.ibm.com/developerworks/aix/library/au-virtualizationagile
13. URL: https://habrahabr.ru/post/98580
14. URL: https://msdn.microsoft.com/en-us/library/cc768520(v=bts.10).aspx
15. URL: https://technet.microsoft.com/en-us/library/hh750394.aspx
16. URL: https://tools.ietf.org/html/draft-sridharan-virtualization-nvgre-00

DOI: http://dx.doi.org/10.20534/AJT-16-11.12-14-15

Sterkhov Alexey Alexeevich,
Methodist, Chairman of the Scientific and Methodological Council,
gymnasium in the name of St. Nicholas the Wonderworker, city Surgut.
E-mail: sterkhov1979@mail.ru

Osipov Anton Olegovich,
Chairman of the Board of school,
gymnasium in the name of St. Nicholas the Wonderworker, city Surgut.
E-mail: tohaosipow@yandex.ru

Android-App prediction lowering the air temperature in a Far North

Abstract: the article describes the technology of creation and implementation of software applications that allow you to predict with extreme precision, to calculate days of the cancellation of classes, according to climatic parameters in the Far North.

Keywords: Android-App, activated day, forecasting, software application.

A geographical location and environmental conditions of the Khanty-Mansiysk autonomous district serve as reason for the certified presence days declared for student high schools of district. But at comparison of weather forecast in the declared certified presence day with data of table, we marked the repeated disparities of the real weather forecast with the declared certified presence days. For the correction of the folded situation it was necessary to write the program that would produce a calculation and prognostication of the certified presence days, and to execute a simulation on the basis of these past winters and define correlation of temperature chart with data of department of education about the certified presence days. The scientific novelty of similar consists in that the worked out application is presently only in Russia, realizing problem data on the platform of Android. Reason of choice for realization of appendix exactly under the operating system Android in language of Java were following: a 1) audience — an appendix did not have to become non-permanent, it must remain useful and actual among schoolchildren, therefore a choice fell on mobile devices; 2) availability — according to research, conducted International Data Corporation, market of smartphones share on the operating system Android more than 80%, that does them more popular and more accessible; 3) mastering — Java — one of the most popular programming languages, but as investigation of -количество of reference sources: textbooks, there are more than enough videocourses for him.

In the process of scientific research from the point of view of methodology and methodology by us was taken for basis of conception of N. V. Ippolitova and N. S. Sterkhova [1], taking into account accenting of attention on meaningfulness of educational-research activity of student, that is underlined by V. P. Nesterova [2]. Researches of I. V. Paramonov served from the technical point of view of one of theoretical bases of work, system studying possibilities of development of appendixes on the platform of Android [3].

Basic task of authorial application — to get data of weather forecast, make the prognosis of the certified presence day and represent information in an user interface (GUI), and in case of the certified presence day, to notify an user PUSH — by notification in 6:00 or 11:00 accordingly. The necessity of server for an appendix is realized by us on PHP. The mechanism of receipt and processing of data is simple enough: PHP a server inquires data every hour by means of CRON and saves data in the database of MYSQL, from where destroys them and passes in an appendix by means of JSON. In an appendix they through parsings will be transformed in an associative array (collection of map is used), the algorithm of prognostication and calculations is after executed.

An algorithm consists of set of terms checking 2 variables — temperature of air and speed of wind. Also there is a calculation of probability of the certified presence day on the basis of dynamics of prognosis on a formula for a 1 changing: probability = 100 — (| a temperature is in 8: 00 | is |a temperature in 11: 00 |) *10 and probability = 100 — (| a temperature is in 11: 00 | is |a temperature in 13: 00 |) *10 for a 2 changing accordingly. Calculations are produced in a separate class and separate stream and hatch in a main class, where and there is a method of conclusion of information in GUI.

Testing allowed to check work of appendix with the different data got from a server. The first tests showed

that on the basis of table of the certified presence days forecasting the certified presence days is fully impossible. The not complete range of temperatures is indicated in a table. This problem was decided simply enough: a method was written in the class of Forecast, allowing to build a prognosis not only for temperatures indicated in a table but also for intermediate temperatures. Then for testing was connected by us system of logiring, by means of that collected data, reflecting program behavior on combination of temperatures in a range from — 24 With to — 37 With and winds from a 0 m/with a to 10 m/s. The analysis of data showed that the calculation of the certified presence day (range of classes, having a right not to visit educational establishment) took place correctly. The method of the visual testing was further used, by setting of appendix on different devices and control of correctness of reflection of elements of graphic interface.

For a receipt, processing of data and co-operating with client application exist different methods. Most optimal for this program is a method of http queries. The main task of server is a receipt of data from the different sources of weather forecast. As basic service of Open Weather Map, free of charge giving valuable prognosis, was chosen on 3 days. For the receipt of data the http query of api is created.openweathermap.org/data/2.5/weather, as a result of implementation of that a server gets an answer in the format of JSON. For more exact tuning, as service of weather was written another PHP Script, allowing by hand to set weather terms, thus, a simulation became possible. Principle of work consists in the regular receipt of meteorological data, maintenance of them in a database and dispatch at a query from client application in the format of JSON.

Thus, on the basis of the conducted work it is possible to do next conclusions: firstly, coming from data of simulation, it be possible to say, that an appendix correctly expects the prognosis of the certified presence day on the basis of meteorological data; secondly, research allowed to educe, that on announcement by Department of the certified presence day not always correctly reflects the dynamics of temperature condition. Consequently, an appendix allows to lean fully against data and to eliminate errors that can be assumed at drafting of prognosis of the certified presence day.

But most essential, to our opinion, there are the further prospects of this development, constrained with the use of her in industries of the Russian economy of strategic value, namely in mastering of petroleum and gas deposits of the Far North. The question is, including, and about mastering of arctic shelf. Maintenance of health of working there people becomes in the conditions of frozen condition of ground of one of priority tasks, including servicemen of the Arctic troops. In an order to prevent probability of frost-bite, workers of oil and gas industry and soldiery must be in good time notified about a possible drop in a temperature, and to accept corresponding measures on maintenance of the organisms from the striking factors related to the drop in temperature. Mobility, compactness and efficiency of the system worked out by us, allows to decide the task of exact and trouble-free prognostication of drop in a temperature and, thus, provide effective activity of man in the conditions of the Far North.

References:

1. Ippolitova N. V., Sterkhova N. S. Methodology and methods of scientific research. – Shadrinsk: ShGPI, – 2011, – 208 p.
2. Nesterova V. P. Design and education-research activity of students in the classroom and in extracurricular activities//Herald of TOGIRRO. – 2015. – No. 2 (32). – P. 48.
3. Paramonov I. V. the Development of mobile applications for the android platform. – Yaroslavl: Yaroslavl State University them. P. G. Demidov, – 2013, – 88 p.

Section 3. Light industry

DOI: http://dx.doi.org/10.20534/AJT-16-11.12-16-18

Babenko Liana Grigoryevna,
Don State Technical University,
postgraduate student, the Faculty of technician and technology
E-mail: liana-babenko@mail.ru

Savelyeva Natalya Yuryevna,
Don State Technical University,
Candidate of Engineering Sciences, the Faculty of the technician and technology
E-mail: saveliefa@list.ru

Dmitrienko Nadegda Alekseevna,
Don State Technical University,
Candidate of Engineering Sciences, the Social and humanitarian faculty
E-mail: stilist4486@mail.ru

Developing the quality indicators and requirements imposed to materials when designing clothes for disabled people

Abstract: In this article a range of material property factors for designing adaptive clothes for people with limited physical abilities is carried out. The quality characteristics shown at different materials are also considered.

Keywords: disabled people, adaptive clothes, functional clothes, wheel-chair, materials, and rehabilitation periods.

The priority of tasks of future developing modern society is usually based on integration of different factors like physical health of disabled people in our society to ensuring the process of recovery a person with destroyed communication ties when the disabled people are provided with facilities ensuring their involvement in main spheres of social activity: work, life and leisure.

Integration is promoted by rehabilitation, i. e. based on implementation of various programs, types of servicing or therapeutic actions to quick recovery of restricted functions [1, 365].

Important conditions of rehabilitation are intended to provide people with limited physical abilities with multi -functional clothes meeting to their basic requirements to high degree of operational comfort and safety. The quality of life of disabled people in many respects depends on their wearing convenient clothes meeting a complex of specific requirements, one of which is matching to a rational packet of materials for designing.

The problem of matching materials for production of functional clothes for disabled people consists in creating and maintaining thermal, operational, ergonomic comfort of disabled people. Physiological features of ensuring comfortable conditions for a person who is in a wheelchair are determined by the need of creating some thermal comfort and its maintenance with the help of thermal control effect. At the same time it is possible to assume that the used materials shall be light, have low price, a high practicality and ease of wearing.

Now there is a huge variety of materials for top, a liner, and also pro-masonry materials with various properties: heat-shielding, thermos protective, with a huge variety protecting a body of the person from negative effects of surrounding and production environment, performing inverse function — environment protection having negative impact on the person.

For design and production of functional clothes additional group of special clothes representing one of the rehabilitation directions process with

special functionality of ergonomic, thermal, operational comfort, safety and esthetic features, it is necessary to add a set of complex requirements and indicators to a quality to materials used to production of special clothes with [2; 3; 4] specific requirements are included and, regulated [5; 6].

It is known that all properties of materials and fabrics for production of special clothes are considered and subdivided into a class of geometrical, mechanical, physical and operational properties. [2; 3; 4].

Some geometrical properties of materials weight, width, length, thickness are take into account. [2, 176].

The main mechanical properties of fabrics and materials for producing special clothes are based on indicators of density, tensile strength and tear, bend deformation (rigidity on a bend), tangential resistance (shift of threads, an falling off or with strewed factors), resistance to attrition, the shrinkage of fabric [2, 105–122].

Physical properties determining hygienic and protective characteristics of overalls are permeability of fabric (water resistance, air permeability, vapor permeability), hygroscopic, thermal and electric properties.

The class of material operational properties unites some features resistance (a property of a material to resist to action, to repeated actions and stretching), physical and chemical factors, etc.

For the first time the complex of indicators of quality determined to designing functional clothes is given in the paper being united in five main subsystems: functional, social, consumer, esthetic, ergonomic and operational indicators. In this work an effective objective is to develop the most complete block diagram of the quality characteristics are shown to materials as adaptive set for daily socks intended for people with disabilities (in the conditions of its operation in the range of expanded temperature condition).

For carrying out an expert evaluation a range of the factors concerning the properties of fabric influencing quality for adaptive set for men with a limited abilities: X1 — with tactile properties; X2 — air permeability; X3 — stability of color; X4 — shrinkage; X5 — mass of material; X6 — moisture-yielding; X7 — resistance to preserve warmth; X8 — heat-shielding properties of materials; X9 — an electric resistance; X10 — ease in leaving (a crease resistance and resistance to pollution); X11 — a heat- and mud-permeability; X12 — resistance attrition was offered.

Survey was conducted among the men with limited abilities moving by means of a wheelchair, the people who are looking after disabled people and health workers of specialized agencies. The number of experts constituted of 12 people for each group being interviewed. Aprioristic ranging was carried out according to a testing technique [3; 4].

Questionnaires for aprioristic ranging are processed by method of rank correlation, to the most significant indicator of the rank R=1 was appropriated, to the least significant was R=n, (where n — number of the analyzed indicators). Processing results of experts' questioning was carried out in accordance to the technique stated in [3; 4; 9]. Assessment of opinions coherence in each of groups of researchers are defined according to the technique given in [2, 10].

As a result of ranging it has been revealed that preferable to production of an adaptive set of clothes intended to men with limited abilities included 8 factors presented in decreasing order, the most essential are: X8 — heat-shielding properties of materials; X12 — resistance to gaps and attrition; X11 — heat — and mud-permeability; X10 — ease in wearing (a crease resistance and resistance to pollution); X5 — mass of material; X9 — an electrified effects; X7 — resistance to preserve warmth; X1 — tactile properties. At the same time inconsistency of various groups of experts on separate properties of materials is stated, as it has been revealed: X7 — resistance to temperature; X8 — heat-shielding properties of materials; X9 — electrified effects; X10 — ease in leaving (a crease resistance and resistance to pollution). Considering specifics of assortment group and special contingent, preferences of disabled men, and also opinion of people who are looking after them are taken account as being the main.

On the basis of the obtained data given in the block diagram the quality characteristics of materials for adaptive set of daily socks for physically disabled people are resulted (in the conditions of wearing in the range of expanded temperature conditions). In this scheme the general requirements matching to a rational packet of materials for production of an adaptive set are determined as absorbability and moisture-yielding ability, air permeability, resistance to attrition and a gap, pleasant tactile properties of fabric, electrified effects, ease in wearing, little material mass. At the same time, each layer of a packet materials has a number of own (original) requirements. Therefore, for the main and lining materials it is resistance to contain warming materials. For creation of an attractive external image, the important role of the main material is its esthetics appearance, and property a heat- mud-air permeability, resistance of materials, and its mass and degree of electrified effects is of great importance for operational properties.

Physiological features of disabled people are determined and the necessity of using a number of original properties of lining materials are pointed out, such as its adequacy to used materials for physiological allocations (sweat, urine and gas generation products), an non traumatic effects and availability without irritating effect on the surface of materials. In work [3, 25] the opportunity of maintenance of sub clothes temperature condition due to use of irritating effect of external receptors of a surface for the first time offered.

Softness and non-traumatic effects of lining material are the unconditional properties providing the safety requirement of the person who is in an adaptation set. Important properties of lining materials are their heat conductivity, air permeability, absorbability and moisture-yielding ability with little weight.

Absolutely new properties ascribed to properties of pro-masonry material of a heater is creating thermal balance, including, maintenance/strengthening of effect of thermal control. This property taking into account physiological features of the considered contingent –a general homeostasis is especially important.

In further researches extent of influence of material properties revealed during the researches on a physiological condition of physically disabled people, including, creation and maintenance of thermal balance in case of operation of a set of functional clothes for daily socks in the conditions of expanded range of temperature condition of the environment will be determined.

References:

1. Фетисова А. В. Социальная интеграция молодых людей с ограниченными возможностями в общество посредством развития сферы культурного досуга как одно из приоритетных направлений государственной молодежной политики//Science Time. – 2014. – № 10. – С. 365–377.
2. Кокеткин П. П., Чубарова З. С., Афанасьева Р. Ф. Промышленное проектирование специальной одежды. – М.: Легкая и пищевая промышленность, – 1982. – 189 с.
3. Романов В. Е. Системный подход к проектированию специальной одежды. – М.: Легкая и пищевая промышленность, – 1981. – 128 с.
4. Чубарова З. С. Методы оценки качества спецодежды. – М.: Легпромбытиздат, – 1988. – 160 с.
5. Сурженко Е. Я. Исследование процесса формирования качества спецодежды на этапе проектирования, – 1978: Автореф/дисс. канд. техн. наук. – 1978. – 214 с.
6. ГОСТ Р 53453–2009/ISO/TS 14415:2005. – Введ. 07.12.09. – М., – 2010.- 16 с. – (Эргономика термальной среды. Применение требований стандартов к людям с особыми требованиями).
7. ГОСТ Р ИСО 28803–2013. – Введ. 01.12.14. – М., – 2010. –52 с. – (Эргономика физической среды. Применение требований стандартов к людям с особыми потребностями).
8. Бекмурзаев Л. А., Приходченко О. В., Савельева Н. Ю. Особенности проектирования одежды для людей с ограниченными возможностями здоровья. Ставрополь: Ставропольское книжное издательство, – 2011. – С. 122.
9. Бабенко Л. Г., Котлярова В. В., Савельева Н.Ю, Дмитриенко Н. А. The methodological procedures using for disabled women' social needs analysis//Молодой ученый – 2015. – Вып. 11. – С. 256–258.

Section 4. Mathematics

DOI: http://dx.doi.org/10.20534/AJT-16-11.12-19-21

Druzhinin Victor Vladimirovich,
Smagin Ivan Romanovich,
National research nuclear University «MEPhI»
Sarov Institute of physics and technology, Department of mathematics
E-mail: Sarov, vvdr@newmail.ru

A generalization of the sums of bernoulli for the case of fractional powers

Abstract: The formulas for approximate computation of the sums of the first n natural numbers raised to the same fractional power from «0» to «3» have been obtained. Different ratios between such sums have been found. The application of these results has been considered.

Keywords: sum of natural numbers, fractional power, Bernoulli numbers.

Let us consider sum

$$B(n;t)=\sum_{k=1}^{n}k^t=1+2^t+3^t+\ldots+n^t, \qquad (1)$$

with integer non-negative t, which we call the sum of Bernoulli considered. These sums have been studied by many mathematicians. In 1617 Johann Faulhaber published the first book where he calculated these sums with powers up to «11» and later he published the second book with powers up to «17». Pierre Fermat suggested the quad- squares and cube-cubes methods to calculate such sums in the letter to Mersenne. Jacob Bernoulli obtained the polynomials named after him. Later Euler found the generating function for the Bernoulli polynomials, and Appel indicated derivative for them. The calculation of these amounts worked well as Jacobi and other mathematicians [1]. In the modern literature of the sum of (1) is calculated using the Bernoulli polynomials $B_t(n)$ by the formula

$$B(n;t)=\frac{1}{t+1}\left[B_{t+1}(n+1)-B_{t+1}\right]. \qquad (2)$$

These polynomials can be obtained by expansion in a power series generating function of the Euler

$$\frac{ke^{kn}}{e^k-1}=\sum_{t=0}^{\infty}\frac{k^t}{t!}B_t(n), \qquad (3)$$

where B_t — Bernoulli numbers, $B_t=B_t(0)$. For small values of $t''10$ these polynomials can be taken from tables in [2]:

$$B_0(x)=1;B_1(x)=x-\frac{1}{2};B_2(x)=x^2-x+\frac{1}{6};B_3(x)=x^3-$$
$$-\frac{3}{2}x^2+\frac{1}{2}x;\qquad B_4(x)=x^4-2x^3+x^2-\frac{1}{30};B_5(x)=x^5-$$
$$-\frac{5}{2}x^4+\frac{5}{3}x^3-\frac{1}{6}x.$$

For large values of t it is necessary to use (3) next. The data to calculate the value of (1) with an arbitrary interval m and with arbitrary initial member of a (not «1») using the Bernoulli polynomials do not exist. There are also other simple approaches to their analysis. In previous articles [3; 4] we have proposed a faster way such calculations of generalized sums

$$S(n;m;t;a)=\sum_{k=1}^{n}\left(a+(k-1)m\right)^t=a^t+\left(a+m\right)^t+$$
$$+\left(a+2m\right)^t\ldots+\left(a+(n-1)m\right)^t, \qquad (4)$$

at a random interval m, an arbitrary initial member a and with integer non-negative powers of t using recursive integral formula

$$S(n;m;t+1;a)=a^{t+1}\left\{\frac{m}{a}(t+1)\int_0^n S\left(\zeta;\frac{m}{a};t;1\right)d\zeta\right\}+$$
$$+a^{t+1}n\left\{1-\frac{m}{a}(t+1)\int_0^1 S\left(\zeta;\frac{m}{a};t;1\right)d\zeta\right\}. \qquad (5)$$

This is the new formula and it is not in handbooks and monographs [1; 2; 5; 6]. It is obtained from the first principles exactly by the method of mathematical induction, and its use does not require knowledge of the Bernoulli polynomials. We show this relation for $m=1$. As $S(n;1;0;1)\equiv B(n;0)=n$, then

$$S(n;1;1;1)\equiv B(n;1)=\sum_{k=1}^{n}k=$$
$$=\int_0^n\zeta\,d\zeta+n\left(1-\int_0^1\zeta\,d\zeta\right)=\frac{n^2}{2}+\frac{n}{2}; \qquad (6)$$

$$S(n;1;2;1)\equiv B(n;2)=\sum_{k=1}^{n}k^2=2\int_0^n\left(\frac{\zeta^2}{2}+\frac{\zeta}{2}\right)d\zeta+$$
$$+n\left(1-2\int_0^1\left(\frac{\zeta^2}{2}+\frac{\zeta}{2}\right)d\zeta\right)=\frac{n^3}{3}+\frac{n^2}{2}+\frac{n}{6} \quad (7)$$

$$S(n;1;3;1)\equiv B(n;3)=\frac{n^4}{4}+\frac{n^3}{2}+\frac{n^2}{4}. \quad (8)$$

This is the well-known equalities. Because the function $B(n;t)$ is continuous and integer t obeys the integral recurrent relations (7). On that base we found approximate expressions for the sums of Bernoulli with fractional powers. The formulas for calculating $B(n;t)$ with $t=0.5;1.5;2.5;3.5$ were given in the article of Indian mathematician Ramanujan [7] in 1915, were given the formula for calculating $B(n;t)$ with $t=0.5;1.5;2.5;3.5$. In a recent paper in the Internet [8] in 2012, another Indian mathematician was given the formula for calculating such amounts for any $0\le t\le 1$. It is slightly different from our formula [9] provides less accuracy.

In this paper, we increased these results and generalize the equality (6–8) for the cas of fractional powers t, i. e. allowed to borrow any $0\le t\le 3$. The formulas are approximate due to irrationalities. The case $0\le t\le 1$ is described in [9], but here we show a little more precise result

$$S_1(n;1;0\le t\le 1;1)=\frac{n^{t+1}}{t+1}+\frac{n^t}{2}-\frac{(1-t)}{2(t+1)}. \quad (9)$$

Equation (9) corresponds to the three boundary conditions (see (6–8)): $S_1(n;1;0;1)=n; S_1(n;1;1;1)=$ $=B(n;1); S_1(1;1;t;1)=1$. The calculations for (9) in the whole range of variation of and n from 1up to 10^7 in comparison with the exact value of S ives an absolute error of $\varepsilon<|0.07|$. Table 1 shows the results.

For the next line segment $1\le t\le 3$, we have obtained the General calculation formula

$$S_2(n;1;1\le t\le 3;1)=\frac{n^{t+1}}{t+1}+\frac{n^t}{2}+\frac{tn^{t-1}}{12}-\frac{(2-t)(3-t)}{12(t+1)}. \quad (10)$$

Formula (10) also satisfies five boundary conditions: $S_2(n;1;1;1)=B(n;1)$; $S_2(n;1;2;1)=B(n;2); S_2(n;1;3;1)=$ $=B(n;3)$; $S_2(1;1;t;1)=1$; $S_2(1;1;0;1)=n$. Note that the first two summands in (9–10) coincide with the first two terms in $B(n;t)$. Absolute error (10) in comparison with the exact value of $S(n;1;1\le t\le 3;1)$ is even smaller than in the first interval $\varepsilon<|0.007||$. In table.2 shows the results for $t=1.5;2.5$.

Table 1. – Values of the exact S and S_1 calculated by (9) quantities of amounts, $\varepsilon=S-S_1$

t	n	2	10	100	1000	10^4	10^6
0.50	S	2.4142	22.4683	671.4629	21097.4559	666716.4592	666667166.4588
	S_1	2.3570	22.4359	671.4767	21097.4881	666716.4975	666667166.4998
	ε	–0.0118	–0.0280	–0.0371	–0.0399	–0.0408	–0.0412
0.10	ε	–0.0037	–0.0071	–0.0080	–0.0081	–0.0081	–0.0081
0.25	ε	–0.0081	–0.0167	–0.0198	–0.0203	–0.0204	–0.0205
0.75	ε	–0.0097	–0.0271	–0.0424	–0.0511	–0.0560	–0.0602
0.90	ε	–0.0049	–0.0153	–0.0276	–0.0373	–0.0450	–0.0570

Table 2 — Values of the exact S and S_2 calculated by (10), $\varepsilon=S-S_2$

t	n	2	10	100	1000	10^4
1.50	S	3.8284	142.6723	40501.2245	12664925.9563	4000500012.4745
	S_2	3.8287	142.6728	40501.2250	12664925.9568	4000500012.4750
	ε	–0.0003	–0.0005	–0.0005	–0.0005	–0.0005
2.50	S	6.6569	1068.2176	2907351.1987	9050897005.4402	28576428779761.9135
	S_2	6.6561	1068.2158	2907351.1964	9050897005.4378	28576428779761.9107
	ε	0.0007	0.0017	0.0023	0.0024	0.0025

Let us discuss applications of the obtained results. The final numerical amounts with exact or approximate analytical solution, play a huge role in mathematics and physics. They allow us to reduce calculations to a new pattern, to achieve specific goals. This parameter, in our case, t is possible to differentiate and integrate, which yields a new formula considered the amount. For example, there is the following relationship

$$\sum_{k=1}^{n}\left\{ln\left(1+(k-1)\right)\right\}\left(1+(k-1)\right)^t=\frac{\partial B(n,t)}{\partial t}. \quad (11)$$

The obtained formulas can be used in discrete spaces and to give the magnitude of error between the squares of the histogram covering the curvilinear trapezoid. They can be useful for specific tasks. Equations (9–10) also allow to calculate multiple sums. For example, raising $S(n;1;1.5;1)$ to the square, you can calculate the sums

$$2\sum_{k_1(<k_2)=1}^{n-1} k_1 k_2 = S(n;1;3;1) - S^2(n;1;1.5;1). \qquad (12)$$

Combination of formulas (9–10) gives formulas for the calculation of the sums of the sums $T = \alpha S(n;1;t_1;1) + \beta S(n;1;t_2;1)$ with arbitrary α and β. For example, the sum

$$\sqrt{2} + 2\cdot\sqrt{3} + 3\cdot\sqrt{4} + \ldots + 9\sqrt{10} =$$
$$= S(n;1;1.5;1) - S(n;1;0,5;1) \approx 120.236.$$

Here is an example on a specific task. Imagine a pyramid, consisting of ten cubes are stacked on top of each other. Edges of a cube are reduced by law: $\sqrt{10};\sqrt{9};\sqrt{8};\supset;\sqrt{1}$. The height of the pyramid is equal to $S(10;1;0.5;1) = 22.468$ (see table 1). The volume of a pyramid is equal to $S(10;1;1.5;1) = 142.673$ (see table 2).

References:

1. Prasolov V. V. Polynomials. MZIMA, – 2003, – P. 131.
2. Graham Z., Knuth D., Patashnik O. Concrete mathematics, – Moscow, "Mir", – P. 313, – 1998.
3. Druzhinin V. V.//NTVP, – No 5, – P. 18–20, – 2016.
4. Druzhinin V. V., Strahov A. V.//AJTNS, – 2016. – No. 9–10. – P 15–17.
5. Gradshteyn I. S., Ryzhik I. M. Tables of integrals, sums, series and products. GIMPL, – Moscow, – 1962. – P. 15–16.
6. Korn G., Korn T. Handbook of mathematics, science, GIMPL, – M. – 1974, – P. 31, 135.
7. Ramanujan S.//J. Indian Math. SOC. – 1915. – No VII, – P. 173–175.
8. Snehal Shekatkar URL://https://arxiv.org/abs/1204.0877v2.
9. Druzhinin V. V., Smagin I. R.//NTVP,– 2016. – No 6, – P. 18–21.

Section 5. Food processing industry

DOI: http://dx.doi.org/10.20534/AJT-16-11.12-22-23

Savriev Yuldosh Safarovich,
Hakimov Shaxruz Shuxratovich,
Majidov Kaxramon Halimovich,
Bukhara engineering-technological institute,
Republic of Uzbekistan,
E-mail: kafedra-03@mail.ru

Technological features of olive seeds

Abstract: Cellular and endocellular structure of the kernel and cover of olive seeds, and their change under the influence of technological parameters have been studied by methods of poremetry, light and scanning electronic microscopy. Chemical, physical-chemical and kinetic methods of researches carried out with use of standard methods of the analysis.

Cellular and capillary-porous structure of physiologically mature seeds of the cotton, safflower, rape, soya and sunflower with the optimum humidity, different sizes, form, initial maintenance of lipids and fibers have been studied. The combination of the listed methods has allowed newly analyzing the structure of olive seeds at cellular level in the volume image. Have revealed interrelation between the structure of seeds and the maintenance lipids and albumens in them, and have estimated its role in formation of structure of materials in technological processing.

Keywords: olive seeds, cotton, safflower, rape, soya, sunflower, porous structure, technological factors.

Introductions: Seeds of some plants contain up to 50 … 70% of lipids from te mass [1]. The greatest quantity of spare lipids is usually concentrated in their basic fabric of seeds — a germ and endosperm; other parts are rather poor in lipids [2].

Vegetable oils are one of the basic fatty components in a food of the person, playing the important role in metabolic processes in the organism [3].

For manufacture of vegetable oils are characteristic the ineffective technology, processes and the equipment. Technological processes differ in multistageness and power consumption.

For the decision of the problem connected with maintenance of necessary consumption level of high quality vegetable oils of the domestic production is necessary perfection of technology of their reception.

In this connection it is actual studying of processes proceeding at extraction of oil and on these basis creation essentially new recourse-saving technologies.

Materials and methods: features of a structure of olive seeds — cotton, safflower, rape, soya and sunflower nowadays cultivated in Republic of Uzbekistan have been studied.

Estimation of results and their statistical reliability carried out with use of modern calculation methods of statistical reliability of measurement results.

Results: seeds of olive cultures processed by the industry represent difficult biological objects and differ on the physical and chemical, physic-mechanical and technological properties.

Processes occurring in seeds, their morphological parts and oil-keeping materials in technological processing and feature of their natural capillary-porous and cellular structure have been studied.

Cellular and capillary-porous structure of physiologically mature seeds of cotton, safflower, rape, soya and sunflower with the optimum humidity, different sizes, form, initial maintenance of lipids and fibers have been studied.

Sharp distinctions in size of cells and their ultrastructure in superficial layer of reserving fabric, basically parenchyma, and also the sizes and localization of lipif spherosomes and albumin globules have revealed.

Differential curve of distributions of pores in the sizes in a cover of oil seeds of the investigated cultures are presented on fig.

On the resulted differential curves maxima of certain groups of pores, both in seeds and for kernels are observed.

In porous system of the cover of sunflower prevails the group of the macropores with equivalent radiuses 1000–6000 Å (52%) and group of the supermacropores with equivalent radiuses 62000–420000 Å (19%).

In the bared cover of seeds of the cotton the group of a passing pores does not exist at all. In porous system of cover of the pore are distributed in the sizes as follows: the considerable quantity — groups of big, macro- and supermacropores in the size 9200–280000 Å (76%), then — groups of a mesopores in the size 37–980 Å (14%), small macropores with equivalent radius 980–9200 Å contains insignificant quantity (4%).

The bared cover of seeds of cotton differs with the high maintenance of group of a macropores in the size 6000–50000 Å.

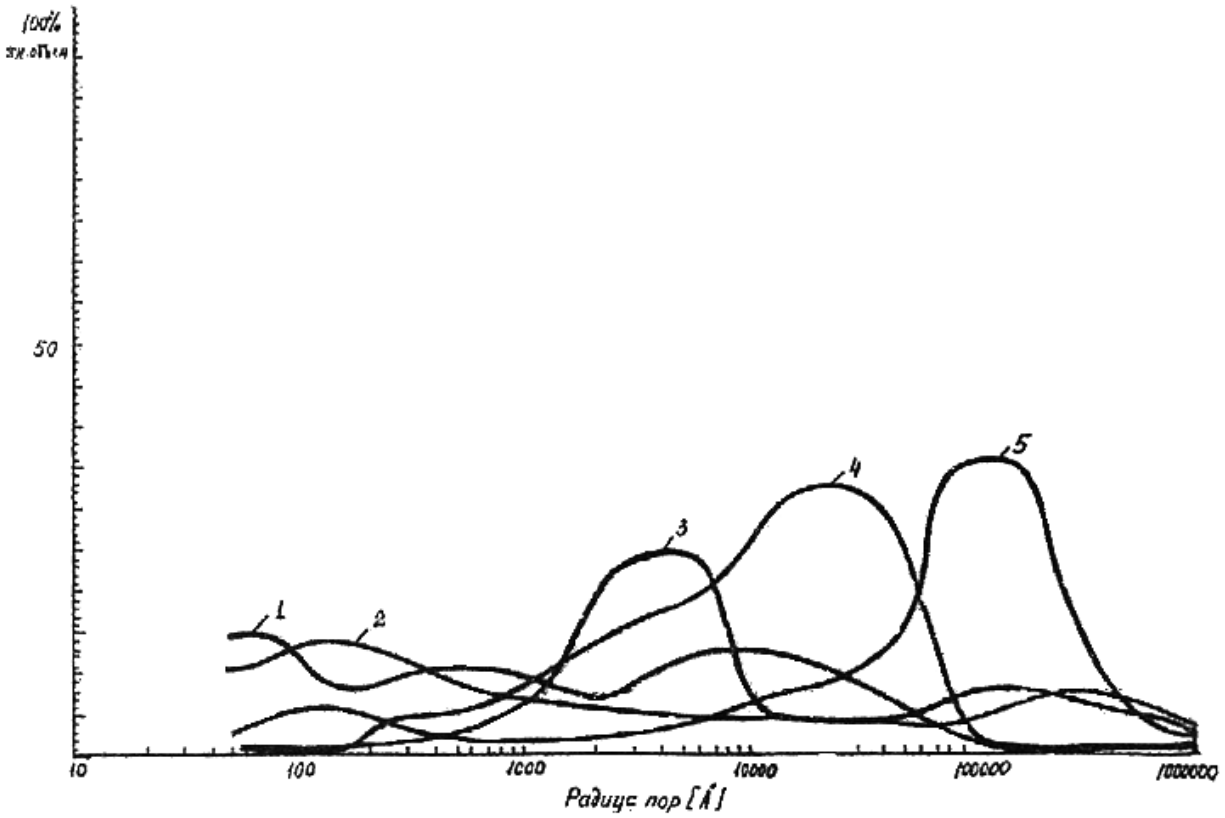

Figure 1. Differential curve of distribution of the pores in the sizes in a cover of olive seeds: 1-rape; 2-safflower; 3-sunflower; 4-cotton; 5-soya.

Discussion: Revealed essential distinctions of a structure of fabrics of intact structures, and properties of natural porous system of kernel and fruit cover of olive seeds will predetermine character of total effect of the response of capillary-porous structure of oil-keeping material with the various maintenance of cover (non-decorticated seeds) on influence of technological kinds of processing.

By studying of cellular and capillary-porous structure of oil-keeping materials in a range equivalent radiuses 37–1000000 Å at different stages of technological processing it is proved that all flowed out free oil from spherosomes destroyed as a result of complex influence of processing methods concentrates in again formed pores and capillaries in the range of the sizes 1000–35000Å. Oil is kept in this pores and capillaries with adsorption and capillary forces which are necessary for overcoming for its extraction.

References:

1. Viability of seeds//Translated from English – M.: Kolos, – 1978 – P. 415.
2. Bohinskiy R. Modern views in biochemistry//Translated from English – M.: Mir, – 1987. – P. 544.
3. Arutyunyan N. S., Kornena E. P., Yanova L. I. and others. Technology of fat processing. – M.: Pishepromizdat, – 1999. – P. 452.

DOI: http://dx.doi.org/10.20534/AJT-16-11.12-24-25

Savriev Yuldosh Safarovich,
Hakimov Shaxruz Shuxratovich,
Majidov Kaxramon Halimovich,
Bukhara engineering-technological institute,
Republic of Uzbekistan,
E-mail: kafedra-03@mail.ru

Structure of some olive seeds

Abstract: Scientific work is aimed on research of structural features of some olive seeds on purpose further optimization of methods of oil extraction.

Cellular and capillary-porous structure of physiologically mature seeds of a cotton, safflower, rape and soya with the optimum humidity, different sizes, form, the initial maintenance of lipids and fibers has been studied. Combinations of the listed methods have allowed newly analyzing structure of olive seeds at cellular level in the volume image. We have revealed interrelation between the structure of seeds and the maintenance of lipids and albumens in them, and have estimated its role in formation of structure of materials in technological processing.

Keywords: olive seeds, cotton, safflower and rape, porous structure, technological factors.

Lipids are an obligatory component of cages though the majority of plants accumulates not much quantity of oils [1–2]. However, there are hundreds cultures at which in fabrics of separate parts the significant amount of fat oils is postponed in a stock.

In process of development of methods and technology the quantity of olive cultures, from which we probably can take oils, continuously extends at the expense of plants with rather low maintenance of oil in fabrics and parts [3].

Development of advanced technologies is connected with studying of laws of formation of capillary-porous system of oil-keeping materials, in particular, olive cultures of local grades.

Materials and methods: Features of a structure of olive seeds — cotton, safflower and rape, cultivated nowadays in Republic Uzbekistan are investigated.

The cellular and endocellular structure of kernel and cover of olive seeds and their change under the influence of technological parameters have been investigated via methods of poremetry, light and scanning electronic microscopy [4–5].

Estimation of results and their statistical reliability have been carried out with use of modern calculation methods of statistical reliability of measurement results.

Results: Distinction of properties of olive seeds is mainly caused by the morphological features genetically put in each separate kind of oil seeds.

Cellular and capillary-porous structure of oil seeds and oil-keeping materials has been studied in the range of equivalent radiuses at different stages of technological processing and in again formed pores and capillaries.

Have been studied processes occurring in seeds, in their morphological parts and oil-keeping materials in technological processing and features of their natural capillary-porous and cellular structure.

Experimental results have been received with use of the newest methods of electronic-scanning microscopy and mercury poremetry, and also with the system method of estimation of size heterogeneity of structural elements of cellular structure from ultramicroscopic (spherosome level) till the biggest pores, capillaries and emptiness.

Combination of the listed methods has allowed newly analyzing structure of olive seeds at cellular level in the volume image. Have revealed interrelation between the structure of seeds and the maintenance of lipids and albumens in them and have estimated its role in formation of structure of materials in technological processing.

Distinctions of seeds in the maintenance of lipids and albumens, the sizes of pores and capillaries have been defined via character of the cellular structure, the sizes of cages, the thickness of cellular walls, quantity and size of lipid spherosomes and albumin little parts, development of cytoplasm matrix. The obtained data is resulted in table 1.

As we see in data of table 1, olive seeds differ among themselves in the basic physical and physical-chemical indicators. It is necessary to note that character of the cellular structure is adequate to properties of capillary-porous structure of kernels.

Table 1. – The basic indicators of porous system of a kernel of olive seeds

Kernel	Volume density, g/cm^3	Volume of the pore, mm^3/g	General porosity,%	Surface area of the pores, m^2/g
Cotton	1.155	78.269	9.046	7.376
Safflower	0.984	212.048	20.874	5.976
Rape	0.961	154.181	14.827	10.272

Distribution of the pores and capillaries in the sizes in a range 37–1000000 Å are resulted in table 2.

Table 2. – Intervals of display of the maximum maintenance of pore groups in the kernel of olive seeds

Kernel	Intervals of maximums, Å
Cotton	37–720; 720–42000; 100000–1000000
Safflower	37–600; 1000–10000; 20000–1000000
Rape	37–600; 7000–320000

As we see in data of table 2, received experimental results have the extreme character.

On the assumption of this the kernel of rape can be considered as bidispersed porous part, and the kernels of cotton and safflower to trydispersed porous parts.

Discussion: By researches on the example of seeds of cotton it is established that oil in the cell is localized in spherosomes which together with albumin globules fill all volume of the cell.

At electron-microscopic level it has been revealed that in the microstructure there are pores, capillaries and air emptiness. Cells of fabrics consist of cellular walls and set of the various structural characteristic details different by the sizes including lipid spherosomes, protein bodies containing spare fibers or globulin, globoids, cellular cytoplasm in which all elements set forth above are introduced together with a water-soluble protein, enzymes and other functional components, i. e. the structure of a kernel of olive seeds is simultaneously multicomponent and heterogeneous, and that predetermines selective character of the response of separate components on action of external fields.

References:

1. Tyutyunnikov B. N. Chemistry of fats. – M.: Food industry. – 1974. – P. 448.
2. Physiology and biochemistry of rest and germination of seeds//translated from English – M.: Kolos, – 1982. – P. 495.
3. Proteins of seeds of grain and olive cultures//translated from English – M.: Kolos, – 1977. – P. 312.
4. Scherbakov V. G. Biochemistry and merchandising of oil-bearing raw materials. M.: Agropromizdat. – 1991. – P. 356.
5. Bikova S. F. Theoretical and experimental bases of creation of essentially new resource-saving technologies of reception of vegetable oils/S. F. Bikova: Abstract of a thesis of doctor of technical sciences, St. Petersburg, – 1996.

DOI: http://dx.doi.org/10.20534/AJT-16-11.12-25-31

Sulaymanova Gulchekhra Hakimovna,
Majidov Kahramon Halimovich
Bukhara engineering technological institute,
Bukhara, Uzbekistan
E-mail: kafedra-03@mail.ru,

Cream-superficial activity of food emulsifiers

Abstract: One of perspective directions of development of butter industry is working out and development of manufacture of butter with the lowered fat content. Now manufacture of such butter has not found a wide prevalence yet. Taking into account were carried out researches of influence of stabilizers of structure on properties of cream with a mass fraction of fat of 40–60% as raw materials for development of oil with the lowered fat content. As the consistence stabilizer used gelatin in quantity from 0 to 2%, as emulsifiers — monoglycerides.

As estimation criteria were used effective viscosity, sedimentation stability of system. Viscosity of cream of 40–50% fat content at entering of emulsifiers changed slightly. At mass fraction of fat more than 60% entering of emulsifiers in cream promoted increase in their viscosity in 1.4–2.1 times. Considerable changes of viscosity were observed at entering of stabilizers into cream. Thus viscosity of cream of 50% fat content came closer to viscosity of control samples at entering into them of the mixture of the stabilizer in quantity of 1% and emulsifiers in quantity of 1%. Viscosity of cream of 40% fat content with addition of the stabilizer less than 2% was lower than viscosity of the control sample, and at a dose of the stabilizer of 2% or its mixtures with emulsifier (0.5% and 1%) was exceeded by viscosity of the control sample in 1.3–1.9 times. Viscosity of cream of 60% fat content at entering into them of 0.5% emulsifiers already was higher than viscosity of control samples in 1.3 times.

Keywords: Dairy butter, fat mass fraction, stability, properties of cream, viscosity and sedimentation stability, maintenance of emulsified fat.

Introduction: Expansion of assortment of articles of food including fat-and-oil products is important problem of food-processing industry in the next years. In this direction ways and measures on overcoming of world financial and economic crisis are considered as the basic program document of Republic of Uzbekistan [1].

The great attention all over the world is given to a problem of a rational and adequate food. In the decision of this problem the important place has expansion of assortment of a foodstuff with the raised food value at the expense of use of additives with functional properties.

Food fats are the important foodstuff. On the physiological norms, the recommended maintenance of fat in a food allowance of the person makes 30–33% — the general power value of food.

Fats are necessary not only as reserve substance and energy source, but also as suppliers of physiologically active connections — irreplaceable fat acids, phosphatides, sterols, vitamins participating in synthesis of cellular membranes and other fabrics of an organism.

Purpose of the scientific work: Decision of problems of quality and safety of food fats and products of their processing is one of priority directions in realization of the concept of state policy in the field of healthy food of the population of republic.

Materials and methods: For analysis of a chemical compound of fats and products of decay of the catalyst were used methods selective extraction, gas-liquid and thin-layer chromatography and nuclear magnetic resonance [2].

The maintenance of trans-isomers defined by the IR-spectroscopy method; separation of triglycerides on molecular weight by the method of high-temperature gas-liquid chromatography [3].

Analysis of positional separation of fat acids in triglycerides was defined by the method of enzymatic hydrolysis with the subsequent calculation of triglyceride structure [4].

Maintenances of monoesters of fat acids, mono-di — and triglycerides defined by the method of thin-layer and gas-liquid chromatography.

The polymorphic crystal structure of fat was studied by the method of X-ray diffraction and the differential-thermal analysis [5].

Results and discussion: One of perspective directions of development of butter industry is working out and development of manufacture of butter with the lowered fat content. It will be co-ordinated with requirements of time and the basic tendencies of butter manufacture in the world [6].

Now manufacture of such butter has not found a wide prevalence yet. It is connected by that decrease in a mass fraction of fat in cream promotes deterioration of conditions of process of oil formation, to infringement of its stability and formation of defects of oil consistence (friability, crumbling, exudation of moisture, disconnectedness of structures, etc.). The reason of it is change of physical and chemical properties of the cream, making direct impact on process of butter forming.

At decrease in a mass fraction of fat in cream from 70 to 40% is observed reduction of their effective viscosity and sedimentation stability, maintenance increase of emulsified fat and decrease in ability to transformation of a dispersion of direct type to a dispersion of return type, characteristic for a butter of traditional structure.

One of possible ways of influence on process of butter forming from dispersions of the lowered fat content is entering into cream of stabilizers of structure — the substances, capable to change physicochemical properties of cream of the lowered fat content so that they as much as possible came closer to high-fatty cream, process of butter forming which proceeds stably. It is possible to refer to them emulsifiers (E) and consistence stabilizers (St).

As emulsifiers are used fat-soluble substances possessing high superficial activity owing to presence in

them polar located hydrophilic and lipophilic groups of atoms. Such structure of emulsifiers causes their ability to concentrate on interfaces of phases, to reduce an interphase tension and to promote formation and stabilization of a fatty dispersion.

As consistence stabilizers are used water-soluble substances possessing expressed hydrophilic properties. Because of this property they allow to keep moisture in a product and keep physical and chemical condition and uniformity formed at participation of emulsifier dispersions.

Positive influence of emulsifiers and consistence stabilizers on process of butter forming is established at development of sandwich fat with a mass fraction of 61.5%. However their influence on cream with lower mass fraction of fat and process of their transformation to oil are studied insufficiently.

Taking into account were carried out researches of influence of stabilizers of structure on properties of cream with a mass fraction of fat of 40–60% as raw materials for development of oil with the lowered fat content. As the consistence stabilizer used gelatin in quantity from 0 to 2%, as emulsifiers — monoglycerides distilled under trademark "Palsgaard-0291" in quantity from 0 to 1% [7].

As estimation criteria were used effective viscosity, sedimentation stability of system (cream + St; cream + E; cream + St +E), organoleptic indicators (taste and smell, consistence), maintenance of emulsified fat, ability of system to destruction under the influence of thermomechanical processing, microstructure of mixtures. As the control product was used cream of 70% fat content without structure stabilizers.

Experiment planning was carried out as full factorial experiment.

The estimation of taste and smell of analyzed samples on specially developed 5-mark scale was in a range of 2.5–4.5 points. For mixtures with a mass fraction of fat of 40% most the appreciation was received by samples with addition of the stabilizer in quantity of 2% or its mixtures with emulsifiers; for mixtures of 50% fat content — samples with addition of the stabilizer of 1% or its mixtures with emulsifiers, and for mixtures of 60% fat contents — samples with emulsifier in quantity of 0.5%. The consistence of analyzed cream was in a range of 1–4 points. Thus for all analyzed samples of cream the tendency of improvement of the consistence was traced at use of structure stabilizers.

Viscosity of cream of 40–50% fat content at entering of emulsifiers changed slightly. At mass fraction of fat more than 60% entering of emulsifiers in cream promoted increase in their viscosity in 1.4–2.1 times.

Considerable changes of viscosity were observed at entering of stabilizers into cream. Thus viscosity of cream of 50% fat content came closer to viscosity of control samples at entering into them of the mixture of the stabilizer in quantity of 1% and emulsifiers in quantity of 1%. Viscosity of cream of 40% fat content with addition of the stabilizer less than 2% was lower than viscosity of the control sample, and at a dose of the stabilizer of 2% or its mixtures with emulsifier (0.5% and 1%) was exceeded by viscosity of the control sample in 1.3–1.9 times. Viscosity of cream of 60% fat content at entering into them of 0.5% emulsifiers already was higher than viscosity of control samples in 1.3 times.

Increase of viscosity of system at addition of stabilizers is caused by formation of additional structural bonds in it that was confirmed by microscopic researches on example of cream of 50% fat content (fig. 1).

At research of sedimentation stability of cream with addition of stabilizers and emulsifiers it is not established any law of its change depending on a mass fraction of fat, dose of the stabilizer and emulsifiers. In some samples is noted the increase of sedimentation stability in comparison with cream of similar fat content without structure stabilizers, in others, on the contrary, its decrease. Average indexes of sedimentation stability on the sediment of fat for cream of 40% fat content with addition of stabilizers of structure have made 81.8%, for cream of 50% fat content — 84.8%, and for cream of 60% fat content — 81.9%. For control cream of 70% fat content this indicator has made 96.0%. On the average at entering of stabilizers of structure sedimentation stability of cream much lower than at control samples. The maintenance of emulsified fat in cream of 40–60% fat content at entering into them emulsifiers tends to growth, and at entering of stabilizers — to decrease. At sharing of emulsifiers and stabilizers the maintenance emulsified fat in cream 40–60% fat content also tend to decrease.

For an estimation of ability of analyzed cream to destruction under the influence of thermomechanical processing of the mixture after pasteurization was cooled to temperature of butter forming and destroyed. In an initial mixture and the received product were defined the maintenance of emulsified fat and calculated ability of system to destruction on parity of maintenance of emulsified fat in the dispersion before and after its destruction. Also hereby established that cream with mass fraction of fat of 40% can collapse under the influence of the mechanical and temperature factor on 90% and more only at addition in them of the stabilizer in quantity of 2% (or its mixtures with emulsifier). The same

degree of destruction of cream with a mass fraction of fat of 50% is observed at entering of 1% and more stabilizer and its mixtures with emulsifier. The cream with the mass fraction of fat of 60% most easily collapse at entering of emulsifiers in quantity of 0.5%. The obtained data accurately shows the tendency of increase in ability of cream to destruction, i. e. to transformation to oil, at use of stabilizers and emulsifiers.

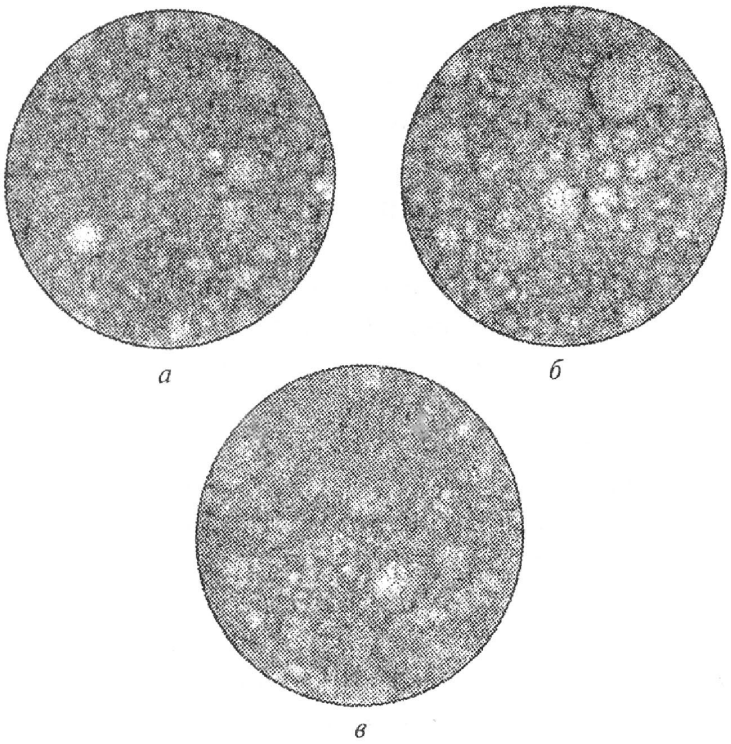

Figure 1. Change of a microstructure of cream at entering into them of structure stabilizers (50% fat content), x280: a- control; b- with addition of 1% emulsifiers; c- with addition of the stabilizer of 2%

Definition of optimum doses of the stabilizer and emulsifiers at which change of initial cream occurs in a direction of reception of system with indicators close to control cream is carried out by the method of the multifactorial analysis of experimental data.

Factors: x_1 — fat mass fraction in cream in a range of 40–60%; x_2 — mass fraction of the stabilizer of 0–2%; x_3 — mass fraction of emulsifiers of 0–1%.

Target parameters: y_1 — taste and smell; y_2 — consistence; y_3 — viscosity; y_4 — ability to destruction (as an indicator uniting condition of dispersion before thermomechanical processing).

The equations of regress describing dependence of indicators $y_1 - y_4$ from factors $x_1 - x_3$ are received. All equations of regress are adequate; the plural factor of correlation varies from 0.83 to 0.92. At the fixed values of the mass fraction of fat in cream (x_1) in the received equations are established dependences of analyzed indicators $(y_1 - y_4)$ from factors x_2 and x_3 at change of fat content of cream from 40.0 to 60.0% with step of 2.5%. On sections of response surface (fig. 2) were defined areas of values of mass fractions of the stabilizer x_2 and emulsifiers x_3 at which indicators of analyzed mixtures of the fixed fat content come closer to control cream.

Analyzing the received results, it is possible to notice that for cream with a mass fraction of fat of 40% the optimum area has narrow enough range: x_2 = 1.70–1.85%, x_3 = 0.40–0.75%. It is limited with discrete step of all analyzed parameters, and in a greater degree with discrete step y_3, y_2, y_1. In optimum area the stabilizer mass fraction has narrower range.

Reduction of its fraction below optimum value leads to decrease in viscosity of system and its ability to destruction. Simultaneously thus worsen organoleptic indicators of cream (taste, smell and consistence).

At definition of optimum areas for cream 42.5–60.0% fat content the taste and smell estimation has appeared less significant at y_1. In a range of fat content from 45.0 to 52.5% physical and chemical indicators were defining (viscosity y_3 and ability to destruction y_4), i. e. in this range entering of stabilizers of structure makes stronger impact on viscosity of cream and ability to destruction than on their taste, smell and consistence.

At higher mass fraction of fat in cream (55.0–60.0%) the big importance in definition of optimum area has viscosity of system — y_3 and its consistence — y_2. It is possible to explain it that in the given range of fat content the superfluous quantity of the stabilizer leads to inflation of viscosity of system, occurrence of its excessive density and stickiness and to deterioration of its consistence.

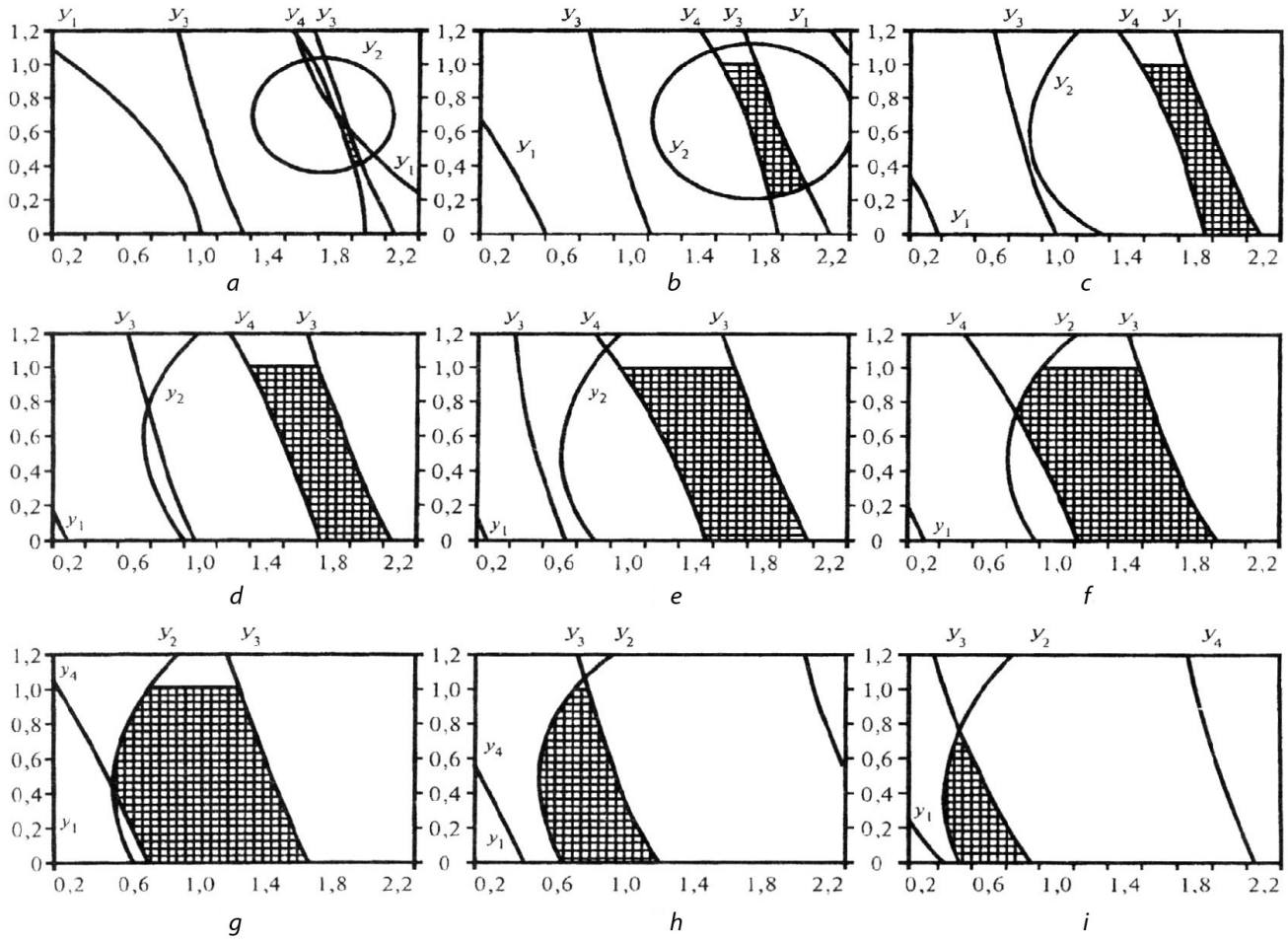

Figure 2. Optimum areas of sections of response surface for dairy-fatty dispersions with the fat mass fraction x_1: 40% (a); 42.5% (b); 45% (c); 47.5% (d); 50% (e); 52.5% (f); 55% (g); 57.5% (h); 60% (i). On an axis of abscissa — stabilizer mass fraction x_2 (%), on an axis of ordinates — emulsifiers mass fraction x_3 (%)

The area of optimum zone of sections of response surface grows with increase in the mass fraction of fat in system from 40.0 to 55.0%, and then decreases in process of growth of a mass fraction of fat. It is necessary to notice that for dispersions with a mass fraction of fat of 40.0–42.5% sharing of the stabilizer and emulsifiers is obligatory. For dispersions with a mass fraction of fat of 45.0–60.0% probably use of two variants: mixtures of the stabilizer with emulsifier or only the stabilizer, i. e. the stabilizer in an analyzed range of fat content of cream makes more significant impact on change of their indicators, rather than emulsifier. As lower fat mass fraction in cream that as higher importance of the stabilizer. At decrease in a mass fraction of fat from 60 to 40–45% the parity of St/E increases from 0.99 to 3.10–3.44.

For each level of fat content of cream on optimum areas it is possible to define minimum E_{min}, average E_{av} and maximum E_{max} quantity of emulsifiers at which addition it is possible to receive cream with the set properties. Optimum values of a mass fraction of stabilizer St at these fractions of emulsifiers are presented in table.

The minimum value of emulsifiers for dispersions of various level of fat content makes from 0 to 0.4%, maximum — from 0.75 to 1.0%. Average value of emulsifiers makes from 0.38 to 0.60%. At increase of dose of emulsifiers from E_{min} to E_{max} (in 2 and more times) the optimum dose of the stabilizer decreases in 1.1–1.6 times. Thus dose application of emulsifiers in limits from minimum to an average of values is economically more proved.

At the minimum value of emulsifiers, equal to zero ($E_{min} = 0$), dependence of a mass fraction of the stabilizer x_2 from fat content of cream x_1 in a range 45.0–60.0% are described by the equation

$$x_2 = -3{,}76 + 0{,}2923x_1 - 0{,}003695x_1^2 \quad (R = 0.99). \quad (1)$$

At average value of emulsifiers E_{av} dependence of a mass fraction of the stabilizer on fat content of cream in a range 40.0–60.0% are described by the equation

$$x_2 = -3{,}316 + 0{,}2647x_1 - 0{,}003407x_1^2 \ (R = 0.99). \quad (2)$$

Dependence of a parity of St/E ($_{x2/x3}$) from a mass fraction of fat of cream is described by the equation

$$x_2 / x_3 = -13{,}18 + 0{,}7554x_1 - 0{,}008718x_1^2 \ (R = 0.97). \quad (3)$$

From the equation (1) it is possible to define demanded mass fraction of the analyzed stabilizer in a range of fat content from 45 to 60% which allows receiving mixtures with organoleptic and physicochemical indicators which are closer to control cream, without usage of emulsifiers.

Table 1.

Mass fraction of fat,%	E_{min},%	St,%	E_{av},%	St,%	St/E	$E_{max,}$%	St,%
40.0	0.4	1.82	0.58	1.78 ± 0.02	3.10	0.75	1.70
42.5	0.2	1.75	0.60	1.72 ± 0.10	2.87	1.0	1.55 ± 0.10
45.0	0	1.87 ± 0.13	0.50	1.72 ± 0.10	3.44	1.0	1.52 ± 0.13
47.5	0	1.83 ± 0.17	0.50	1.63 ± 0.22	3.26	1.0	1.40 ± 0.20
50.0	0	1.65 ± 0.30	0.50	1.43 ± 0.28	2.86	1.0	1.20 ± 0.35
52.5	0	1.40 ± 0.40	0.50	1.17 ± 0.38	2.34	1.0	1.08 ± 0.27
55.0	0	1.08 ± 0.42	0.50	0.87 ± 0.48	1.74	1.0	0.83 ± 0.22
57.5	0	0.82 ± 0.30	0.50	0.65 ± 0.22	1.30	1.0	0.63 ± 0.05
60.0	0	0.50 ± 0.20	0.38	0.37 ± 0.15	0.99	0.75	0.30

From the equation (2) it is possible to define demanded mass fraction of the stabilizer in a range of fat content from 40.0 to 60.0% at its sharing with emulsifier. Having defined value x_2 and having substituted it in the equation (3), it is possible to calculate demanded value x_3 for any analyzed fat content of cream.

Thus, the conducted researches have allowed to establish emulsifiers (distilled monoglycerides) and the stabilizer (gelatin) on change of properties of cream of 40–60% fat content and to define influence their optimum doses, allowing to approach properties of cream of the lowered fat content to cream of 70% fat content (without structure stabilizers) and by that to improve conditions of their transformation to a ready product — butter with the lowered fat content.

Conclusions: Basis of emulsifying ability of different soluble emulsifiers, including food emulsifiers, is their superficial activity.

Except property of emulsifiers — to lower a superficial tension on border of section of phases as a result of spontaneous concentration of its molecules in the superficial layer — necessary conditions of stabilization of concentrated emulsions are density of the protective layers stabilizing emulsions, and presence of the structurally-mechanical barrier which is carried out by permolecular structures in the form of phase superficial films of emulsifiers.

For achievement of enough high structural viscosity — durability of covers of droplets of emulsion — in them should occur micellar structuration with occurrence of lyophilic gel as a result of concentration increase of its superficial-active substance in adsorption layer

Basically asymmetry of structure of molecules of superficial-active substance is observed only in solutions of superficial-active semicolloids in which the certain fraction of all dissolved particles is in colloid-disperse condition, and other part — in molecular-disperse condition.

Mono- and diglycerides are received by etherification of glycerin with fat acids or glycerosis of food fats and oils. Glycerosis of fats is an exchange of radicals between triglycerides and glycerin, being special case of interesterification. Used as emulsifier the product of glycerosis contains 35–70% of monoglycerides, 30–40% of diglycerides, 10–20% of triglycerides, and the rest part — glycerin and fat acids. Concentrated monoglycerides are received by molecular distillation.

On research of superficial activity of the technical mixture of mono-, di- and triglycerides in comparison with pure monoglycerides, allocated with molecular distillation, it is shown that monoglycerides lower the superficial tension on border of cotton oil-water system at temperature 70 °C much more strongly than a mixture of mono- and diglycerides.

Decrease of a superficial tension depends on length of the hydrocarbonic chain of a radical of fat acid of monoglyceride, exactly: superficial activity of monostearate is less than glycerin monopalmitate and monolaurate, i. e. superficial activity of these substances from nonaqueous

solution increases on border with water with reduction of a hydrocarbonic chain that is typical for all hydrophobic superficial-active substances.

Researches of a superficial tension of solutions of some glycerides in cotton oil on border with water are conducted. Superficial activity for solutions of monoglycerides of caprylic, capric, lauric, palmitic, linoleic and oleic acids has been thus studied at various temperatures.

At analysis of a superficial tension of solutions of monoglycerides of stearin, pelargonic, 12-hydroxystearin, 9.10-dihydroxystearin and 9.10.12-trihydroxystearin acids has been noted difficult solubility of di- and trihydroxymonoglycerides in cotton oil, therefore measurements of superficial tension of these monoglycerides carried out for their water solutions on border with cotton oil.

Superficial tension of solutions glycerin monostearate in cotton oil was measured on border with water. It has been thus shown that superficial activity, for example, glycerin monostearate, approximately in 6 times lower than 9.10.12-trihydroxymonoglycerides.

Definition of factor of superficial activity of α -monostearate and butyl alcohol at its calculation under the empirical formula has shown that at temperatures lower than 40 °C the formula ceases to be true.

Thus, the given researches can be a basis for practical use of monoglycerides on the basis of different fatty raw materials in this or that technological process by manufacture of food production, because the properties, nature, chemical structure of superficial–active substances cause character of interaction with them entered systems.

References:

1. Karimov I. A. "World financial-economic crisis, ways and measures on its overcoming in the conditions of Uzbekistan." T: – Uzbekistan, – 2009.
2. Rudakov O.B, Vostrov I. A., Fedorov S. V., Filipov A. A., Selemenev V.F, Pridantsev A. A. "Guide of chromatographer" Voronezh: Aquarius – 2004.
3. Cazes J., Scott R. P. W. "Chromatography theory" New York – 2002.
4. Tereshuk L. V. Lactic-fatty composition: Kemerovo technological institute of food industry-Kemerovo, – 2006 – P. 209.
5. Polyanskiy, K. K. Differential thermal analysis of food fats. K.K Polyanskiy, C. A. Snegiryov, O. B. Rudakov – M.: DeLi print – 2004. – P. 85.
6. State Standard P 53776–2010. Refined and deodorized palm oil for food industry. Technological conditions. Introduction. – 2011. – 04–01. – M.: Standartinform, – 2010 – P. 16.
7. Arutunyan N. S., Kornena E. P., Yanova L. I., and other. Technology of processing of fats. – M: Pishepromizdat, – 1999. – P. 452.
8. Kornena E. P., Kalmanovich S. A., Martovshuk E. V. and other. Assessment of oils, fats and products of their processing/Edited by Pozdnyakovskiy V. M. – Novosibirsk, – 2007 – P. 272.
9. Sulaymanova GH, Rahimov MN, Madjid KH The influence of electromagnetic fields on the degree of purification cottonseed oil. Magazine "Fat industry" – Moscow, – 2015. – No 5. – S 18–19.
10. Sulaymanova GH, KH Mazhidov Stabilizers and emulsifiers production of low-fat butter. "The Uzbek chemical journal" – Tashkent, – 2015. – No 3. – S. 76–79.

Section 6. Technical sciences

DOI: http://dx.doi.org/10.20534/AJT-16-11.12-32-35

Bekmuratova Zulfiya Tleumuratovna,
Karakalpak State University named of Berdakh,
department of «Chemical mechnology», senior teacher
Alimova Halimahon,
Dr.Sci.Tech., Tashkent institute textile and light industry,
department of "Technology of silk and spinning»
Avazov Komil Raxmatovich,
Tashkent institute textile and light industry,
department of "Technology of silk and spinning»,
Senior Research Fellow Applicant
E-mail: komil.avazov@mail.ru, avazov-komil@umail.uz
Habibullaev Doniyor Anvardjanovich,
Tashkent institute textile and light industry, an independent researcher

Technology of producing textile products of medical use

Abstract: In the article is researched the opportunities' of technical equipment for making high qualified woven unsterile medical cotton bandages with using reduced technical range. Its given technological process and receipt of bleaching severe yarn, from taken bandage of new pattern of given width on the machine Fittex (Italy). By Method of experimental research is given technological parameters of production bandage patterns on new way. It is worked out reduced on 5 transformations technology of producing new medical goods.

Keywords: Keywords: woven unsterile medical cotton bandage, production for medical, production technology, the wide of the bandage.

Medical dressings are necessary as they considerably contribute to improving the healing efficiency of drugs. The gauze can be used for making medical dressings such as lengths of fabric, bandages, napkins, both single-layered, and multilayered, surgical tampons, gauze turundas, swabs, medical bolsters, balls, for gel-type and salve dressings, compresses, immobilization of medicinal agents and preparations.

During the development of the new sample of bandage the weft yarn is laid in circular line on the set width of the bandage. Thanks to it the fringe is not formed neither along the edges of bandage, nor at a cut like it happens in gauze bandages, thereby simplifies their operation, excludes possibility of leaving the smallest threads of a dressing on wounds. There is a necessity to improve this kind of product of the textile industry. The production of the raw, then bleached gauze is carried out by two separate, differing from each other technologies and the equipment at textile factories (textile machinery and finishing equipment).

The object of the research is textile products of medical use. The experimental research method establishes the technological parametres of manufacturing of the unsterile medical cotton bandage woven according to the new method.

According to existing technology, the full cycle of manufacturing of gauze bandage in the traditional way includes spinning, weaving and whiting, after that it is sent to a pharmaceutical factory where it is made into medical product.

The goal of the research is to develop a more reduced technology of production of medical cotton bandage by using an experimental research.

The bandage produced in a new way on the FITTEX (Italy) machine tool surpasses the traditional gauze bandage in all respects.

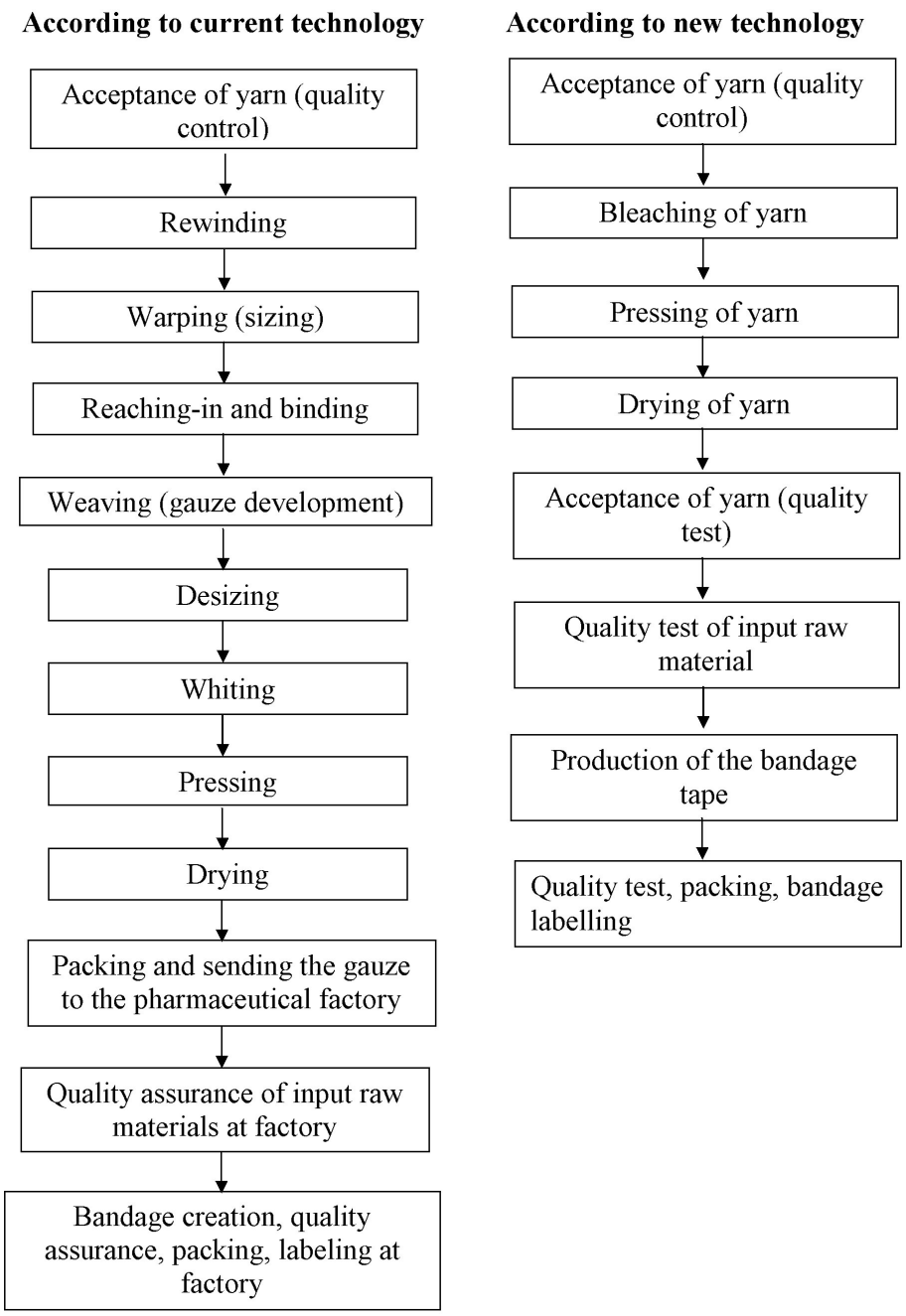

Figure 1. The technological chain of the development of the medical cotton gauze bandage and the bandage of new type

The new technology of development of the woven unsterile medical cotton bandage consists of the following basic stages: whiting of a raw yarn, pressing and drying of the bleached yarn, development of the tape of the bandage on the machine tool, getting of the finished goods (fig 1.).

To obtain the new sample of bandage the raw yarn is bleached. The basic and raw weft yarn with linear density of 20 tex, reeled up on the punched cones, is delivered from textile factory.

Acceptance of a grege yarn is carried out according to national standard (OST) –17–198 considering appearance and physical-mechanical properties [1]. A class of yarn appearance is defined according to GOST 15818, which is characterized by presence of small knots, unevenness on short pieces, and presence of trash [2].

The necessary technological documents have been developed by us and confirmed by the corresponding organizations.

The described woven unsterile medical cotton bandage in conformity with TSh-Uz-14847912–0001–01 [3] and to Industrial Regulations Pr-92 Uz-03873–14847912–178–04 [4], registered by Uzstandard [5], having License #000037 [6] and the Registration certificate # Uz TT 006/656/11 of the Ministry of Health of Uzbekistan [7] are developed on the reduced technological chain in comparison with the traditional one.

Preparation of the yarn for bleaching is carried out in the bleaching shop where reels with a gege yarn is loomed up in special drums, which are then loaded into the bleaching unit — autoclave. The yarn is bleached according to the formula confirmed by Industrial Regulations.

Engineering Process and the Bleaching Recipe of Yarn.

Table 1.

Bleaching (liquor ratio 1: 13)		
1	penetrating agent	1 g/l
2	stabilizer	2,6 g/l
3	antifoamer	0,1 g/l
4	caustic soda	2,4 g/l
5	peroxide	8 g/l pH –10 –11,5
flushing		
1	hot	60´ (80° C)
2	cold	20’
3	cold	20´ (pH-7)

To bleach the yarn chemical components are loaded into an autoclave, the process is conducted for 3–6 hours at a temperature of up to 100° C. The bleached yarn is wrung out in a centrifuge and sent into the drying chamber where at a temperature of up to 110° C the drying process is conducted. According to the technology of obtaining any medical drugs, first the input raw material is checked; only then the final product is made from it. Laboratory researches of the bleached yarn were conducted on physical and chemical properties as entrance raw materials in accordance with STP Uz-14847912–001–00 [8] and must correspond to requirements. If the results of tests are unsatisfactory even by one indicator, the bleached yarn is not accepted for manufacturing bandage.

Thus, the control of entrance raw materials before obtaining the new sample of the bandage is conducted, which is important from the point of view of economy of time, raw materials and all basic auxiliary means. After the drying process the bleached yarn moves to Fittex machine tools where the bandage tape is produced. The general principle of the formation of a cloth is kept on these machine tools. The basis is formed by a knitted structure through making a weft with tubular needles.

It is possible to develop 12; 8; 6; 4 cloths of a bandage — tape on the machine tool in parallel, with the width provided by standard documents 14cm; 10cm; 7cm; 5cm., accordingly.

According to the new way of manufacturing of woven unsterile medical cotton bandage, the technological process is reduced to 5 transitions in comparison to the existing one. At the achievement of the set diameter of the bandage-tape roll on the machine tool, removal is carried out. Bandage- tape rolls are cut on tape-cutting devices at length of 5 metres. In accordance with the technology packing is provided on the SWIFT equipment and the bandage of the new type is wrapped in propylene paper, the edges being welded. Packing is thought to be distinct. The woven bandage is packed in the container, according to TshUz –14847912–001–00. The obtained woven unsterile medical bandage surpasses gauze bandage on all indicators [9]. For the purpose of preventing of possible adverse influence on the health of the person, medical products are subject to obligatory hygienic tests. In this respect sanitary-chemical, toxicological, physical and chemical researches of the bandage of the new sample were carried out in the Research Institute of Sanitary, Hygiene and Occupational Diseases (NIICGPz) with the aim of receiving the Hygienic Certificate [10].

Results of toxicological and hygienic tests have shown, that they do not possess skin-irritating, skin-resorptive and general toxic effects, and do not have sensitizing properties either [11]. Like all medications and medical equipment, the new type of bandage has passed clinical tests in three basic medical institutions, namely, in the Research Centre of Surgery named after academician V. V. Vahidova, in the Second Tashkent State Medical Institute, and in the Research Institute of Traumatology and Orthopedics. Natural researches of the new type of bandage have been carried out on volunteers for the purpose of revealing the presence or absence of side-effects during the use of bandage. Bandages of the new type were used for imposing on limbs for 10–12 hours over 10 days. Objective and subjective sensations of patients were also considered. Bandages were used on 17 patients during operation as a dressing and on 15 patients in the form of a pressure dressing and fixing bandage after angiographic study.

The results of the survey of volunteers have shown that the bandage does not cause irritation, itching, peeling of a skin [12] and it is also convenient for imposing dressings due to its elasticity and durability. It also fixes perfectly the sterile dressing on limbs [13]. After sterilization in an autoclave, it keeps the whiteness, hygroscopicity, capillarity, and can be used as a dressing material during the operation and after it [14].

The woven unsterile medical cotton bandage obtained in a new way, in comparison to the traditional bandage prepared from gauze, does not get garneted, which makes them more practical for imposing of fixing pressing dressings, for the preparation of a dressing material for operation. The carried out researches have allowed us to draw a conclusion, that the bandage of the new type correspond to the developed specifications on hygroscopicity, elasticity, durability, capillarity, and keeps the properties after sterilization.

On the basis of an experimental research the new technology of the production of the woven unsterile medical cotton bandage reduced to 5 transitions has been developed. All necessary technological requirements of the new sample of the bandage are prepared and confirmed in due time. On the basis of toxicological, hygienic and operational properties of the new product line, after approbations of the unsterile medical cotton bandage in the clinical medical conditions conducted in due time, the new type of medical bandage is created according to the new method of production, and it meets the requirements on all accounts.

References:

1. OST-17-198 2.
2. GOST 15818.
3. Bekmuratova Z. T. Tsh Uz 1447912–001–2001 "The Woven Medical Unsterile Bandage" – 2001, – UDN 615.468.2:006.354 group F 12, joint-stock company "Катекс".
4. Industrial Regulations PR 42 Uz. 03873–14807912–178–04, – 2001, joint-stock company "Катекс".
5. State standards and guideline Republic of Uzb. The informational index quarter I, – 2003.
6. The licence, series FF – No 000037, – Tashkent, – 1999. – 8.06.
7. The Registration certificate – No Uz TT 006/656/11 Ministry of Health, Republic of Uzb.
8. STP Uz-14847912–001–00 for the Bleached yarn.
9. Bekmuratova Z. T. "On the Issue of Working out the Specifications on Manufacturing of the Woven Bandages ", the Bulletin, Karakalpak Branch, AS Uzb. – 2005. – No 3, – P. 49–50.
10. Ministry of Health of Uzb. Scientific Research Institute of Sanitary, Hygiene and Occupational Diseases: the Hygienic certificate – No 017, 5.12 is accredited by Uzbek State Standard NSS.UZ.07.NSO.111. – 2000.
11. Ministry of Health of Uzb. Research Institute of Sanitary, Hygiene and Occupational Diseases. The certificate for hygienic examination of the bandages. from 11.10. – 2000. Tashkent.
12. Research Center of Surgery named after aacademician V. V. Vahidov Ministry of Health of Uzb. The certificate on carrying out of clinical tests of samples. from – 17.10. – 2000. – Tashkent.
13. Research Institute of Traumatology and Orthopedics, Ministry of Health of Uzb. The certificate on clinical tests of the products of medical use. from – 13.10. – 2000. – Tashkent.
14. The Second Tashkent State Medical Institute, Ministry of Health of Uzb. The certificate on clinical tests of products of medical use. from – 3.10. – 2000, – Tashkent.

DOI: http://dx.doi.org/10.20534/AJT-16-11.12-36-44

Adurasul Mamataliev,
Senior staff scientist applicant, "Phosphate fertilizer" laboratory
Institute of General and Inorganic Chemistry
of the Academy of Sciences of the Republic of Uzbekistan

Shafoat Namazov,
Doctor of science, professor, chief of "Phosphate fertilizer" laboratory,
Institute of General and Inorganic Chemistry of the Academy
of Sciences of the Republic of Uzbekistan
E-mail: igic@mail.ru

Atanazar Seytnazarov,
Doctor of Science, chief scientist, "Phosphate fertilizer" laboratory
Institute of General and Inorganic Chemistry
of the Academy of Sciences of the Republic of Uzbekistan
E-mail: igic@mail.ru

Beglov Boris,
Doctor of Science, academician, "Phosphate fertilizer" laboratory
Institute of General and Inorganic Chemistry
of the Academy of Sciences of the Republic of Uzbekistan
E-mail: igic@mail.ru

Alimov Umarbek,
PhD in technique, senior scientist "Phosphate fertilizer" laboratory,
Institute of General and Inorganic Chemistry
of the Academy of Sciences of the Republic of Uzbekistan
E-mail: umaralihonalimov@mail.ru

Ammonium Nitrate Melt, Ammonium sulphate and phosphogypsum based nitrogen-sulphur containing fertilizers and their commodity

Abstract: In this article the samples of nitrogen-sulphur containing fertilizers in which the molar ratio of ammonium sulphate to ammonium nitrate varied from 1:1 to 1:8, have been prepared. The phosphogypsum, waste production of JSC "Ammophos-Maxam", as additive was used in amount of 5; 10 and 15% of the total weight of ammonium nitrate-sulphate. The composition, density, viscosity, strength and dissolution rate of granules, hygroscopic point of water vapor sorption kinetics and sorption moisture capacity to them was determined. The introduction of 62.3% of ammonium sulfate and 15% of phosphogypsum into the melt of ammonium nitrate increases the strength of the product granules from 1.32 to 7.86 MPa.

Keywords: ammonium nitrate, melt, ammonium sulfate, phosphogypsum, nitrogen-sulphur containing fertilizer composition, and properties.

Introduction

Ammonium nitrate is a concentrated, efficient and the most common in the world as a nitrogen fertilizer [1]. In Uzbekistan, three major JSC "Maxam-Chirchik", "Navoiazot" and "Ferghanaazot" produce ammonium nitrate in the amount of more than 1 million 750 thousand tons per year.

However, ammonium nitrate has some drawbacks. Firstly, it is caking during the storage. Secondly, it is its explosion hazard. The third drawback is determined by its composition. The ammonium nitrate is half the nitrogen in the ammonium form and the other half is in the nitrate form. Nitrate nitrogen in the soil is not fixed and washed out of ammonium nitrate in terms of the normal moisture and irrigation. Therefore, ammonium nitrate is not used for fertilizing of winter crops during sowing spring and autumn is as the main fertilizer. These

drawbacks can be eliminated, if on the basis of ammonium nitrate to produce ammonium nitrate sulfate. Ammonium form of nitrogen is being in the ammonium nitrate and ammonium sulfate is in a well available to plants that is relatively a little mobile and is washed out of the soil [2]. The advantage of ammonium sulfate — nitrate to ammonium nitrate is also the presence of sulfur in it, which is a part of proteins and amino acids in the formation of the crop. According to the physiological role of sulfur in plant nutrition should be put on the third place after the nitrogen and phosphorus [2].

For the first time mechanical mixture, and ammonium nitrate melt with ammonium sulphate were made in Germany [3]. The higher the content of ammonium sulfate in ammonium nitrate, the less is hygroscopicity, caking and explosiveness. About decrease of ammonium nitrate explosibility in the presence of ammonium sulfate is in [4–6]. In [4], it was investigated that the influences of chlorine, sulfate and nitrite ions on ammonium nitrate decomposition in a strongly acidic aqueous solution at its boiling temperature. It has been found that sulphate ions do not revealed catalytic activity in the decomposition of NH_4NO_3 as opposed to chlorine ions, which allow the rapid expansion of NH_4NO_3 to N_2O and H_2O.

In [5] the ammonium nitrate was modified by chemical fertilizers, such as $(NH_4)_2HPO_4$, $NH_4H_2PO_4$, $(NH_4)_2SO_4$, and K_2SO_4 NH_4Cl, and then it was mixed with fuel oil and sawdust to produce explosives. It is found that the detonation of explosives is not started in the presence of 25% $(NH_4)_2SO_4$ in a modified NH_4NO_3.

In [6], the non explosive composite material is patented, comprising ammonium sulfate nitrate. As product has the following composition: 14–35% of ammonium sulfate $(NH_4)_2SO_4$; 60–85% of a double salt $(NH_4)_2SO_4 \cdot 2NH_4NO_3$; combination of the double salt $(NH_4)_2SO_4 \cdot 3NH_4NO_3$ and ammonium nitrate is up to 5%. This material is used as a fertilizer, which has the necessary level of nitrate ions. It has an excellent stability against detonation, higher density, and humidity resistance.

Let no one be confused by the above-mentioned double salts. These salts were discovered in the study of solubility in the system of $(NH_4)_2SO_4 – NH_4NO_3 – H_2O$ wide temperature from –20 to + 100 °C and the concentration range [7–13] and in the melting system of $NH_4NO_3 – (NH_4)_2SO_4$ [14].

In agriculture, it is widely used that product containing 65–67% of sulphate and 33–35% of ammonium nitrate (this molar ratio of $(NH_4)_2SO_4$: NH_4NO_3 is slightly greater than unity), obtained by simple mixing of these salts. Before entering the salts are screened of large caked pieces subjecting to crushing in the mixer, and then ammonium sulfate heat to 120 °C, and ammonium nitrate to 40–60 °C [3].

The most advanced approach for preparing ammonium sulphate nitrate is a dry mixture of ammonium sulfate with 83% solution of ammonium nitrate. Mixing is carried out in screw machines, from which the mass with approximately 6% of moisture content. This mass is crushed between two cast-iron rollers with spikes, dried to 0.1–0.2% of moisture content in a tumble dryer and dissipated.

The fraction with the larger size pieces more than 4 mm is crashed and returned to the screen, and the fraction of particles less than 0.8 mm are returned to the mixer.

It can be obtained the ammonium sulfate nitrate by neutralization of a mixture of sulfuric and nitric acids. The carbonator reactor equipped with a stirrer, is simultaneously fed a 50% nitric acid, 68% sulfuric acid and ammonia. Because the exothermicity and neutralization reaction a temperature in the saturator reaches 145–150 °C and heat is enough to vaporize the water introduced with acids. The gases (ammonia) from the saturator and water vapor flow into the distillation column from where the ammonia is returned to the saturator. Continuously melting that flows from the reactor contains 2.5–3% free acid. Excess melt acidity decreased to 0.1–0.3% by introducing ammonia into neutralizer-down. The melt containing 97–98% dry salt and 2–3% moisture from neutralizer-down is directed to crystallization, which is carried on the surface of the cooling drum. [3]. The neutralized mixture of nitric and sulfuric acids also can be dried and granulated in the apparatus equipped fluidized bed [15].

Melt containing 80% of ammonium nitrate and 20% of ammonium sulfate can be granulated and in the granulation towers [16–18].

Currently, the Russian has developed the production of complex fertilizers, nitrogen sulphate NS 32: 5 (ammonium nitrate with the addition of 21% ammonium sulfate). This corresponds to a mole ratio of $(NH_4)_2SO_4$: $NH_4NO_3 = 1: 6$) [19]. The novel sulfur-containing nitrogen fertilizer does not rebate, and in some cases exceed standard forms of nitrogen fertilizer on the effect on the yield and quality of grain of spring wheat.

Nitrogen of the fertilizers are better absorbed by this plant, its application rate is more than by 21%, and nitrogen washing out from the soil is less than with ammonium nitrate [20, 21]. In [19] it was shown that the introduction of sulfate anions in the form of ammonium sulfate in the ammonium nitrate melt leads to reduction initial rate of thermal decomposition of ammonium nitrate and

no increase of the decomposition rate during the process in comparison with the kinetic laws decomposition of pure ammonium nitrate.

As effect observed is associated with a reduction in the concentration of molecular nitric acid in the melt due to its ionization with sulfate anion. Under the same environmental conditions explosion safety of high-temperature processing of complex fertilizers based on ammonium nitrate and ammonium sulphate mixtures are higher than for ammonium nitrate, produced as a fertilizer.

We have been also conducted studies to obtain ammonium nitrate melt based nitrogen-sulphur fertilizers with the additive in it two perspective additives, ammonium sulfate and phosphogypsum, composition, physico-chemical and product properties are summarized in this study.

Materials and Methods

As crystalline ammonium sulfate previously milled in a porcelain mortar until the particle size of 0.063 mm. Phosphogypsum is from JSC "Ammophos-Maxam" that is in the form of calcium sulfate as dihydrate ($CaSO_4 \cdot 2H_2O$) with a moisture content of 18–20%. Therefore, before adding it to ammonium nitrate, the latter is dried in an oven at 90 °C, and then it is milled in a porcelain mortar. Composition of the dry phosphogypsum (wt.%.): P_2O_{5total}. 1.59; P_2O_{5accep}. 1.48; $P_2O_{0wat.sol}$. 1.12; CaO_{total}. 37.47; CaO_{accep}. 19.08; $CaO_{wat.sol}$. 11.26; SO_{3total}. 54.49; $SO_{3accep.}$. 27.4; $SO_{3wat.sol}$. 16.88.

Experiments were carried out as follows. AN sample is melted in a metal cup by electric heating. Ammonium sulfate was added to the nitrate in an amount such that the ratio of the starting components $(NH_4)_2SO_4$: NH_4NO_3 mixture is ranged from 14.5: 78.8 to 59.2%: 32.0%.

Phosphogypsum additive is taken in amount of 5; 10 and 15% of the total weight of the mixture. The mixture was thoroughly stirred. The melts were kept at 190 °C for 15 minutes. The melt is poured into the granulator, representing the thimble with a perforated bottom, the diameter of the hole was at 1.2 mm. With pump the top of the thimble are pressurized and the melt was sprayed on the tenth floor of a building on the plastic film, lying on the ground. The fertilizer granules obtained were analyzed according to known techniques [22]. Pellet strength measurement was performed on the devise MIP-10–1 [23]. It should be note that when mixing the melt of ammonium nitrate and ammonium sulphate with phosphogypsum according to the ratio of NH_4NO_3: $CaSO_4 \cdot 2H_2O$ in varying degrees double decomposition reaction occurs:

$$2NH_4NO_3 + CaSO_4 \cdot 2H_2O \leftrightarrow Ca(NO_3)_2 + (NH_4)_2SO_4 + 2H_2O$$

Therefore, we tested how the conversion is in the ammonium nitrate melt. Determining the degree of conversion of NH_4NO_3 was performed as described in [24].

There was studied the dissolution rate of the granules 2 mm. To this pellet was sunk into the glass with 100 ml of distilled water and observing visually, fixed time of its complete dissolution. The temperature was room was, and the test was five-time.

The nitrogen-sulphate fertilizers melt density determined by pycnometric method, and viscosity — viscometer using WPJ-2. For this purpose samples of nitrate with the addition of ammonium sulfate and phosphogypsum melted, mixed thoroughly, cooled to room temperature and milled. The resulting powders were injected into the pycnometer, and the viscometer, which is then placed in a thermostat filled with glycerol.

Thermostat temperature was raised to a predetermined value. The powder in the pycnometer and viscometer melted. If the melt level is not reached in the pycnometer mark powder added to it. And if the melt exceed the mark, the excess melt cleaned by cotton placed on the end of the wire. Temperature was controlled with a contact thermometer.

The melt is kept at a predetermined temperature for 5–7 minutes, and then the measurements were made.

Point hygroscopic of fertilizer granules with size 2–3 mm at 25 °C is determined by exsiccator method [25]. Sorption moisture content of fertilizers also determined exsiccator method [25] with a relative humidity of 48.5; 62.5; 69.5; 80; 90 and 100%. For these samples of fertilizer is above the acid kept for 31 days. The results are shown in Table. 1, 2, and 3 and Fig. 1–3.

Results and its discussion

As it is seen from Table 1 that with increasing amounts of ammonium sulfate injected into melt of ammonium nitrate, from 14.5 to 59.2% decreased the total nitrogen content in the product from 27.58% to 24.89%, while the sulfur content is increased in the product from 6.63% to 15.27%. With increasing amount of additive phosphogypsum from 5 to 15%, the sulfur content is also increased from 4.89 to 6.63% at a ratio of $(NH_4)_2SO_4$: NH_4NO_3 = 1: 8, and from 15.27 to 15.96% when $(NH_4)_2SO_4$: NH_4NO_3 = 1:1. With increasing fraction as ammonium sulfate and phosphogypsum in ammonium nitrate melt increased strength of the resulting fertilizer granules. Thus, the strength of the granules of ammonium nitrate (mark "pure") is 1.32 MPa (0.67 kg/granule). Most maximum strength of granules of ammonium sulfate nitrate reached 7.86 MPa at a ratio of $(NH_4)_2SO_4$: NH_4NO_3 = 1:1 with 15% of phospho-

Table 1. – Composition and commodity properties nitrogen-sulphur containing fertilizers

Ratio of initial components	Content in the products, weight,%							Conversion degree of NH_4NO_3, %	Strength of granule, MPa	Complete dissolution time of granule, sec.
	NH_4NO_3	$(NH_4)_2SO_4$	Phosphogypsum ($CaSO_4 \cdot 2H_2O$)	N_{total}	$N_{amm.}$	$N_{nit..}$	S			
Гранулированный NH_4NO_3 марки «ч»	100	–	–	35	17.50	17.50	–	–	1.32	44.6
$(NH_4)_2SO_4 \cdot 8NH_4NO_3$	78.8	16.2	5	29.86	16.12	13.74	4.89	3.58	6.46	76.34
$(NH_4)_2SO_4 \cdot 8NH_4NO_3$	74.6	15.4	10	29.14	16.09	13.05	5.77	5.22	6.52	77.72
$(NH_4)_2SO_4 \cdot 8NH_4NO_3$	70.5	14.5	15	27.58	15.26	12.32	6.63	6.87	6.60	79.20
$(NH_4)_2SO_4 \cdot 7NH_4NO_3$	76.9	18.1	5	30.64	17.21	13.43	5.38	6.35	6.68	82.48
$(NH_4)_2SO_4 \cdot 7NH_4NO_3$	72.8	17.2	10	29.02	16.31	12.71	6.22	8.44	6.72	84.04
$(NH_4)_2SO_4 \cdot 7NH_4NO_3$	68.8	16.2	15	27.37	15.35	12.02	7.10	10.08	6.74	85.90
$(NH_4)_2SO_4 \cdot 6NH_4NO_3$	74.5	20.5	5	30.23	17.27	12.96	5.96	9.12	6.82	88.62
$(NH_4)_2SO_4 \cdot 6NH_4NO_3$	70.6	19.4	10	28.66	16.35	12.31	6.78	11.55	6.88	90.14
$(NH_4)_2SO_4 \cdot 6NH_4NO_3$	66.6	18.4	15	27.08	15.44	11.64	7.59	13.20	6.90	91.76
$(NH_4)_2SO_4 \cdot 5NH_4NO_3$	71.4	23.6	5	29.82	17.34	12.48	6.68	12.89	6.98	94.52
$(NH_4)_2SO_4 \cdot 5NH_4NO_3$	67.7	22.3	10	28.24	16.41	11.83	7.46	14.71	7.03	96.08
$(NH_4)_2SO_4 \cdot 5NH_4NO_3$	63.9	21.1	15	26.74	15.58	11.16	8.25	16.38	7.06	97.54
$(NH_4)_2SO_4 \cdot 4NH_4NO_3$	67.3	27.7	5	29.29	17.54	11.75	7.69	16.26	7.13	100.20
$(NH_4)_2SO_4 \cdot 4NH_4NO_3$	63.7	26.3	10	27.76	16.63	11.13	8.44	17.82	7.19	101.98
$(NH_4)_2SO_4 \cdot 4NH_4NO_3$	60.2	24.8	15	26.18	15.67	10.51	9.17	19.61	7.21	103.82
$(NH_4)_2SO_4 \cdot 3NH_4NO_3$	61.3	33.7	5	28.45	17.75	10.70	9.16	19.43	7.29	107.20
$(NH_4)_2SO_4 \cdot 3NH_4NO_3$	58.1	31.9	10	26.91	16.77	10.14	9.79	21.02	7.33	108.56
$(NH_4)_2SO_4 \cdot 3NH_4NO_3$	54.8	30.2	15	25.47	15.89	9.58	10.45	22.67	7.37	110.34
$(NH_4)_2SO_4 \cdot 2NH_4NO_3$	52.1	42.9	5	27.14	18.05	9.09	11.38	22.20	7.45	113.54
$(NH_4)_2SO_4 \cdot 2NH_4NO_3$	49.3	40.7	10	25.72	17.11	8.61	11.89	24.14	7.51	114.82
$(NH_4)_2SO_4 \cdot 2NH_4NO_3$	46.6	38.4	15	24.28	16.14	8.14	12.46	25.87	7.59	116.24
$(NH_4)_2SO_4 \cdot NH_4NO_3$	35.8	59.2	5	24.89	18.64	6.25	15.27	25.76	7.69	119.42
$(NH_4)_2SO_4 \cdot NH_4NO_3$	33.9	56.1	10	23.56	17.65	5.91	15.59	27.38	7.77	121.08
$(NH_4)_2SO_4 \cdot NH_4NO_3$	32.0	53.0	15	22.25	16.67	5.58	15.96	29.03	7.86	124.34

gypsum. In this case, the product contains 22.25% of N and 15.96% of S.

The same parameters at a ratio of $(NH_4)_2SO_4$: NH_4NO_3 = 1: 8 with the addition of 5% phosphogypsum equal to 6.46 MPa, 29.86% and 4.89%, respectively. When the same ratio of $(NH_4)_2SO_4$: NH_4NO_3, but with the addition of 15% of phosphogypsum contains by 27.58% of N and 6.63% of S, granule strength is 6.60 MPa.

High strength fertilizer granules of the nitrogen-sulphate indicate its thermal stability.

The introduction of ammonium sulfate phosphogypsum into the melt of ammonium nitrate increases the degree of conversion of ammonium nitrate to calcium nitrate.

Thus, if the ratio of $(NH_4)_2SO_4$: NH_4NO_3 = 1: 8 with a 5% of phosphogypsum addition conversion degree of ammonium nitrate is 3.58% at the 15% of phosphogypsum addition, this indicator rises to 6.87%. When the ratio of $(NH_4)_2SO_4$: NH_4NO_3 = 1: 1 ammonium nitrate conversion degree increases from 25.76 to 29.03%.

The time of complete dissolution of granules of pure ammonium nitrate is 44.6 seconds. With the increase of the share as ammonium sulfate and phosphogypsum in the mixture with ammonium nitrate, time completely dissolution of nitrogen-sulphur fertilizers granules has been growing steadily and reach its maximum 124.34 seconds for sample with the ratio of the starting components $(NH_4)_2SO_4$: NH_4NO_3 = 53%: 32% to 15% addition of phosphogypsum. This suggests that the resulting fertilizer will slowly washing out of the soil than pure ammonium nitrate.

Table 2. – Rheological properties of nitrogen-sulphur containing fertilizers melt

Ratio of initial substances components	Phosphogypsum content in the mixture, %	Density, (g/cm³) at temperature, °C				Viscosity, (cps) at temperature, °C			
		175	180	185	190	175	180	185	190
$(NH_4)_2SO_4 \cdot 8NH_4NO_3$	5	1.589	1.578	1.565	1.557	8.14	7.68	7.22	6.76
$(NH_4)_2SO_4 \cdot 8NH_4NO_3$	10	1.621	1.612	1.598	1.589	8.98	8.47	7.98	7.49
$(NH_4)_2SO_4 \cdot 8NH_4NO_3$	15	1.654	1.643	1.629	1.620	9.82	9.29	8.76	8.22
$(NH_4)_2SO_4 \cdot 7NH_4NO_3$	5	1.685	1.675	1.661	1.653	10.65	10.11	9.53	8.95
$(NH_4)_2SO_4 \cdot 7NH_4NO_3$	10	1.716	1.706	1.693	1.681	11.49	10.86	10.31	9.68
$(NH_4)_2SO_4 \cdot 7NH_4NO_3$	15	1.749	1.739	1.724	1.714	12.33	11.72	11.07	10.41
$(NH_4)_2SO_4 \cdot 6NH_4NO_3$	5	1.782	1.771	1.757	1.746	13.17	12.45	11.84	11.14
$(NH_4)_2SO_4 \cdot 6NH_4NO_3$	10	1.817	1.803	1.790	1.779	14.01	13.31	12.62	11.87
$(NH_4)_2SO_4 \cdot 6NH_4NO_3$	15	1.848	1.836	1.822	1.805	14.84	14.07	13.38	12.63
$(NH_4)_2SO_4 \cdot 5NH_4NO_3$	5	1.873	1.867	1.856	1.838	15.69	14.88	14.15	13.35
$(NH_4)_2SO_4 \cdot 5NH_4NO_3$	10	1.906	1.899	1.885	1.870	16.52	15.60	14.93	14.06
$(NH_4)_2SO_4 \cdot 5NH_4NO_3$	15	1.940	1.931	1.918	1.899	17.36	16.49	15.69	14.82
$(NH_4)_2SO_4 \cdot 4NH_4NO_3$	5	1.974	1.964	1.953	1.931	18.20	17.32	16.46	15.54
$(NH_4)_2SO_4 \cdot 4NH_4NO_3$	10	2.012	1.997	1.984	1.962	19.05	18.11	17.24	16.27
$(NH_4)_2SO_4 \cdot 4NH_4NO_3$	15	2.037	2.025	2.016	1.993	19.87	18.87	18.01	16.99
$(NH_4)_2SO_4 \cdot 3NH_4NO_3$	5	2.069	2.058	2.045	2.024	20.71	19.68	18.78	17.73
$(NH_4)_2SO_4 \cdot 3NH_4NO_3$	10	2.103	2.091	2.079	2.055	21.55	20.46	19.55	18.45
$(NH_4)_2SO_4 \cdot 3NH_4NO_3$	15	2.131	2.123	2.112	2.086	22.39	21.25	20.32	19.21
$(NH_4)_2SO_4 \cdot 2NH_4NO_3$	5	2.166	2.155	2.147	2.117	23.22	22.09	21.09	20.96
$(NH_4)_2SO_4 \cdot 2NH_4NO_3$	10	2.198	2.188	2.170	2.148	24.06	22.86	21.87	21.68
$(NH_4)_2SO_4 \cdot 2NH_4NO_3$	15	2.225	2.219	2.206	2.179	24.90	23.64	22.63	22.42
$(NH_4)_2SO_4 \cdot NH_4NO_3$	5	2.260	2.252	2.238	2.210	25.73	24.47	23.46	23.04
$(NH_4)_2SO_4 \cdot NH_4NO_3$	10	2.292	2.284	2.271	2.243	26.57	25.28	24.12	23.27
$(NH_4)_2SO_4 \cdot NH_4NO_3$	15	2.326	2.309	2.292	2.275	27.41	26.17	24.86	23.54

Further studies determined the rheological properties of fertilizers melts derived. The results are summarized in Table 2 above.

As seen from the above materials, the density and viscosity of the ammonium nitrate melt significantly decreased with increasing amount of additives. Pure am-

monium nitrate is melted at 170 °C melts and naturally flows. However, addition of phosphogypsum and ammonium sulphate leads to increase of its melting point.

The mixture of ammonium nitrate with a molar ratio of ammonium sulfate and phosphogypsum at molar ratio sulphate to nitrate varying from 1: 1 to 1: 8 begins to melt at 175 °C and while the melt has a high viscosity, but it is flowing easily. An increase in the mass fraction of ammonium sulphate with 14.5 to 59.2 of $(NH_4)_2SO_4$ and phosphogypsum addition and from 5 to 15% increases the density and viscosity of a nitrate-sulphate melt at 175 °C from 1.589 to 2.326 g/cm^3 and 8.14 to 27.41 cps, respectively.

With an increase the temperature of the melt viscosity and density is decreased.

Fluid state of the melts of two-component fertilizer with the addition of ammonium sulfate and phosphogypsum in ammonium nitrate gives possibility to granulate them in the granulation tower.

There are given below the results of determination of hygroscopic point, kinetics of water vapor sorption and sorption moisture capacity of nitrogen-sulphur fertilizer granules (Table 3).

Table 3. – Hygroscopic point and moisture of the nitrogen-sulphur containing fertilizers

No samples	Ratio initial components	Content in the products, weight.%			Hygroscopic point, %	Moisture, %
		NH_4NO_3	$(NH_4)_2SO_4$	Phosphogypsum ($CaSO_4 \cdot 2H2O$)		
1	$(NH_4)_2SO_4 \cdot 8NH_4NO_3$	78.8	16.2	5	47.8	0.60
2	$(NH_4)_2SO_4 \cdot 8NH_4NO_3$	74.6	15.4	10	47.5	0.63
3	$(NH_4)_2SO_4 \cdot 8NH_4NO_3$	70.5	14.5	15	47.3	0.65
4	$(NH_4)_2SO_4 \cdot NH_4NO_3$	35.8	59.2	5	52.7	0.42
5	$(NH_4)_2SO_4 \cdot NH_4NO_3$	33.9	56.1	10	52.4	0.44
6	$(NH_4)_2SO_4 \cdot NH_4NO_3$	32.0	53.0	15	52.1	0.46
7	NH_4NO_3 mark «ch»	100	–	–	62.0	0.20

Table 3 presents data of initial moisture content of the first sample is 0.60%, the second 0.63%, the third — 0.65%, the fourth — 0.42%, the fifth — 0.44%, the sixth — 0.46%, the seventh — 0.20% (AN mark "pure"). Values of the hygroscopic points for the tested fertilizers are the following: for the first sample — 47.8%, for the second — 47.5%, for the third — 47.3%, for the fourth — 52.7%, for the fifth — 52.4%, for the sixth — 52.1% and for the seventh sample (AN) — 62.0%. Relative humidity in Uzbekistan is characterized by the following figures: the average monthly minimum — 46%, the average maximum — 74%, average — 60%. According to a scale hygroscopic of N. E. Pestova, all samples of ammonium sulfate-nitrate are highly hygroscopic, i. e. they are more hygroscopic than the original ammonium nitrate. The reason for the low value hygroscopic points of products is due to the fact that the salt mixture is more hygroscopic than its component parts [26].

Fig. 1 and 2 show that the kinetic curves of water vapor sorption by granules of fertilizers under isothermal conditions at 25 °C and a relative humidity are 48.5; 62.5; 69.5; 80; 90 and 100%.

As can be seen from Fig. 1 and 2, with relative humidity of 80; 90 and 100% for all samples equilibrium is achieved within the test period. When humidity 69.5% pure AC (sample 7) and for samples 1, 2 and 3 is also not established an equilibrium during the test period. For the fourth, fifth and sixth samples the equilibrium occurs only after 29–31 days. When the relative humidity of 62.5% is for samples 1–6 equilibrium occurs within 10–12 days, and for the seventh sample (pure AN) in 4 hours. At a humidity of 48.5% for samples 1–6 equilibrium is reached within 4–5 days. In this sample moisture sample –7 is not moistened, but it is dried.

Sorption moisture content is the most important indicator of the quality of fertilizers, for such it indicates the maximum amount of water absorbed, in which fertilizers retain their appearance and friability. Fig. 3 presents the curves of sorption moisture capacity for fertilizer samples as 1; 4; 6 and 7. The curves for samples 2, 3 and 5 are not shown in the figure, for such they are very close to curves for samples 1, 4 and 6. From this figure can be seen that the pure AN (sample 7) at 48.5% moisture air naturally does not absorb moisture, and the first, fourth and sixth samples adsorb 3.08; 2.91 and 2.76% of moisture, respectively. However, the granules retain their original appearance and friability. At a relative humidity of 62.5% in the first sample moisture content reaches 6.87% in the fourth — 6.75%, in the sixth — 6.58% in the seventh (pure AN) — 1.80%. The granules thus maintain their appearance, but it is lumped a bit.

When the relative humidity of 69.5%, moisture increase in pure AN is 27.9%, in the first sample is 26.27%, in the fourth — 24.15% and in the sixth — 23.08%. At the same time, all samples are liquefied. It was found that the granules of pure AN when the moisture 3.5% strongly become compressed and lose their friability, and nitrogen-sulphur fertilizer samples retain the appearance and friability even when the moisture content of 5–6%. When the moisture equal to 7%, granules lose their ability to sowing only.

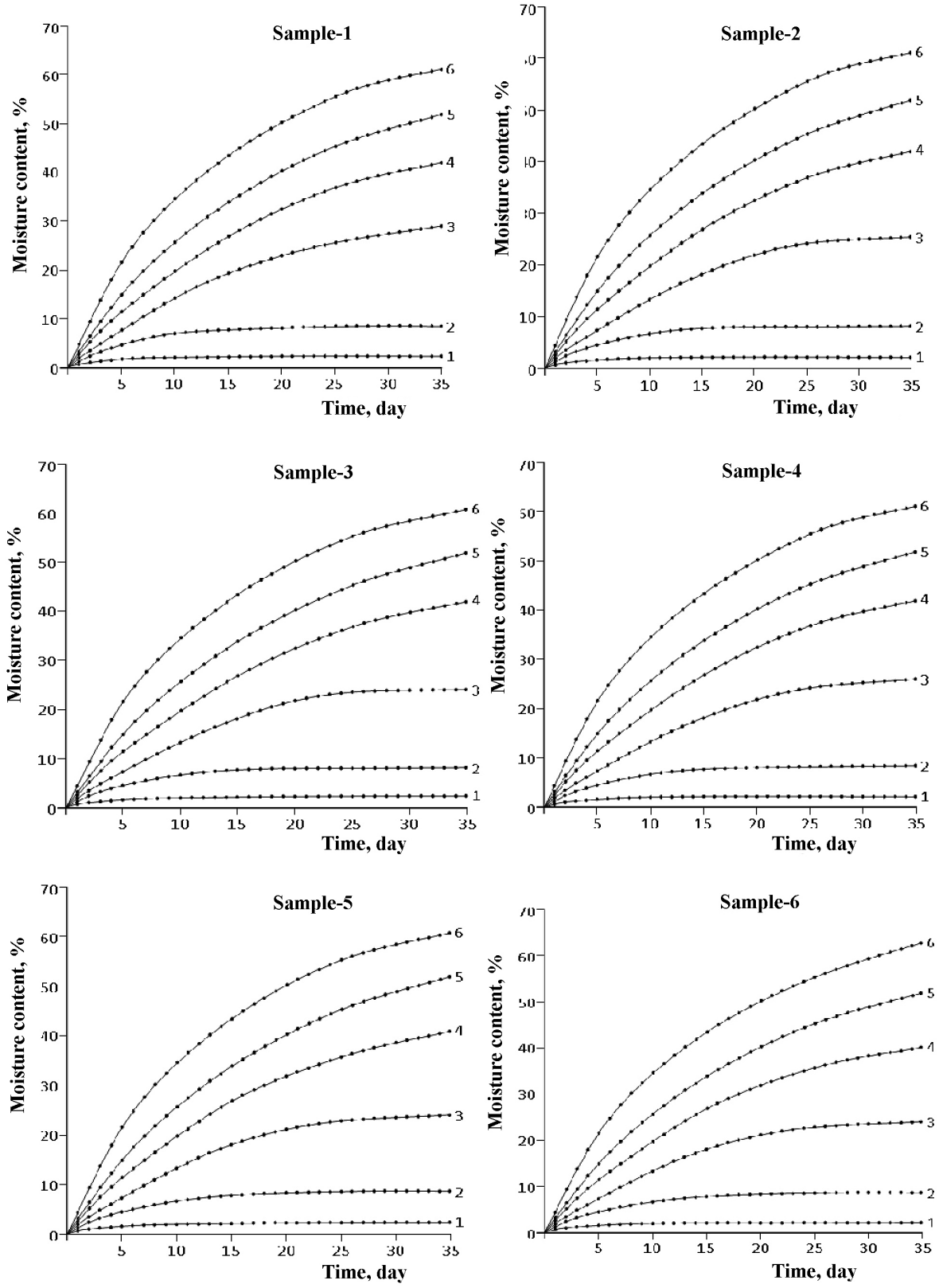

Figure 1. The kinetics of water vapor sorption by samples of nitrogen-sulphur fertilizer at a relative humidity: 1–48.5%; 2–62.5%; 3–69.5%; 4–80%; 5–90%; 6–100%

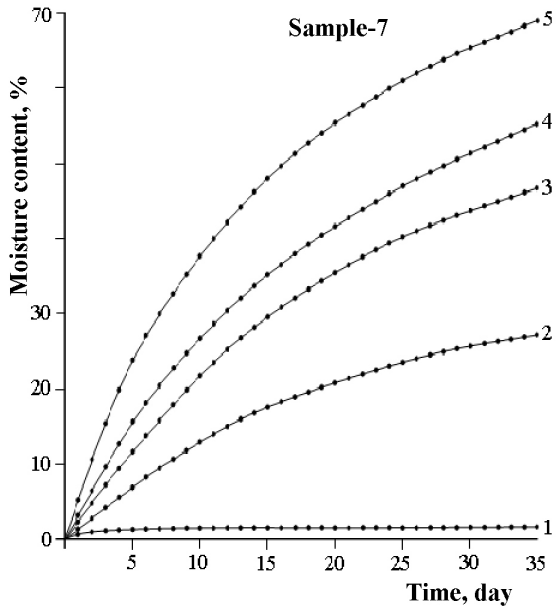

Figure. 2. The kinetics of water vapor sorption pure AN under relative moisture: 1 – 62.5%; 3 – 69.5%; 4 – 80%; 5 – 90%; 6 – 100%

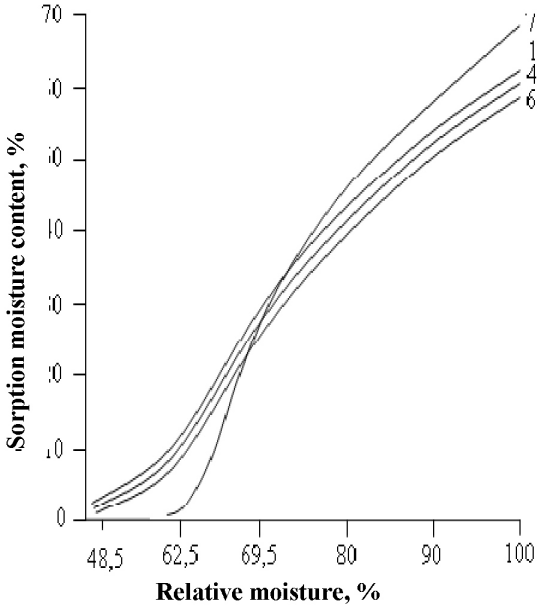

Figure 3. Dependence sorption moisture AN and nitrogen-sulphur fertilizers from the relative moisture

Conclusion

Thus, the results of the determination of physico-chemical properties show that novel kind of nitrogen-sulphur fertilizer produced based on ammonium nitrate melt, ammonium sulfate and phosphogypsum should be backed in paper or plastic bags.

References:

1. Ammonium nitrate. Properties, production, application/A. K. Chernyshev, B. V. Levin, A. V. Tugolukov, A. A. Ogarkov, V. A. Ilin. – M., – 2009, – 544 p.
2. Milaschenko N. C. Ammonium sulphate – available form of nitrogen fertilizer//Agrochemical bulletin. – 2004, – No 2, – P. 3.
3. Posin M. E. Mineral salts technology. Chapter II. – L: "Chemistry", – 1970, – 1558 p.
4. Biskupski A., Kolaczkowski A., Masal C., Schroeder J., Simonides J., Sorich B. Effect of supplements on the decomposition of ammonium nitrate. I. The effect of chloride ions, sulphate, nitrite//Pr. Nauk. Inst. technol. nieorg. i nawoz. miner. PWrocl. – 1981, – No 22, – P. 15–30.
5. Tang Shuang-Ling, Lü Chun-Xu, Zhou Xin-Li, Wang Yi-Lin, Liu Zu-Liang. Investigation of the modified ammonium nitrate II. Influence of inorganic chemical fertilizers//Chin. J. Appl. Chem. – 2004, – 21, – No 4, – P. 400–404.
6. US Patent 6,689,181. IPC C05 C 1/00. Sulfate of ammonium nitrate/Highsmith R. E., Kweeder J. A., Correale S. T. – Publ. – 10.02.2004 – RZhHim – 2004, no 19 (II).
7. Sokolov V. A. Equilibrium and complexing in the system of H_2O – NH_4NO_3 – $(NH_4)_2SO_4$//Proceedings of the USSR Academy of Sciences. Chemical Series – 1938, no 1, – P. 123–135.
8. Emons H. H., Kloth H. Investigation of system of ammonium sulfate – ammonium nitrate – water//Wiss Z. Techn. Hochschule Chem. Leuna – Merseburg – 1968. 10, – No 2–3, – P. 102–106.
9. Turlej Jan., Pieniazek Tadeusz. Dual salt of system of NH_4NO_3 – $(NH_4)_2SO_4$ – H_2O//Przem. Chem. – 1981, – 60, – No 7–8, – P. 418–422.
10. Shenkin Y. S., Ruchnova S. A. System isobar solubility of NH_4NO_3 – $(NH_4)_2SO_4$ – H_2O at atmospheric pressure//Journal of Inorganic Chemistry. – 1970, – V. 15, – No 4, – P. 1145–1147.
11. Vyazenova I. A., Soltus T. L. NH_4NO_3 System study of $(NH_4)_2SO_4$ – H_2O at 25 °C//Affairs. ONIITEHIM in Cherkassy 03.12.90, – No 721–90 hp.
12. Pagaleshkin D. A., Grishaev I. G., Dolgov V. V. The study of solubility in system of NH_4NO_3 – $(NH_4)_2SO_4$ – H_2O//Chemical industry today – 2013, – No 3, – P. 4–8.

13. Kogan V. B., Ogorodnikov S. K., Kafarov V. V. Handbook of solubility. – Volume III, book 2 – L.: "Nauka", – 1970, – 1170 p.
14. Nikonov I. N., Bergman A. G. Polyterm of converse mutual systems of potassium and ammonium sulfates and nitrates//Journal of Applied Chemistry. – 1942, – V. 15, – No 6, – P. 437–446.
15. Ovchinnikov L. N., Kruglov V. A., Shirokov S. G., Fedosov S. V. Investigation of the process of granulation of sulphate-nitrate and sulfate-urea solution in a fluidized bed//Proceedings of the universities. J. Chemistry and chemical technology. – 1981, – V.24, – No 8, – P. 1049–1050.
16. Taran A. L., Shmelev S. L., Olevskiy V. M., Kuznetsov V. V., Rustambekov M. K., Filonov A. M., Taran A. V. Study the possibility of granulation towers of ammonium nitrate with the addition of ammonium sulfate//Chemical Industry. – 1991, – No 12, – P. 743–749.
17. Taran A. L., Konohova N. V. The research and development of NS production technology – containing mineral fertilizer in granulation towers//Advances in chemistry and chemical technology. – 2009, – V. 23. – No 7, – P. 72–75.
18. Taran A. L., Konohova N. V., Taran Yu. A., Yakovlev D. S. Check of the adequacy of the mathematical description of the granulation process of ammonium nitrate with ammonium sulfate as a filler in the towers during the actual process//Chemical industry today. – 2011, – No 6, – P. 21–27.
19. Kazakov A. I., Ivanova O. G., Kurochkin L. S., Plishkin N. A. Kinetics and mechanism of thermal decomposition of ammonium nitrate and sulphate mixtures//Journal of Applied Chemistry. – 2011. – 84. – V. 9, – P. 1465–1472.
20. Zavalin A. A., Safran S. A., Chernova L. S., Dubrovskikh L. N. A novel form of nitrogen fertilizers under spring wheat//Fertility. – 2009, – No 1, – P. 19–20.
21. Zavalin A. A., Safran S. A., Chernova L. S., Blagoveshchenskaya G. G., Dukhanina T. M., Bayramov L. E., Dubrovskikh L. N. Assessment of the effectiveness of a novel form of nitrogen fertilizer//Agrochemistry. – 2009, – No12, – P. 11–17.
22. Methods for analysis of phosphate raw materials, phosphate and compound fertilizers, feed phosphates/M. M. Vinnik, L. N. Erbanova, P. M. Zaytsev. – M.: Chemistry, – 1975, – 213 p.
23. State standard 21560. 2–82. Mineral fertilizer. Test methods. – M.: State Standard, – 1982, – 30 p.
24. Friedman S. D., Skum L. S. The solubility of potash chloride in nitroammophos//Chemical Industry. – 1971. – No 1. – P. 44–47.
25. Pestov N. E. Physico-chemical properties of granular and powdered chemicals. – M.: Publishing House of the Academy of Sciences of the USSR, – 1947, – 239 p.
26. Posin M. E., Zinyuk R. Y. Physical and chemical bases of Inorganic Technology: Educational supplies for higher education. – L.: Chemistry, – 1985. – 384 p.

DOI: http://dx.doi.org/10.20534/AJT-16-11.12-44-46

Nabiyev Akram Botirjonovich,
lecture of Namangan State University,
Republic of Uzbekistan
E-mail: akramnabiyev@umail.uz

Researching of influence of the electromagnetic field to the petroleum viscosity

Abstact: In this research work the results of influence of electromagnetic field on reologic peculiarity of petroleum are given. Also was observed decreasing more than 20 °C of energy of active of petroleum influence on electromagnetic field.

Keywords: high-viscosity reologic peculiarity, flowing, electromagnetic field, high frequency

It is commonly known that, during the transportation of high-viscosity oil via pipelines, the increasing of its fluidity is of prime importance.

Fluidity: some factors affect especially on reologic peculiarity of oil which is inclined, such as its component, structural functions, temperature, physical and

chemistry peculiarity [1]. As usual, two ways are widely used in order to increase fluidity.

First, in the oil pipeline there is a heat work regime which is constant and believable provision, second without heating system, it is used mixture of various gas condensates and from extra breaking granules in environment temperature.

Besides, regular use of either of the two methods considers to be effective. As mentioned, a considerable energy is necessary for all of this that can lead to the increase of oil cost. That is why, currently styles are globally produced demanding less energy. In this work it is cited to test report on influence of electromagnetic field of oil reologic peculiarities.

The sample of Mingbulak oil was put to the rotary facility "Rsostat-2–1", the correlation of shifting speed on the pressure voltage at various temperatures under influence of electromagnetic field was researched [2].

It is observed in influence of high frequency electromagnetic field that status of oil viscosity lessening low temperatures.

1 – Picture. Depending upon the temperature tension of moving when the value equals to the speed of moving 800 c^{-1}.

1. For primary petroleum (the petroleum which wasn't met the influence of the high frequency electromagnetic fields);

Shifting of sticky connections speed (T=40 °C).

2. The next petroleum after the influence of the high frequency electromagnetic field.

1) For first oil;

2) Influence of HVEF is for oil.

From above mentioned dependence we can see that the movement of the high frequency electromagnetic field exceeds, and it doesn't demand additional heating and the flow from the pipe gets improved. That's to say, it is required the considerable small quantity of shifting intensity to get the shifting speed of 800 c^{-1} after the influence of electromagnetic field under the temperature of 45 °C.

It can be explained with the situation of Newton that it is passed into the low temperature.

From the graphic we can see, in high frequency the oil movement increases, it is not required extra heating and the current enhances from pipelines. In an aim of researching, sticky connection temperature with logarithmic was monitored.

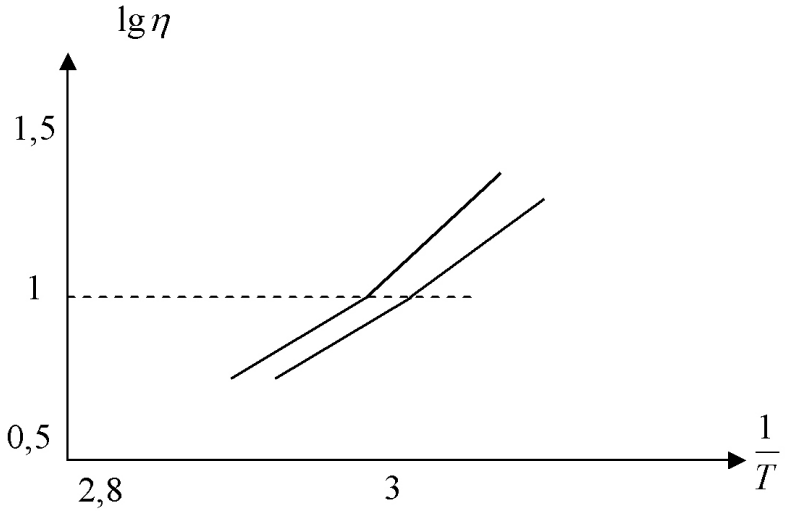

Figure 1. 2-picture. Sticky connection temperature (in Frankel equation coordinators)
1 – state; 2 – influence HVEF T= 20 °C

From the graphic we can see T = 20–60 °C temperature interval sticky changes with a few breaking. In an influence HVEF, this connection is corner tangency so activation energy organizes the smallest and adjustable 1–43,2–25 kj/мol in comparison with first state.

In higher temperatures activation energy remains the same. In an influence HVEF various stirred structural functions happens with breaking, oil sticky lessens and changes proportion set voltage.

Especially, in a low temperature, it has changed noticeable which energetic point shown its advantage.

The connection has its breaking, when it goes some temperature, in structure space passing may occur being shown [3; 4]. It goes without saying, while oils have higher sticky will be transferred to high-viscosity electromagnetic, its sticky lessens, fluidity increases in a low temperatures.

We think that the decreasing of viscosity degree of electromagnetic field dependents under the influ-

ence it is due to appearing of joining. We can see breaking of logarithmic dependence in the 2nd picture and space passing in the structure seized certain temperature in the 3rd and 4th pictures.

Relative low temperatures are structured parathion and petroleum associates, with increasing of the temperature it is formed detached phase. The mass of broken fragments are increased due to relatively little and poled.

References:

1. Lukoshkin G. S. Gathering and preparation of oil, gas and water to transport. – M.: Nedra, – 1972. – 324 p.
2. Kasparyans K. S. Trade preparation of oil. – M.: «Nedra» – 1966. – 363 p.
3. Nabiyev A. B., Sultonov A.S, Abdurahimov S. A. Problems of transportation of local high-viscosity oil. Fargona Polytechnics Institute, V materials of Republic scientific- practical forum – Fargona – 2009. – 132–133 p.
4. Nabiyev A. B., Abdurahimov S. A. Reologic features of transported compositions from mastic oil fields. Chemistry and Chemistry technology journal, – 2010, – No 1, – 63–65 p.

DOI: http://dx.doi.org/10.20534/AJT-16-11.12-46-49

Usmanov Abdukhamid,
Tashkent institute of chemical technology (Uzbekistan),
Junior assistant, Department of Food Safety
E-mail: abduhamid-86@yandex.com; sherzod-mamatov@mail.ru
Rakhimdjanov Makhamadjan,
Tashkent institute of chemical technology (Uzbekistan),
Professor, Department of Food Safety,

The effectiveness of the research of refining of cotton seed oil by local bentonite that activated by thermoradiation and acids

Abstract: Bentonite has been activated by thermoradiation and acids, and it has been applied in adsorptive refining. The safety index of adsorptive refined cotton seed oil has been researched.

Keywords: Bentonite, the infrared radiate, the high-frequency radiation, sulfate acid, alkali.

Introduction

Nowadays in the Republic of Uzbekistan it is an important issue to alter imported adsorbents to local ones which are used in refining cotton seed oil in The oil industry. Therefore, our basic concern is to apply local raw materials in an adsorbing refining of cotton seed oil. In this matter, we have chosen the bentonite which is produced in Navbakhor in Navoi region and Logon in Fergana region. In 1998, in Navbakhor bentonite mine was explored by geologic exploration and was applied as a source of bentonite. Fergana Logon mine was found in 2009, nowadays, it has been excavating. The chosen bentonite has alkaline substance, in order to use it in food industry it is necessary to neutralize it.

Materials and methods

As a material: 500 gr bentonite, sulfate acid 10%, microwave oven, distilling water for neutralization, sieve (with the diagonal of 0,16 mm holes) Lovibond machine, (to clarify the color of cotton seed oil), disintegrator (to grind a bentonite), water pump or electrical pump (to separate the mixture of bentonite and oil).

Methods: The bentonite of Navbakhor and Logon mine were chosen as an example. Physical-chemical index of it is studied according to this mineralogical features of the bentonite was investigated with sciagram.

500 gr bentonite from both samples has been taken and it has been neutralized with water until it has become neutral and it has been soaked in sulfate acid 10% for a while. Then bentonite has been flushed with water till it is neutralized consequent to that it has been heated in microwave oven with capacity 17 l, with the tension of 900 watts, with 220 V, until 9–10% of moisture left. Dried bentonite has been grinded and sieved. Then the oil has been refined with bentonite. The colour index of refined cotton seed oil is appropriated by Lovibond machine.

Results of research

According to the outcome the mineralogical structure is given in the following chart.

Table1.

Outcomes of test	Component of bentonite										
	Al_2O_3	SiO_2	TiO_2	CaO	Fe_2O_3	K_2O	Na_2O	P_2O_5	MgO	SO_3	Other elements
The bentonite of Navbakhor, %	13,69	57,91	0,35	0,48	5,10	1,75	1,53	0,43	1,84	0,75	13,71
The bentonite of Logon, %	17,56	50,11	–	0,37	13,69	2,38	1,0	–	1,92	0,1	12,87

Table 2. – The mineralogical structure of bentonite

The name of substace	An inactivated bentonite of Navbakhor,%	An activated bentonite of Navbakhor,%	An inactivated bentonite of Logon,%	An activated bentonite of Logon,%
montmorillonite	67,3	63,66	69,3	66,7
hydromica	27,8	27,8	26,9	26,9
Kaolinite	4,9	4,9	3,8	3,7

Table 3. – The chemical structure of the bentonite Fergana

The name of substance	An inactivated bentonite,%	An activated bentonite,%
Silica	18,9	17,5
R-beldspar	9,7	9,6
Plagioclase	2,2	2,7
The total of adsorbent	58,9	57,1
Calcite	1,0	5,1
Dolomith	6,6	5,8
Iron disulfates	–	2,2
Phosphate	2,2	1,5
Chlorite	0,5	0,5
Paligorskit	+	–
Semihydrate	+	–

If the bentonite is like a powder, adsorption of elements which gives colour will be active. The activated bentonite has been added to purify cotton seed to oil in 1% in ratio and it has heated up to 70°C in magnetic mixer and it should be mixed. In reference materials, it was written that to refine cotton seed oil we can use adsorbent till 5% in ratio. However, using in excess of bentonite can be caused for sourness in a taste and reducing the date of expiry. Nowadays, the factories which produces cotton seed oil planned to use an adsorbent 1% in ratio in the industry. In order to separate bentonite from the mixture, it has been filtered out. The colour has been clarified in the machine which identifies it. The results are given here:

Table 4. – The results of cotton seed oil which was refined with local bentonite

Area of local bentonite	The colour's index of oil before refining			The weight of used bentonite	The weight of used cotton seed oil	The colour's index of oil after refining		
	Red	Blue	Yelow			Red	Blue	Yelow
The Logan	14	1	35	3,008	100,050	9	0,1	35
The Navbakhor	14	1	35	3,005	100,040	6	0	35

As we see from the chart, effectiveness of the bentonite which produced in Navai differs from the bentonite which produced in Fergana to 1,5 red index. From these results we can deduce that the bentonite of Navbakhor is more effectively than the other. The bentonite which weighed 500 gr, has been flushed with water until it has been neutralized. After it has been soaked in sulfate acid and it has been heated in IR kiln with tension 220 V, and 710 mm wavelength during 20 minutes with high temperature inside 410×600×700 mm volumetric closed system. After, it was dried, it was grinded, therein scraps' size should be smaller than 0,16 mm.

In order to refine cotton seed oil it has been added an appropriate amount of bentonite to oil and heated

up, then it has been mixed in magnetic mixer. For the purpose of separating bentonite from the mixture, it has been clarified in machine which identifies colours. The result are given here:

Table 5. – The result of cotton seed oil which was refined with local bentonite

Area of local bentonite	The colour's index of oil before refining			The weigh of used bentonite, gr	The weight of of used cotton seed oil, gr	The colour's index of oil after refining		
	Red	Blue	Yelow			Red	Blue	Yelow
The Logan	14	1	35	3,078	100,400	5,5	0,1	35
The Navbakhor	14	1	35	3,015	100,080	4	0	35

The effectiveness of the bentonite which produced in Navoi differs from the bentonite which produced in Fergana to 5 red index.

From this, it has been determined that the bentonite of Navbakhor mine is more effectively in comparison between charts 4 and 5. According to this, the colour of cotton seed oil is reduced from 14 red index to 4 red index.

In this, two methods the reduction of cotton seed oil using activated bentonites becomes 3–5%.

An amount of toxic elements and radionuclides in the structure of adsorption refined cotton seed oil has been investigated. According to this analysis, we take 0,05000–2,0000 analogical scales and put it in autoclave with teflon.

Then we pour concetrated nitric acid and 2 ml of hydrogen peroxide. We close the autoclave and in the Berghof laboratory equipments it was proxided programming speedwave™ MWS-3+.

According to the programming it can be expanded and the degree of expanding (in autoclave till12).

After expending totally, it is poured to nitric acid of 2% to bottle with capacity of 50 ml, by the mark on it. Investigated object is tested with optician emissive spectrometer with inductive argon plasma or analogical spectrometer with this method, we can appropriate elements by their optimal wave adsorbing, they were submitted in the program, according to this the quality of elements will be appropriated.

An amount of taken outcome is calculate with the following formula.

$$Z = \frac{N \times 10}{C}$$

N – an amount of metal in spectrum mg/kg

C – concentration of prepared solution

Table 6. – The safety index of adsorptive refined cotton seed oil

The name of oil product	Appropriated concept ration of elements not much from mg/kg					
	Zn	Cd	Pb	Cu	As	Hg
The cotton seed oil which is refined with bentonite of Logon	0,0269	Not appropriated	0,0012	0,0175	Not appropriated	Not appropriated
The cotton seed oil which is refined with bentonite of Navbakhor	0,0135	Not appropriated	0,0022	0,0331	Not appropriated	Not appropriated
An allowable amount	5,0	0,05	0,1	0,5	0,1	0,03

As we see the chart, all safety index of refined cotton seed oil is conformed to an allowable amount. Besides that we can also take it to consider that bentonite of Navbakhor mine has purified the zinc better than the bentonite of Logon mine, while the bentonite of Logon mine has purifed the copper and lead better than the bentonite of Navbakhor mine.

Table 7. – The amount of radionuclides in the adsorbtive refined cotton seed oil.

The name of index	Signs of index			The conformation of index
	Documet norms	In practice		
Radionuclides		The oil which is refined by Logon bentonite	The oil which is refined by Navbakhor bentonite	
Cesium (Cs)-137, Bq/l, not much from	60	1,9	3,7	Conformed
Strontium (Sr)-90, Bq/l, not much from	80	0,5	0,4	Conformed

The amount of radionuclides, which was given in that schedule, is conformed to Rules of Sanitation, and Conformed 0283–10.

Conclusion

According to the research, Navbakhor bentonite is more effectively than Logon bentonite. In the result of adsorptive refining of cotton seed oil, it has decreased to 4 red index of the colour of oil. Oil has been produced with 95–97% of productivity after adsorptive refining. The aim is by activating local bentonites to refine adsorptively the cotton seed oil, besides this, to reduce the color index of cotton seed oil as the requirement of state standards and it has been cleared that it has conformed to the safety index of people's health.

It means that this refined cotton seed oil is edible for use.

References:

1. Руссу В. И., Окопная Н. Т., Стратулат Г. В., Ропот В. М. Исследование адсорбционных процессов и адсорбентов. – Ташкент: Фан. – 1979. – С. 257–259.
2. Дубин М. М. Адсорбенты, их получение, свойства и применение. – Л.: Наука, – 1975. – С. 92.
3. Надиров Н. К. Теорические основы активации и механизма действия природных сорбентов в процессе осветления растителных масел. – М.: Пищевая промышленность, – 1973. – С. 97–98.
4. Руководство по методам исследования, техническому контролю и учету производства в масложировой промышленности. – Ленинград: ВНИИЖ, – 1975. – Т. 2. – С. 223.

DOI: http://dx.doi.org/10.20534/AJT-16-11.12-49-52

Hamrokulova Muborak,
senior teacher, Fergana politexnical institute
Qodirov Yuldoshxon,
professor, Tashkent chemical-technological institute
E-mail: Ulug85bek77@mail.ru

Reserch on the refining process of prepressed cotton oil

Abstract: This work deals with research on high temperature neutralization of prepressed cotton oil at the presence of carbamide and usage of different excesses and strength of alkali. It has been determined that the excess of refined oil at all alkali strength is higher than without its application, but on the contrary, the chromaticity of refined oil is higher without application of carbamide, the difference in the chromaticity decreases if alkali solution in low concentration is used.

Keywords: cotton oil, carbamide, prepressed, refined, research, neutralization, soapstock.

Cotton oil is difficultl-refined oil among vegetable oils, because of the maintenance of colouring pigments in it, such as gossypol and its derivatives [1]. In this connection at cotton oil refining it is necessary to find optimum regimes for the extraction of gossypol from it and its derivatives that give the dark-painted colour to oil. One of extraction methods of gossypol, especially its derivatives is presented in the work [2], such as the changed and connected forms in which are available free aldehyde groups with the help of carbamide. To remove changed forms of gossypol carbamide is used at the refining high-acid cotton oils obtained from low-grade seeds. It is noted that at the refining high-acid cotton oil the chromaticity decreases and the output of refined oil increases at use of alkali solution with concentration 700, 800 g/l, carbamide solution with concentration of 50–55%, in number of it 0,1–2,0% from weight of initial oil. It has been determined that the optimum quantity of carbamide is 0,1% from weight of initial oil.

In order to improve the quality of oils, decrease in its losses at high-temperature neutralization of prepressed cotton oil, before addition of alkali solution, it has been loaded aqueous carbamide solution with concentration of 50% in number of 1,0% from weight of initial oil. In experiments it has been used prepressed cotton oil with neutralization number 3,03 mg KOH, chromaticity on

Lovibond: in a layer of 1,0 sm 10 red unit, 18 blue at 35 yellow units. At neutralization it has been also used alkali solution with concentration 700; 508; 400; 296,7; 201,2 g/l, excess of alkali 0,5; 1,0; 1,0; 1,2% from oil weight, a quantity of water for coagulation of soap stock makes 4,0% from oil weight, neutralization temperature — 60^0 C, duration of neutralization — 30 minutes, duration of process of concretion — 6–8 hours.

Acid number of the refined and unrefined cotton oil is defined by the present method [3], chromaticity in the colorimeter Lovibond.

Mean of results of researches is presented in tab. 1., from which follows that with decrease in the strength of caustic alkali at excess of 0,5%, the consumption of alkali 7,78 kg/t the output increases, the chromaticity decreases and the acid number of refined oil almost does not change with use of carbamide and without it. It is necessary to note that the output of the refined oil in all strengths of alkali higher at carbamide use, than without its application. The chromaticity of refined oil on the contrary, higher without carbamide application, the chromaticity difference decreases at use of the solution of alkali of low concentration. For the research of the influence of duration of soap stock coagulation on indicators of the refined oil experiments have been carried out at the temperature of neutralization $25–30^0$ C, the consumption of alkali 7,78 kg/t, and its excess 0,5% from the oil weight.

Results of research (tab. 2) show that at the duration of soap stock coagulation 6–8 hours the output of the refined oil is lower than at the duration of coagulation process 48–50 hours, except for concentration of alkali 296,7 and 201,2 g/l. The chromaticity of the refined oil is almost equal, except for at the strength of alkali 700/g/l.

And at the duration of soap stock coagulation 48–50 hours there are the maximum output and high chromaticity of the refined oil.

Table 1. – Influence of carbomide on the refining process of cotton oil

Strength of alkali, g/l	**Output**		**Indicators of refined oil**	
	Soap stock %	**Oil %**	**Chromaticity in 13,5 sm layer, r. unite. at 35 yellow**	**Acid number, mg KOH**
Carbomide consumption 1,0%				
700,0	8,97	93,36	22,0;3,0blue	0,297
508,0	8,74	93,67	17,2; 1,0 blue	0,287
400,0	8,89	93,76	17,2; 1,0 blue	0,291
296,7	10,76	94,16	14,5; 1,0 blue	0,284
201,2	11,49	93,77	15,0; 1,0 blue	0,285
Without carbomide				
700,0	10,08	92,64	26,0; 7,0 blue	0,3
508,0	12,48	92,89	27,0; 7,0 blue	0,3
400,0	10,70	92,96	17,0; 1,0 blue	0,297
296,7	10,88	93,88	16,0; 1,0 blue	0,298
201,2	11,68	93,94	18,0;1,0 blue	0,293

It is obtained at the strength of alkali 700 g/l, and the further decrease in the strength of alkali leads to the decrease in the chromaticity of the refined oil. It is necessary to note that the highest chromaticity of the refined oil is attained at the strength of alkali 700 g/l with application of carbamide and without it, and also at the duration of coagulation process 48–50 hours. From this it follows that in the neutralization process at high temperature and high strength of alkali the large quantity of heat which was possibly promotes an increase of temperature on a boundary of phases deposits. It is thus possible that native gossypol passes in the changed form that does not enter interaction with the caustic sodium and gives phaeochrous colour to the neutralized oil.

At increase in the coagulation process, it is possible to be the desorption of colouring substances from soapstock in the refined oil. The maximum output of the refined oil at the coagulation duration of soapstock 48–50 hours is possible connected by that thus there is an allocation of neutral fat which passes from soapstock in oil.

At high-temperature neutralization prepressed cotton oil irrespective of presence and absence of carbamide, the decrease in the strength of alkali positively influences on the decrease in chromaticity of the refined oil, i. e. at the strength of alkali 400; 296,7; 201,2 g/l the chromaticity of the refined oil almost does not change. At the strength of alkali 700; 508 g/l the chromaticity of the refined oil considerably differs from the refined without

carbamide application in comparison with its application at excess of alkali 1,0 and 1,2% from the oil weight (tab. 3). Carbamide presence at high-temperature neutralization prepressed cotton oil positively influences on the decrease in the chromaticity of the refined oil if to use strong caustic alkali solutions, i. e. 700; 508 g/l are used.

Table 2. – Influence of the duration of concretion process on cotton oil indicators

Strength of alkali, g/l	Output		Indicators of refined oil	
	Soapstock %	Oil %	Chromaticity in 13,5 sm layer, r. unite. at 35 yellow	Acid number, mg KOH
Duration of the coagulation process 6–8 hours				
700,0	9,20	92,68	16,0;2,5 blue	0,282
508,0	9,97	92,07	16,0;1,0 blue	0,280
400,0	11,36	91,82	16,0;2,0 blue	0,284
296,7	10,63	93,70	12,0;0,9 blue	0,281
201,2	11,11	93,88	13,0;0,5 blue	0,284
Duration of the coagulation process 48–50 hours				
700,0	7,78	94,19	22,0;4,0 blue	0,30
508,0	10,26	93,75	16,0; 1,5 blue	0,289
400,0	10,76	93,13	16,0;1,0 blue	0,289
296,7	11,56	93,47	12,8; blue	0,287
201,2	11,77	93,54	12,9;0,5 blue	0,288

The output of the refined oil is more at application of all strengths of caustic alkali with carbamide use than without its application, and is considerable higher an output at the strength of caustic alkali 700; 508 g/l.

Factory data testifies that steaming and roasting pulp is carried out with the big maintenance of peeling (i. e. in peeling with considerable quantity, than it is provided by the order) in the obtained oil the quantity of pigments giving blue coloring to oil increases. It is necessary to note that if in initial prepressed cotton oil it contains more pigments giving blue coloring to oil the increase in the excess of alkali does not influence positively on the decrease in the chromaticity of the refined oil (tab. 3)

Table 3.

Strength of alkali, g/l	Output of soap stock, %	Output of soap stock, %	Indicators of refined oil	
			Chromaticity in 13,5 sm layer, r. unite. at 35 yellow	Acid number, mg KOH
Excess of alkali 1,0% from the oil weight, alkali consumption 13,22 kg/t, carbamide consumption 1,0% from the weight				
700,0	12,85	93,09	12,0	0,229
508,0	13,63	93,61	11,0	0,219
400,0	13,79	93,42	12,0	0,20
296,7	15,77	92,26	11,0	0,20
201,2	17,64	92,63	12,0	0,21
Excess of alkali 1,0% from the oil weight, alkali consumption 13,22 kg/t, without carbamide consumption				
700,0	13,98	88,02	19,0; 3,0 blue	0,253
508,0	15,72	88,33	19,0; 0,1 blue	0,261
400,0	13,50	92,65	12,0	0,237
296,7	15,02	92,12	13,0	0,239
201,2	17,22	90,95	12,0	0,229
Excess of alkali 1,2% from the oil weight, alkali consumption 15,4 kg/t, carbamide consumption 1,0% from the oil weight				
700,0	14,31	91,61	12,0	0,221
508,0	22,50	85,36	13,0	0,217
Excess of alkali 1,2% from the oil weight, alkali consumption 15,4 kg/t, without carbamide				
700,0	19,32	85,50	22,0; 2 blue	0,227
508,0	26,20	80,11	21,0; 0,2 blue	0,229

At high-temperature neutralization prepressed cotton oil with the application of various strengths of alkali at presence and absence of carbamide it is revealed interesting regularity, i. e. the difference in outputs and the chromaticity of the refined oil is observed at the big and small excess of alkali. It is necessary to note that especially big difference in outputs and chromaticity is observed at the strength of alkali 700; 508 g/l and excess of alkali of 0,5% from the oil weight i. e. 93,36–92,64% and 93,67–92,89% (tab. 1), and at excess of alkali of 1,0% from the oil weight accordingly makes 93,09–88,01% and 93,61–88,33% (tab. 3). The difference in chromaticity at excess of alkali of 0,5% from the oil weight 22 r.unit. 3,0 blue –26 r. unit 7 blue; and 17,2 r.unit 1,0 blue.-27 r.unit 7 blue (tab. 1), at excess of alkali of 1,0% from the oil weight of 12 r. unit –19 r.unit 3,0 blue. And 11 r.unit –19 r.unit 0,1 accordingly. The small difference on the output and chromaticity is observed at the strength of alkali 400; 296,7; 201,2 g/l and excess of alkali of 0,5% from the oil weight i. e. 93,76–92,96%, 94,16–93,88%, 93,77–93,94% (tab. 1), and at excess of alkali of 1,0% from weight of oil i. e. 93,42–92,65%, 92,26–92,12%, 92,63–90,95 (tab. 2) Accordingly the difference in chromaticity at excess of alkali of 0,5% from the oil weight, 17,2 r.unit 1,0 blue –17 r.unit 1,0 blue, 14,5 r.unit 1,0 blue — 16,0 r.unit 1,0 blue, 15,0 r. unit 1,0 blue — 18 r. unit 1,0 blue (tab. 1.), at excess of alkali of 1,0% from the oil weight 12–12 r. unit; 11,0–13,0 r. unit; 12,0–12,0 r.unit (tab. 3).

The further research is directed on studying of the influence of carbamide on the indicators of the refined oil at high-temperature neutralization of prepressed cotton oil with acid number 8,96 mg the KOH, chromaticity in 1 sm layer is not visible. Experiments have been carried out at the excess of alkali of 1,2% from the oil weight and the consumption of alkali 20 kg/t. Mean of results of researches are presented in table 4 from which follows that in all used strengths of alkali the output of the refined oil is higher in the presence of carbamide than at its absence.The chromaticity of the refined oil is higher in the presence of carbamide than without its application if it is not to considered the blue coloring of the refined oil. Blue coloring in the refined oil is much lower in the presence of carbamide than in its absence in all strengths of caustic alkali used by us. It is necessary to note that the increase in the output of the refined oil in the presence of carbamide is not in regular intervals with change of the strength of alkali. The maximum increase in the output of the refined oil is achieved at the concentration of alkali 201,2 g/l (3,22%), and the minimum increase in the output of oil is attained at the concentration of alkali 700 g/l and 296,7 g/l (0,1 and 0,18%).

Table 4. – Refining indicators of cotton oil

Strength of alkali, g/l	**Output**		**Indicators of refined oil**	
	soap stock,%	**oil,%**	**chromaticity in 13,5 sm layer, r. unite. at 35 yellow**	**Acid number, mg KOH**
Carbamide consumption 1,0% from the oil weight				
700,0	21,39	85,58	19,0; 8blue	0,289
508,0	25,91	82,83	26,0; 6blue	0,291
400,0	25,60	83,84	17,0; 8blue	0,284
296,7	27,91	82,46	20,0; 8blue	0,293
201,2	29,44	83,99	20,0; 7blue	0,293
Without carbamide				
700,0	17,44	85,48	13,0; 12 blue	0,290
508,0	26,90	80,77	22,0; 10 blue	0,291
400,0	27,16	81,93	20,0; 9 blue	0,287
296,7	28,84	82,28	15,0; 11 blue	0,291
201,2	30,32	80,77	17,0; 11 blue	0,292

References:

1. Мартовщук В. Н., Мгебришвили Т. В., Боровский А. Б., Палманович С. А. «Оптимизация процесса рафинации труднорафинируемых растительных масел совмещенного с механо-химической активацией». Известия Вузов. Пищевая технология, – 1989, – No 11, – С. 89.
2. А. с. 1564179 СССР, МКИ С 11 В 3/00. Способ рафинации хлопкового масла/А. Т. Ильясов, В. Пак, Р. Мирзакаримов, Т. И. Искандаров, А. Н. Мирзаев. БИ – 1973.
3. Руководство по методам исследования, технологическому контролю и учету производства в масложировой промышленности, – Т. 1. Книга 2, Л. ВНИИЖ, – 1967, – 890 с.

Section 7. Physics

DOI: http://dx.doi.org/10.20534/AJT-16-11.12-53-62

Usachev Valery M.
Russia, Republic Of Tatarstan,
City Of Naberezhnye Chelny.
E-mail: usachevvm1@yandex.ru

The beginning of the theory of space as an ideal quantum liquid (IQL)

Abstract: The author of this article (in 1967) sets out a number of new ideas and hypotheses about the physical nature of the elementary particles and physical interactions that are necessary and sufficient to the crisis in the field of theoretical physics to overcome.

These ideas, hypotheses and evidence are here in a very accessible way for professionals and for those, the physics course in High Schools and Colleges have studied.

Keywords: quantum liquid space, photon, electron, proton, physical interaction.

The beginnings of the theory of space as an ideal quantum liquid (IQL)

Note: all physical variables, constants, and calculations are here in an "absolute System of physical units" GCSE.

1 Definition

1.1. "The beginnings of the theory " — it is new ideas, scientific hypotheses and mathematical proof of its adequacy with regard to the basic scientific theories and facts of objective reality.

1.2. "ideal quantum liquid (IQL)" — it is a liquid almost absolute zero Kelvin, in which:

a) the temperature depends on the concentration of photons (quasi-particles);

b) the value of the internal friction (dynamic viscosity) is very close to Zero;

c) the physical properties are independent of the geometric volume (from infinity to zero).

Molecular-kinetic theory based on ancient and medieval hypothesis of the atomic structure of matter and the "ether" is set and, therefore, can not explain why there are physical interactions (electroweak, strong and gravitational) through the void.

This was because it seemed completely empty the entire space between the smallest particles of matter ether. (Thus, it was impossible to offer a logical hypothesis of interaction of the physical body with the other physical objects in the distance.)

Since the beginning of the twentieth century appears the hypothesis of relativistic expansion of space as the constant expansion to infinity of all the particles of matter. In this hypothesis, the "expansion of the universe" is interpreted as "the expansion of space-time continuum." This is the phenomenology of relativistic paradigm completely contradicts the real discrete quantum-mechanical nature of the microcosm and macrocosm.

In the middle of the 60s of the last century not the adequacy of the Interpretation of the physical phenomena of objective reality reaches its peak. Then all the great physicists of the world, recognized this fact.

The author of this article in September 1967 proposed a number of basic ideas and hypotheses, which are necessary and sufficient for the overcoming of this crisis in theoretical physics. Listed below are these ideas, hypotheses and evidence in a very simple Form for professionals and those who studied the course in physics for secondary schools.

2. The basic ideas and hypotheses

2.1. The basic "elementary" particles (photons, electrons, protons, neutrons) interpreted (in a simple analogy) as different aggregate states ideal quantum liquid space (IQLS):

electron (and photon) is interpreted as a "vapor bubble" in IQLS;

"Proton" can be interpreted as the ball of the plurality of concentric spheres of liquid crystal in IQLS;

neutron can be interpreted as a foam formed from a mixture of these particles (electron, proton and "Photon-neutrino"), which again decays into an electron, proton, and "photon-neutrino" for 15 minutes;

positron in this set of interpretations looks like a bubble cavitation in IQLS.

2.2. Based on 2.1., electrostatic forces of repulsion and attraction between electrons and protons are easy to explain on the basis of the laws of classical thermodynamics.

Since the electron is hot "vapor bubble" in IQLS, but the proton is very cold "LCD ball" in IQLS, the same particles are removed from each other, but different particles are approaching each other, to equalize the temperature in a physical system "IQLS-particles" (according to the second law of thermodynamics about the increase in entropy).

Experiments led by Academician Kapitsa and theory of quantum liquids (Academician Landau), showed that the photons appear or disappear in a quantum liquid, if it increases or decreases the temperature.

Therefore, in an ideal quantum fluid space (IQLS) around "hot" electrons form a zone of high concentration of photons, but around the "cold" protons (and positrons) in IQLS formed a zone of low concentration of photons. This allows us to understand the physical nature "of the electric fields of charged particles" (with opposite "signs").

2.3. Based on 2.1. and 2.2. we conclude that the elementary particles and photons in a perfect quantum liquid space (IQLS) are formed of different aggregate States IQLS. Localization (individualization) of a particle (and its internal structure) is formed by surface tension between phase condition IQLS.

2.4. Starting with 2.1.-2.3. it follows that the diameter of the surface electrons, protons and positrons in a free state must be equal to each other, if equal modules of electric charges "e" of these particles. (Under this condition, the resultant force of surface tension is equal and oppositely directed internal electrostatic force, which seeks to break the particle.)

2.5. Starting from 2.1.-2.4., One can understand (explain) why the proton density is three orders higher than the electron density. (Since the density of gas condensate at three orders of magnitude greater density of atmospheric gases under normal conditions).

2.6. Starting with 2.1.-2.5., an electron as a "bubble steam" in a perfect quantum liquid space (IQFL) easily and elastically deformed, the higher the energy of colliding particles with him. So that the diameter of the electron cannot be measured in particle collisions in accelerators.

2.7. Based on these fundamental new ideas, the author formulated the system of equations (for the first time in August-September 1967):

$$h\nu = us = mc^2 \qquad (1)$$

expressing the fundamental law of conservation and transformation of energy-mass; where

h — is the Planck constant;

ν — is the frequency of the quantum;

u — is the surface tension of the perfect quantum liquid space (IQLS);

s — is the total surface area IQLS formed a photon (or "elementary particle" and its internal structure);

m — is the mass;

c — is the constant speed of light.

The left side of the Formula (1) is the formula for the Planck energy $E = h\nu$ for photons (quanta of electromagnetic radiation). The right side of this formula expresses the value of the total kinetic energy $E = mc^2$ for a particle with inertial mass m and the translational velocity c. The Central part of the (us) Formula (1) expresses the potential energy, which is equal to the work of the forces of surface tension IQLS in the processes of synthesis — annihilation of particles and quanta from one to another.

2.8. Total electrostatic energy of the electron is directly proportional to the square of the electric charge and inversely proportional to the classical radius of the electron (in accordance with the classical theory of electricity).

Therefore, based on the idea of the electron as a "vapor bubble" ideal quantum fluid space, you can simply calculate the values of u and d, solving two equations with two unknowns:

2.1) $2e^2 / d = us$;

2.2) $2e^2 / d = mc^2$.

Where:

e — electric charge of the electron;

u — factor surface tension ideal quantum fluid space;

d — is the diameter of the electron;

$s = 3{,}14\,d^2$ — is the surface area of the free electron;

m — is the electron mass;

c — is the speed of light.

Substitution of known constants, we can solve the system of equations 2.1) and 2.2), and calculate the two new constants: the diameter of the electrically charged "elementary particles" $d = 0{,}563 \times 10^{-12}\,cm$;

and the new fundamental physical Constant the surface tension of the ideal quantum liquid space (i. e., the strong interaction)

$u = 0{,}823 \times 10^{18}\ erg/cm^2 = 0{,}823 \times 10^{18}\ din/cm$.

Note: The system of equations (1) shows a direct proportion to the mass of elementary particles and the surface area of an ideal quantum fluid space that forms the "elementary particles" (and its internal structure). This was confirmed experimentally. For example, "mass defect" is directly proportional to a change in the surface of the nuclei of atoms (and the release of atomic energy) in the synthesis and decay of atomic nuclei.

2.9. Presented in paragraph 2.1.- 2.8. the basic ideas and Formulas (1) of the law of conservation and transformation of energy-mass exhibit a unique combination of all the fundamental physical interactions on the basis of the principles and laws of classical physics.

2.10. For example, "wave-particle duality in quantum physics it is easy to understand, watching the bubbles of steam that rise from the bottom of the vessel on the water surface. The bubble moves not strictly in a straight line, but a spiral helical path around a vertical axis. Similarly, "elementary particle and photon (i. e., "liquid-crystal ball" or "vapor bubble") moves in IQLS not in a straight line, but a spiral-helical path.

2.11. Thus, the length of the "de Broglie waves" is the length of the pitch of the helical trajectories of particles and quanta. Therefore, the frequency of de Broglie waves", this value is the number of rotations that occur per second (particle or quantum around the axis of the helical path).

2.12. The rotation of particles and photons around the axis of the helical path can be "right" or "left" (50/50). Thus, it is easy to explain such phenomena as the "double refraction of light", "transverse electromagnetic waves", "spin" and its sign ("+" or "–").

2.13. The idea of the physical nature of the space as a perfect quantum liquid easily explains the reason for the existence of the law of universal gravitation (gravity). Indeed, just looking at the bubbles on the surface of tea or coffee in the Cup, it is easy to see that they are approaching each other with acceleration, forming Islands of foam. This is because water molecules evaporate from the surface of each bubble. The location of these molecules is occupied by the molecules of the surface layer of the surrounding liquid. Therefore, each bubble is constantly "pulling on" the surface layer of the liquid. Because of this, it attracts other bubbles. The same thing happens in a perfect quantum liquid space with all the particles and the physical body. Only instead of molecules in an ideal quantum fluid space, there are gravitons — the smallest quanta of energy ("Nano"- bubbles), in accordance with formula (1).

2.14. From the laws of classical physics and the beginnings of the theory of IQLS (perfect quantum liquid space) the author received formula "lifetime", "frequency", "energy" and "length of step of a screw trajectory of a photon as a function of time t its free movement in space of the universe (IQLS):

$$T_0 = (\nu_0 / K)^{1/2} \quad (2)$$

$$\nu_t = \nu_0 - Kt(2T_0 - t) \quad (3)$$

$$E_t = h[\nu_0 - Kt(2T_0 - t)] \quad (4)$$

$$\lambda_t = c / \left[\nu_0 - Kt\left(2T_0 - t\right)\right] \quad (5)$$

In these formulas here and further:

T_0 — possible full life-time quantum in the case of free movement in IQLS from the Moment of its radiation with the energy $E_0 = h\nu_0$ until complete dispersion of its energy in it ($E_{t=T_0} = 0$);

t — period movement (from the Moment of the radiation);

ν_t — frequency as a function of time t ;

E_t — energy of the quant (photon) as a function of time t ;

ν_0 — frequency of the quant (photon) at the time of its radiation (t=0);

K — factor offset (indicated capital letter of last name brilliant physics experimenter, academician P. L. Kapitsa);

λ_t — length step of the spiral helical trajectory ("the de-Broglie-wave"), as a function of time t of the motion of the free quantum;

h — Planck constant;

c — constant speed of light.

3. Proof. (Mathematical principles of the theory of space as a perfect quantum liquid and particles and photons as different physical states IQLS, localized by surface tension IQLS.)

Theory IQLS (ideal quantum liquid space) expresses the law of conservation and transformation of energy-mass equation system:

$$h\nu = us = mc^2 \quad (1)$$

On the basis of ideas about space as objectively real quantum liquid with a very small coefficient of friction η (but not reduced to zero when the absolute temperature is not equal to 0), and on the basis of ideas about the Photon as the bubble vapor-liquid-room with a surface area of spherical surface geometrically equal to $s = \pi d^2$ (where d is the diameter of the Photon), we find the formula fully kinetic energy of the photon according to the principles of classical physics.

To do this, we consider the de-Broglie wave to the photon as a complex helical trajectory of the ball bladder with step-screws, equal to λ and the frequency of rotation around the axis of the helical trajectory is equal to ν. That is, how two simple movement of the ball: forward, (with a speed of light parallel to the axis of the screw trajectory of the movement of the photon) and rotation with the angular velocity $\omega = 2\pi\nu$, and the speed $V = \omega R$ perpendicular to this axis (on the tangent to a circle with Radius R of the cylinder screws). Then, according to classical mechanics the complete kinetic energy E of the Photon-bubble with the mass m and moment of inertia $I = mR^2$ is obtained from the summation of the kinetic energy of the translational and rotational movements:

3.1) $E = 0{,}5mc^2 + 0{,}5I\omega^2 = 0{,}5mc^2 + 0{,}5m(R\omega)^2 = 0{,}5mc^2 + 0{,}5mV^2$.

Please note that by the formula (1) $mc^2 = us$, and that $m = us/c^2$. Substituting the corresponding expressions in the formula, a full energy of the photon, we obtain:

3.2) $E = 0{,}5us\left(1 + V^2/c^2\right)$.

On the other hand, since the total energy of the photon is given by a formula-Planck $E = h\nu$, then, from the equation $h\nu = 0{,}5us\left(1 + V^2/c^2\right)$, so we get $V = c$, so as $h\nu = us$.

That is, tangential (to the tangent to a circle with Radius R) component of the speed of the photons with respect to the axis of the trajectory is always equal to the speed of light *c* (i. e. the same as the translational component parallel to the axis of the screw).

HENCE. From equations 3.1) and $V = c$ follows immediately:

1) the energy $E = h\nu$ is full kinetic energy $W = 0{,}5mc^2 + 0{,}5mV^2 = 0{,}5mc^2 + 0{,}5mc^2 = mc^2$ with the free motion of photons in a spiral helical path. That is, from classical mechanics immediately $W = E = h\nu = mc^2$;

2) module full speed of a photon in a spiral helical path exceeds the constant c is the velocity of light propagation in $\sqrt{2}$ times (it ≈1,414 c);

3) according to the formula (1), knowledge of the frequency ν of the photon at time t, we can determine not only the photon energy according to the formula $E = h\nu$ and mass m according to the formula $E = mc^2$, but its diameter d (such as " bubble steam" IQLS) and the radius R of the helical trajectory (at time t).

For example, due to the fact that $s = \pi d^2 = h\nu/u$, the diameter of the bubble-photon is found by the formula

3.3) $d = \sqrt{h\nu/\pi u}$.

For a Photon of violet light ($\nu = 0{,}76\times10^{15}\ Hz$), so we get:

$d = (6{,}62\times10^{-27}\times0{,}76\times10^{15})^{1/2}/(3{,}14\times0{,}823\times10^{18})^{1/2} = 1{,}4\times10^{-15}(cm)$.

Hence, the largest diameter of a photon of visible light (violet) is about 0.3% of the diameter of the free electrons. According to the formula $\omega = 2\pi\nu$ and $V = \omega R$ you can calculate the radius R of spiral helical path around the axis of direction. Since $V = c$, we have:

3.4) $R = c/(2\pi\nu)$.

Therefore, for light purple $R = 6\times10^{-6}$ cm, see, that is billions of times greater than the diameter $d = 1{,}4\times10^{-15}\ cm$ photon.

Thus, in accordance with the energy of photons at a certain point in time, we can calculate all the parameters of the photon, on the basis of the principles and laws of classical physics. (This confirms the prophecy P. Dirac, who claimed that "the generally accepted interpretation of quantum field theory should be considered as a palliative without any future".)

In modern theoretical physics, when moving from the source to the receiver, all the photons remained unchanged for billions of years. The understanding of space as a perfect quantum liquid requires new perspectives on Photon, given the loss of their energy. As the temperature of ideal quantum liquids just above absolute zero, the viscosity is very low. But at large distances between stars, galaxies, the photons lose energy to do work against friction forces in IQLS. Thus, in accordance with the principles and laws of classical physics, we find the equation of energy (and other parameters photons) depending on time (or distance), if these losses must be considered.

When the ball moves in a fluid, the friction force f is found by the Stokes formula:

$f = 3\pi\eta dV$, where:

η — ratio of the viscosity of the liquid;

d — diameter of the ball;

V — the speed of his movement in the liquid.

The speed of the movement of the bubble-Photon along a spiral trajectory is always invariable. According to the rule of addition of velocities in classical physics it is equal to $\sqrt{2}\,c \approx 1{,}414\,c$, because we found that both parallel and tangential (along the tangent to the circle with radius R) the speed of the photon relative to the axis of the helical path is equal to the speed of light c. The diameter d of a photon by the formula 3.3) $d = \sqrt{h\nu/\pi u}$. Therefore, the equation for finding the absolute value of the friction force in the motion of a photon in a spiral

helix in accordance with the Stokes formula becomes:

3.5) $f = 3\pi\eta(h\nu / \pi u)^{1/2} \times 2^{1/2} c$.

Write the differential equation for the infinitesimal energy loss ΔE photon infinitesimal path length ΔL of its movement in a spiral helical path for an infinitely small time interval Δt. On the one hand, the magnitude of the energy loss ΔE is equal to the friction force f on an infinitely small interval of length spiral helix $\Delta L = 2^{1/2} c\,\Delta t$. That is,

3.6) $\Delta E = 3\pi\eta(h\nu / \pi u)^{1/2} \times 2^{1/2} c\Delta L = 6\pi^{1/2} c^2 \eta (h/u)^{1/2} \times$
$\times \nu^{1/2} \Delta t$.

On the other hand, infinitely small change in the size of the energy of the photon can be found according to the formula of M. Planck, such as $\Delta E = h\Delta\nu$, where $\Delta\nu$ — infinitely small change in the frequency of a photon to an infinitely small time interval Δt. Then we can write a differential equation of the type:

3.7) $h\Delta\nu = 6\pi^{1/2} c^2 \eta (h/u)^{1/2} \nu^{1/2} \Delta t$, that is,

3.8) $\Delta t / \Delta\nu = \nu^{-1/2} (hu)^{1/2} (6\pi^{1/2} c^2 \eta)^{-1}$.

In the right part of this differential equation the value of $\nu^{-1/2}$ depends on changes in the frequency of the photon. Other factors $(hu)^{1/2}(6\pi^{1/2}c^2\eta)^{-1}$ — constant values, the product of which also has a constant coefficient K_1. That is,

3.9) $K_1 = (hu)^{1/2}(6\pi^{1/2}c^2\eta)^{-1}$.

On this basis, we can write an integral equation of the type

3.10) $\int_0^T dt = K_1 \int_{\nu_0}^0 \nu^{-1/2}\, d\nu$.

We take a certain integral over the entire frequency range from the beginning ν_0 (at the moment of emission of a photon) to 0 Hz (when the final consumption of its energy), and we get the following formula full time T_0 free movement of the photon to the complete dissipation of its energy in a ideal quantum liquid space (IQLS):

3.11) $T_0 = 2K_1 \nu_0^{1/2}$.

From this formula, we get:

$$\nu_0 = KT_0^2 \qquad (2),$$

where the constant $K = (1/2K_1)^2$, that is,

3.9') $K = 9\pi\eta^2 c^4 h^{-1} u^{-1}$.

The formula (2) offers the possibility to calculate the decrease in the frequency ν_0 of the photons at the preset distance from the source to receiver; or, on the contrary, the calculation of distances between source and receiver radiation in space, if you know the frequency ν_0 at the moment of emission and the target frequency ν_t at the time of admission. In fact, if $t_0 = 0$ taken at the moment of emission of a photon with the original frequency radiation ν_0, and full time possible "life" of a photon T_0; then at each moment of time t after the moment of radiation (excluding the gravitational effect and the Doppler effect) instantaneous frequency value ν_t can be found by the formula

3.12) $\nu_0 - \nu_t = KT_0^2 - K(T_0 - t)^2 = Kt(2T_0 - t)$.

Hence (by the Planck formula $E = h\nu$) for each quantum of electromagnetic radiation are calculated all the parameters as a function of time t when its free movement in ideal quantum liquid space (IQLS):

$$T_0 = (\nu_0 / K)^{1/2} \qquad (2)$$

$$\nu_t = \nu_0 - Kt(2T_0 - t) \qquad (3)$$

$$E_t = h[\nu_0 - Kt(2T_0 - t)] \qquad (4)$$

$$\lambda_t = c / [\nu_0 - Kt(2T_0 - t)] \qquad (5)$$

Formula (2) to (5) follows from the continuity of the functions of the lifetime of the photon in all the way L along the axis of the spiral helical path of free movement in IQLS (between the time of radiation $t_0 = 0$ to time $t = L/c$). That is, these formulas follow from the logical assumption that at time t, (if the frequency of the photon decreases to ν_t), then the remaining "life" T_t Photon will be less by the amount of time t. This means that $T_t = T_0 - t$.

We can prove, justice, such a logical assumptions mathematically.

In time ($t_0 = 0$) Photon left the source of the radiation with the frequency ν_0. By the formula (2), we can find the time T_0 (until complete dispersion of the energy of the photon in the IQLS):

3.13) $T_0 = (\nu_0 / K)^{1/2}$.

Let at time t the frequency of the first photon is obtained by the formula

(3) der Wert $\nu_t = \nu_0 - Kt(2T_0 - t)$. Let at the same time, radiates a second Photon with the same frequency ν_t.

Full time live T_t second Photon, we find by the formula (2):

3.14) $T_t = (\nu_t / K)^{1/2}$.

Replace this expression, the frequency ν_t to the same value $\nu_t = \nu_0 - Kt(2T_0 - t)$ from equation (3), we get:

3.15) $T_t = [(\nu_0 - Kt(2T_0 - t)) / K]^{1/2} =$.

We have noticed that $\nu_0 / K = T_0^2$ according to formula (2). So we get:

3.16) $T_t = \left(T_0^2 - 2T_0 t + t^2\right)^{1/2} = [(T_0 - t)^2]^{1/2}$, so that $T_t = T_0 - t$.

That evidence.

The theory of dissipation of energy of quantum of EMR (photons) in the case of motion in ideal quantum liquid space (IQLS) leads to completely different formula of the law of the «galactic red shift» than «law

Hubble» ($V = Hr$). From the formula (6) implies that the energy dissipation of EMR happens is that the difference between the square root of the frequency $\nu_0^{1/2}$ EMR in the parent galaxy and the square root of its frequency $\nu_t^{1/2}$ (received on Earth) is constant for all frequencies at the same distance between the source and the radiation detector. That is to say:

$$\nu_0^{1/2} - \nu_t^{1/2} = K^{1/2} t \qquad (6)$$

or

$$\nu_0^{1/2} - \nu_t^{1/2} = K^{1/2} r / c \qquad (6')$$

Constant coefficient Kapitza K "galactic red shift", we can calculate in theory IQLS by the formula 3.9') as a mathematical multiplication of the different degrees of the fundamental physical constants (which in fact is the most important physical parameters of ideal quantum liquid space):

3.9') $K = 9\pi\eta^2 c^4 h^{-1} u^{-1}$, wo

K — is a constant "galactic red shift" (or "factor Kapitza");

π — number "Pi";

η — is the coefficient of internal friction in a ideal quantum liquid space (IQLS), (or "constant superweak interaction");

c — is the constant speed of light;

h — is the Planck constant;

u — factor surface tension ideal quantum liquid space (IQLS), (or "constant of the strong interaction").

Under the new formula "galactic redshift" astrophysics can calculate the distance r to distant galaxies, the more accurate than they are farther away from us. (The greater the distance r, the smaller the% error due to the Doppler effect, compared with the true the magnitude of the galactic red shift EMR).

K — factor can be calculated by the observed value of z relative red shift in the emission spectrum of nearby galaxies. The distances to these galaxies is well calculated with different methods of astronomy in the last century. The relative displacement z is expressed by the formula $z = (\nu_0 - \nu_t)/\nu_t$, from which it follows that $\nu_0 - \nu_t = z\nu_t$ und $\nu_0 = \nu_t(z+1)$.

Astronomy already in the first third of the last century has found that, on average, for the observed next to us galaxies (on a distance of one mega parsec) of the relative redshift of the Master-line spectrum is approximately equal to $z = 0{,}0016706$.

The Mpc distance light travels during time

$t = 1{,}0340487 \times 10^{14}\, sek$. $t = 1{,}0340487 \times 1014\, сек$.

From these data according to the formula (6)

3.17) $K = (\nu_0 - 2\nu_0^{1/2}\nu_t^{1/2} + \nu_t)/t^2 = \nu_t[z + 2 - 2(z+1)^{1/2}]/t^2$ can be calculated, if the photons from galaxies with a distance of one megaparsec has a frequency $\nu_t = 0{,}53060612035 \times 10^{15}\, Hz$ (mid-visible range), this parameter gives us the calculated value $K = 0{,}34736 \times 10^{-19}\, sek^{-3}$.

Now, knowing the observed value $z = 11{,}9$ for galaxy **UDFj-9546284**, we can calculate the time of the movement of the light from galaxy to us, according to the formula

3.18) $t = [(\nu_0^{1/2} - \nu_t^{1/2})^2 / K]^{1/2} = [(\nu_0 - 2\nu_0^{1/2}\nu_t^{1/2} + \nu_t)/K]^{1/2}$.

For the average frequency of the visible range of light from this galaxy $\nu_t = 0{,}53060612035 \times 10^{15}\, Hz$ according to the formula $z = (\nu_0 - \nu_t)/\nu_t$ calculate

$\nu_0 = \nu_t(z+1) = \nu_t(11{,}9+1) = 12{,}9\nu_t$.

There fore: $t = [\nu_t(13{,}9 - 2 \times 12{,}9^{1/2})/K]^{1/2}$

$t = [0{,}53060612035 \times 10^{15}(13{,}9 - 7{,}1833)/0{,}34736 \times$
$\times 10^{-19}]^{1/2} = 3{,}203124 \times 10^{17}$ (sec).

It is the time, in seconds, the light goes from the galaxy **UDFj-9546284** up to us.

That is, the distance r of us up in the galaxy **UDFj-9546284** is:

$r = 3{,}203124 \times 10^{17} / 3{,}15576 \times 10^7 = 10{,}15 \times 10^9$ (light years).

So, galaxy **UDFj-9546284** at a distance of 10 billion 150 million light years away from earth.

Know coefficient $K = 0{,}34736 \times 10^{-19}\, sek^{-3}$ we can calculate new physical constant η — coefficient of internal friction of the ideal quantum liquid space. As was shown above

3.9') $K = 9\pi\eta^2 c^4 h^{-1} u^{-1}$, wo

K — is a constant "galactic red shift" (or "factor Kapitsa");

π — number "Pi";

η — is the coefficient of internal friction in a ideal quantum liquid space (IQLS), (or "constant super weak interaction");

c — is the constant speed of light;

h — is the Planck constant;

u — factor surface tension ideal quantum liquid space (IQLS), (or "constant of the strong interaction").

So $\eta = [K/(9\pi c^4 h^{-1} u^{-1})]^{1/2}$, where:

$K = 0{,}34736 \times 10^{-19}\, sek^{-3}$ and $u = 0{,}823 \times 10^{18}\, erg/cm^2$ new physical constant, the received theoretically and on the basis of experienced scientific data. Substituting the known numerical values of the constants and calculating, we obtain: $\eta = 2{,}882 \times 10^{-36}$ (Poise).

4. Let us prove that the idea of the physical nature of the "physical vacuum" as the ideal quantum liquid space (IQLS), and electrons and quanta of elec-

tromagnetic waves, as bubbles of steam (ideal gas of quasi-particles"), corresponds to objective reality and all the principles and laws of classical physics and quantum mechanics.

If a free electron in a perfect quantum liquid space (IQLS) is an analogue of the vapor bubble in the water, in this case, some physical properties of the electron must comply with the laws of classical molecular-kinetic theory. Therefore, the pressure force "steam" on the inner surface of the bubble-electron must be equal to the force of the pressure surface tension IQLS on "steam" inside the electron.

The energy W of the compressed gas at pressure p volume V, according to the molecular-kinetic theory is determined by the formula $W = pV \times 3/2$. This means that on the one hand, pressure from the inside to the surface of the electron is equal to the formula

4.1) $p = 2W/3V$.

On the other hand, according to the theory of surface tension, pressure IQLS on pairs of electrons, find the Laplace formula

4.2) $p = 4u/d$, where d is the diameter of the bubble-electron, and

u — is the surface tension IQLS.

According to the classical theory of electrical potential energy E of the electron (diameter d) can be expressed by the formula:

4.3) $E = 2e^2/d$, where e — is the electric charge of the electron. In absolute system of physical units CGSE (up to the second mark)

E = $0{,}82 \times 10^{-6}$ Erg.

According to the classical law of conservation and transformation of energy value E must be equivalent to the total kinetic energy of the mass m of the electron:

4.4) $2e^2/d = mc^2$ (in full accordance with the experimental results).

Geometrically, the area s of the surface of the electron is determined by the formula

4.5) $s = 3{,}14d^2$.

Substituting this expression in $us = mc^2$, we get:

$u \times 3{,}14 \times (5{,}64 \times 10^{-13}\,см)^2 = mc^2$.

Substituting known values and calculations, we find (as shown above), the surface tension of IQLS:

$u = 0{,}823 \times 10^{18}\ erg/cm^2 = 0{,}823 \times 10^{18}\ din/cm$.

Now the pressure inside the electron will be found by the formula 4.2) Laplace:

$p = 4 \times 0{,}823 \times 10^{18} / 5{,}64 \times 10^{-13} = 0{,}584 \times 10^{31}(Bar)$.

The geometric volume of the electron will be found by the formula

4.6) $V = 3{,}14d^3/6$, that is,

$V = 3{,}14 \times (5{,}64 \times 10^{-13})^3/6 = 0{,}94 \times 10^{-37}\left(cm^3\right)$.

Substituting the values of pressure p and volume V of the electron in equation 1) and calculating, we get:

4.7) $W = pV \times 3/2 = 0{,}584 \times 10^{31} \times 0{,}94 \times 10^{-37} \times 3/2 = 0{,}82 \times 10^{-6}(Erg)$.

That is, the calculations confirm that, in accordance with the principles and laws of classical and quantum physics, the electrostatic energy of the electron is equivalent to its internal thermal energy. In addition, the energy of surface tension equivalent to the total energy of the electron mass. These equations are equivalent to the system of equations "triple Formula (1) of the law of conservation and transformation of energy, according to the theory of ideal quantum liquid space (IQLS). Now it's proven.

5. One more time, in a few words, as in the theory of the ideal quantum liquid space (IQLS) appears the System of the equations

$$h\nu = us = mc^2 \qquad (1).$$

Here (in the examples for photons and electrons):

h — is the Planck constant;

ν — frequency quanta;

u — constant surface tension ideal quantum liquid space (IQLS) (or constant of the strong interaction);

s — is the total surface area of a ideal quantum liquid space (IQLS) forming a photon or "elementary particle" (and its internal structure);

m — is the mass of the quantum (or particles);

c — is the speed of light.

Theoretically and experimentally proved the existence of inside the well-known quantum liquids dissolved gas of quasi-particles". This phenomenon can be interpreted as "sparkling water" (or "sparkling wine"). It was also proven that the free movement of quasiparticles inside the quantum fluid occurs as a wave process. "Wavelength" is defined in accordance with the equation de Broglie: $\lambda = h/m\nu$.

In a ideal quantum liquid space (IQLS) this relation is true for the movement of all particles and quanta (from zero speed to the speed of light).

In accordance with the ideas of the theory of the ideal quantum liquid space (IQLS) λ — step helical trajectories of particles and quanta. Formed such trajectory through drip-cluster hierarchical structure IQLS (like all liquids, according to the theory of academician Frenkel).

NOTE

You can just see the wave-like movement and the helical trajectories of gas bubbles in a glass of soda water (or sparkling wine).

Knowing the step length $\lambda = h / mv$, we can easily calculate the period T of rotation of the particles (or quanta) around the axis of the trajectory $T = \lambda / v = h / mv^2$. Here

5.1) $mv^2 = h / T$.

Da $1 / T = v$ — number of cycles per second particles (or quanta) around the axis of the helical path. Therefore, for a photon the expression $mv^2 = hv$, s identical to the formula

5.2) $hv = mc^2$.

Clarify the physical meaning of this formula.

It is easy to explain on the basis of understanding the physical nature of space as a perfect quantum liquid (IQLS). For the formation of a photon ("steam bubble diameter) is necessary against the forces of surface tension IQLS to do work equal to us.

I. e. for the formation of a steam bubble in a perfect quantum liquid space (IQLS), require energy quantum

5.3) $hv = us = 3{,}14d^2u$.

Experimental and theoretical total energy quanta is determined by the Planck formula $E = hv$. Therefore, for photons, we can write the equality $us = hv$.

On the other hand, in accordance with section "**3. Proof**", of the evidence" (see above) we find the equation $hv = mc^2$:

The corollary. From equations 3.1) and $V = c$ follows immediately:

the energy $E = hv$ is full kinetic energy $W = 0{,}5mc^2 + 0{,}5mV^2 = 0{,}5mc^2 + 0{,}5mc^2 = mc^2$ movement of photons (quanta) in a spiral helical path. That is, from classical mechanics should directly $W = E = hv = mc^2$).

From these two equations, we get for the energy of the photons in ideal quantum liquid space (IQLS) the third equality:

5.4) $us = mc^2$.

Thus, proceeding from the principles of the theory of space as a perfect quantum liquid, we came to the conclusion formula of the law of conservation and transformation energy/mass in all the processes of synthesis-Annihilation "of elementary particles and quanta of energy: $hv = us = mc^2$.

Values of h, u, c in this system of equations are the fundamental constants. Thus, the variables v, s, m is directly proportional to each other.

From the above, it follows that the full (according to the quantum theory) the energy $E = hv$ the photon is equal to, on the one hand, the potential energy us (the surface tension) of the IQLS, and, on the other hand, it is a complete kinetic energy $W = mc^2$, the movement of this vapor bubble (photon) along a helical trajectory with a speed of 1,414 c (in accordance with the laws of classical mechanics).

It is easy to explain, from our understanding of the physical nature of the space as a ideal quantum liquid (IQL): to create a photon or an electron ("vapor bubble") should work, thermal energy of the quasiparticles against the forces of surface tension IQLS.

6. The calculation of the number of quasi-particles of one free electron.

According to the ideas of the classical molecular-kinetic theory (ILC), the temperature T it is a quantitative measure for the energy of the thermal motion of molecules. This average kinetic energy of the translational motion of the individual molecules is directly proportional to the absolute temperature of the body T:

6.1) $mv^2 / 2 = (3 / 2)kT$.

In accordance with the principles of classical physics and the theory of space as a ideal quantum liquid space (IQLS), a free electron is a vapor bubble (or ideal gas of quasi-particles") in it. Therefore, according to the third Newton's law (equality of action and reaction), and according to the law of conservation and transformation of energy-mass, we can say that the thermal energy $E = (3 / 2)pV$ electron must be exactly equal to the potential energy us tension of its surface:

6.2) $us = (3 / 2)pV$, where

u — factor surface tension of an ideal quantum liquid space (IQLS) (or constant of the strong interaction);

s — surface of the electron as a "vapor bubble";

p — is the pressure in the electron as the "vapor bubble";

V — volume of the electron as "vapor bubble".

The pressure p in an ideal Gas is expressed by the fundamental formula of the kinetic theory of gases $p = nkT$, where n — the number of particles per volume V (the concentration). As $n = N / V$, where N — the total number of particles, therefore $pV = nkTV$ expresses what

6.3) $us = (3 / 2)pV = (3 / 2)NkT$.

According to the system of equations of the Formula (1), which expresses the law of conservation and transformation energy/mass in the theory of an ideal quantum liquid space (IQLS), we obtain the equation:

6.4) $us = mc^2$, where

m — mass of the electron;

c — the speed of light.

According to the equation $us = (3 / 2)pV$, the potential energy of the surface tension of the electron (like the vapor bubble) is equal to its total internal thermal energy, which is equivalent to the total energy mc^2 the

electron mass; on the other hand, $mc^2/2$ can be considered as the kinetic energy of the chaotic thermal motion of free electrons (as any molecules of an ideal gas). But in this case the energy of thermal motion of the electron is expressed through its absolute temperature:

6.5) $mc^2/2=(3/2)kT$.

The surface of the electron it is also a "corpuscle" gaseous bodies (spherical surface + quasiparticles). According to the molecular kinetic theory (MKT) continuous interaction with each other should be set between dynamic balance, which is expressed in the fact that the kinetic energy (RMS) of the particles in this system must be equal to $(3/2)kT$. Internal interaction of the quasiparticles with the surface of the electron manifests itself in the form of oscillations (vibrations) of an electron in a ideal quantum liquid space (IQLS) with average square velocity chaotic translational motion is equal to the speed of light c.

From equation

6.3) $us=(3/2)pV=(3/2)NkT$,

6.4) $us=mc^2$ and

6.5) $mc^2/2=(3/2)kT$ we get an equation

6.6) $us=Nmc^2/2$, from which it follows that:

6.7) $N=2$.

That is, a free electron consists of two quasiparticles localized in a ideal quantum liquid space (IQLS) its surface tension.

7. The basic law for ideal quantum liquid space (IQLS).

The author in 1985 receives a formula — law for quantum condensed environments. Namely, that the elementary quantum of action (fundamental Planck's constant) is equal to the product of three physical quantities, which define the properties, composition and structure of quantum condensed matter:

$$h=mvd \qquad (7);$$

where:

h — is the Planck constant,

m — mass of elementary particles for a given environment,

d — is the diameter of the "elementary particles" for this environment,

v — velocity of propagation of the elementary quantum of action h in this environment.

According to the classical theory of the structure of liquids Y. I. Frenkel, ideal quantum liquid space (IQLS) also has a fractal-hierarchical drip-cluster structure. But, of course, for each level of this structure, the average diameter of a droplet cluster has a different diameter droplets (from the infinitely large to the infinitely small). Thus, the product of two variables md varies from level to level and decreasing m and d, in the limit tends to zero. Accordingly, the value $v=h/md$ (the same condition) is committed to the infinitely large value.

Based on these considerations, according to the formula (7), we can calculate the value of the sound velocity v in molecular quantum liquids, if known mass m and diameter d of the molecule. (Or you can calculate the diameter d of the molecules, quantum liquids, if known mass m and speed v for these fluids. And so on, and others).

You can check the execution of the basic law ($h=mvd$) quantum condensed media". (For example, in a known cryogenic physics quantum of liquid helium-II.)

The mass of an "elementary" particles (^4_2He) is defined as

$m=6{,}65\times10^{-24}$ (g). The density of this quantum Fluid, 7 times less than that of water, so about to $0{,}14$ (g/cm^3). Therefore, we calculate the diameter d of the atom (on the basis of the dense packing of balls of atoms in the quantum liquid) so:

1) the number n of atoms in a cubic centimeter as

$n=0{,}14/\left(6{,}65\times10^{-24}\right)=0{,}02\times10^{24}$ (cm^{-3});

2) specific volume V_1 fluid for a single atom we find so

$V_1=1/n=50\times10^{-24}$ (cm^3);

3) we multiply with the factor of packaging of the specific volume V_1 the liquid, and we get the volume V of a sphere-Atom

$V=0{,}74\times50\times10^{-24}=37\times10^{-24}$ (cm^3);

4) according to the formula $V=3{,}14d^3/6$, we find

$d=\left(6\times37\times10^{-24}/3{,}14\right)^{1/3}=70{,}70^{1/3}\times10^{-8}=4{,}135\times$

$\times10^{-8}$ (cm);

5) now, theoretically we can find the speed of the dissemination of own oscillations (the quasiparticles) in the quantum-liquid Helium-II according to the formula $v=h/md$:

$v=6{,}626\times10^{-27}/\left(6{,}65\times10^{-24}\times4{,}135\times10^{-8}\right)=$

$=0{,}24\times10^5$ (cm/sek).

That is, v=240 m/sec, what is to be proved.

Experiment under the direction of academician P. L. Kapitza identified the speed of sound in the quantum liquid Helium-II even earlier, in 1940, about (240 ± 10)m/sec.

References:

1. Kapitsa P. L.: "PROBLEMS of LIQUID HELIUM" (Report at the General meeting of the Academy of Sciences of the USSR, – 1940).
2. Kuznetsov B. G.: "the Principles of classical physics" – Moscow, – 1958.
3. Frisch C. E. and Timoreva A. C.: "the General physics Course, so 1" – Moscow, – 1956.
4. Jaworski B. M., Detlaf A. A.: "the physics Course, so 3, wave processes, optics, atomic and nuclear physics" – Moscow, – 1967.
5. Dukov C. M.: "Electron, the history of the discovery and study of properties" – Moscow, – 1966.
6. Kalashnikov S. G.: "Electricity" – Moscow, – 1977.
7. The primary sources and the works of the great physicists (from I. Newton to our days).

Section 8. Chemistry

DOI: http://dx.doi.org/10.20534/AJT-16-11.12-63-66

Daminova Shahlo Sharipovna,
Tashkent Chemical Technological Institute,
Department of «Technology of silicate materials and rare precious metals»,
Scientific Researcher
E-mail: daminova-sh@mail.ru

Kadirova Zukhra Chingizovna,
Tashkent Chemical Technological Institute, Center of Excellence,
Dr. Engineering, PhD in Chemistry,
E-mail: zuhra-kadirova@yahoo.com

Sharipov Khasan Turabovich,
Professor, Tashkent Chemical Technological Institute,
Department of "Technology of silicate materials and rare precious metals",
E-mail: sharkhas@yandex.ru

Sorption of Ag(i) ions on Pad 400 impregnated resin

Abstract: The polymer matrix (PAD-400) was impregnated by diethyldithiophosphate and used for sorption of silver ions from solutions. The impregnated sorbents were characterized by FTIR, SEM and DTA data. It was established that silver ions have been sorbed from solutions with impregnated sorbents due to formation of the metal-impregnate surface complexes. The sorption process is described better with Freundlich equation.

Keywords: sorption, diethyldithiophosphate, silver ions.

1. Introduction

Study of organothiophosphorus acids and their derivatives are very actual due to wide possible applications [1, 863] in hydrometallurgy [2, 149], waste water treatment [3, 1636]. Dialkyldithiophosphoric acid compounds are well known agents for impregnation of polymeric sorbents used for sorption of metal ions [4, 201] applied for extraction of noble metals [5, 545] due to formation of stable metal complexes [6, 369].

The aim of study is preparation of PAD-400 resin impregnated by diethyldithiophosphoric acid $((EtO)_2PS)_2H$ for sorption of Ag^+ ions from nitrate solutions.

2. Experimental

PAD-400 (Purolite) is a commercial granular macroporous styrene-divinylobenzene resin (moisture retention — 55%, grading < 1180 μm, uniformity coefficient — 1.43, mean diameter — 543 μm, pore volume (Hg) — 0.7 ml/g, mean pore diameter (Hg) 362 Å, surface area (BET) — 684 m^2/g). Diethyldithiophosphoric acid $((i\text{-}EtO)_2PS)_2H$) was purchased from Sigma Aldrich GmbH. Before impregnation PAD-400 was rinsed with methanol and then with water to remove impurities. 7 g of potassium diethyldithiophosphate dissolved in 250 cm^3 of methanol was added to 10 g of PAD-400, all ingredients were shaken for 3 h at 293 K. After impregnation, SIR was rinsed by deionized water. The concentration of diethyldithiophosphoric acid in PAD-400 matrix was determined by using gravimetric method. The content of $(EtO)_2PS)_2H$ in PAD-400 was ~ 50% (CHNS-analyzer EA-1108, Carlo-Erba). The prepared impregnated sorbent was used in further metal sorption studies in batch reactor. The metal ions contents were analyzed by using atomic absorption spectroscopy (Aanalyst–800, Perkin Elmer) after sorption from 0.05–0.02–0.04 mol/l solutions. The ligand coordination was studied

by FTIR absorption spectra in the range of 400–4000 cm^{-1} (FTIR 2000, Perkin-Elmer), KBr pellets. The SEM/EDX data obtained by Zeiss EVO MA 10/Aztec Energy Advanced X-Act (Zeiss SMT LTD/Oxford Instruments).

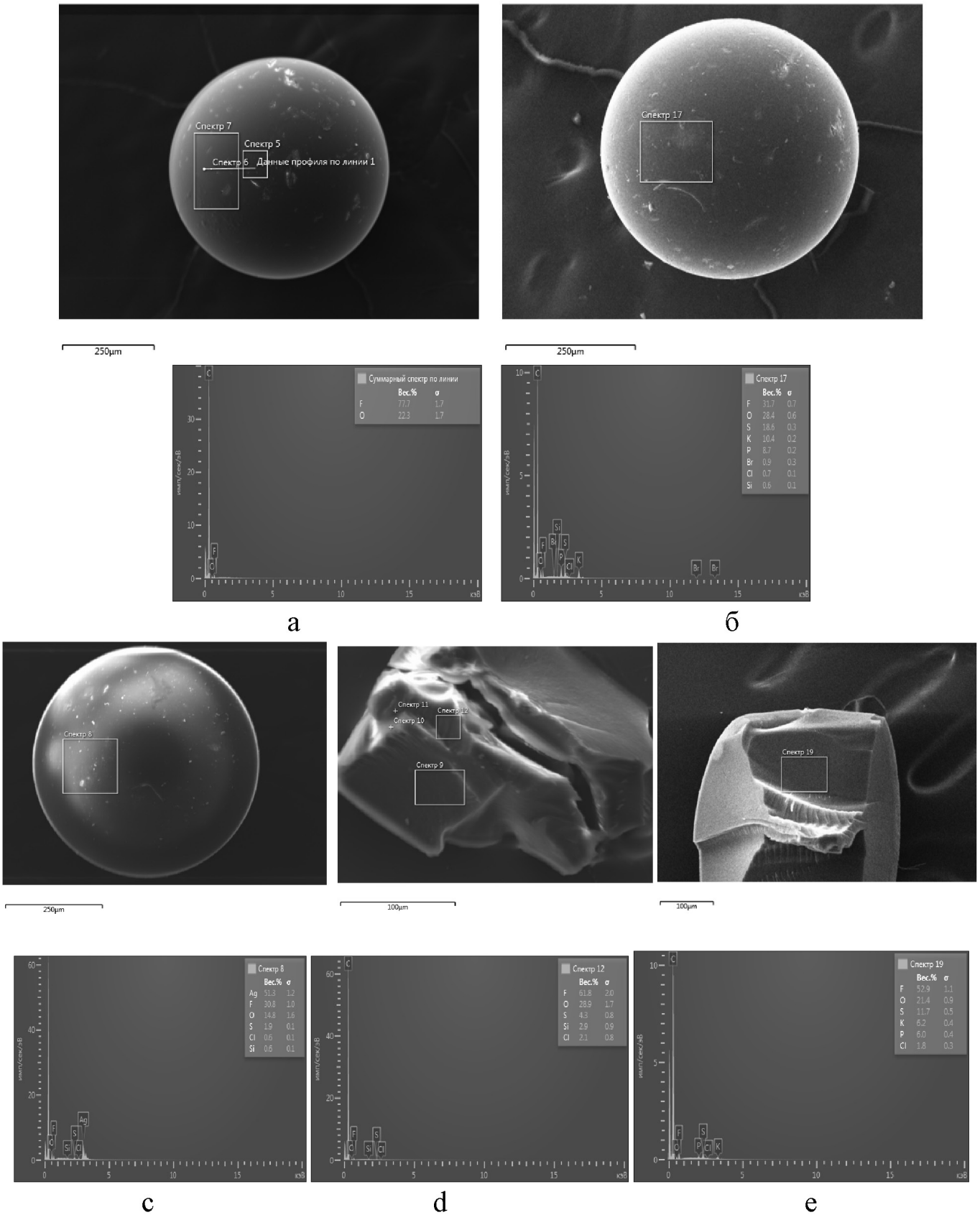

Figure 1. Microstructure of the PAD 400 granule (a) and the PAD 400 granule impregnated by $(EtO)_2PS_2K$ (b), PAD 400 granule after Ag^+ ions sorption (c), the inner part of PAD 400 granule after Ag^+ ions sorption (d) the inner part of the PAD 400 granule impregnated by $(EtO)_2PS_2K$ after Ag^+ ions sorption (f)

3. Results and discussion

The microstructure of the PAD 400 granule (a) and the PAD 400 granule impregnated by $(C_2H_5O)_2PS_2K$ (b) shows on Fig. 1. The SEM-EDX analysis indicates the PAD-400 granules have some content of F (Figure 1a). The surface of the impregnated sorbent granule is characterized by P, S and K peaks from $(C_2H_5O)_2PS_2K$ (Fig. 1b). The appearance of the silver EDX peaks on the granule surface can evidence the silver ions sorption with the PAD 400 sorbents (Figure 1 c). However, silver ions have not been detected inside of the PAD-400 granules (Figure 1d), as well as, the PAD-400 granules impregnated with diethyldithiophosphoric acid, although, the presence of PSS-groups within the impregnated granules is confirmed by EDX (Figure 1e).

Obviously, the influence of steric factors causes a good impregnation and sorption for the PAD-400 sample (pore size 362 Å). The silver ions sorption capacity (q_e) of sorbents have been determined for sorbents experimentally for each sorbent system. According obtained isotherm graph the sorption parameters were calculated from the Langmuir and Freundlich models (Table 1) The characteristic S-shape of the sorption curve has a plateau indicating that the adsorption on impregnated sorbents is step-multilayer process. Indeed, the sorption process is described better with Freundlich equation, which gives an indication on the significant contribution of the chemical interaction in comparison with the physical adsorption. Sorption mechanism can be considered with both physical sorption of metal ions on the adsorbent surface and strong chemical reaction in the presence of the impregnated sorbent, which increases the metal sorption on impregnate. It is shown that sorption increases from the initial PAD-400 sorbent to the impregnated sorbents.

Table 1 – Calculated parameters of the Ag^+ ions sorption on the PAD-400 sorbents

Sorbent	Langmuir					Freundlich		
	q_o		b	R^2	D	K_f	n	R^2
	mmol/g	mg/g	l/mmol		kJ/mol			
PAD-400	17.24	1862.07	0.28	0.9070	–20.46	3.85	1.09	0.974
$(i\text{-}EtO)_2PS_2K$–PAD400	13.33	1440.00	0.95	0.8670	–21.47	5.79	1.93	0.9770

The FTIR spectrum of the PAD400 sample has polystyrene characteristic frequencies, e. g. 1600–1700 cm^{-1}, 705–795 cm^{-1} bands identified as the stretching and deformation vibrations frequencies of monosubstituted aromatic hydrocarbons. The presence of absorption bands at 2925–3081 cm^{-1} and at 1350–1512 cm^{-1} related to n to ν_{as} and ν_s vibrations of aliphatic C-C bonds, C-H, CH2, CH3. The styrene absorption bands at 708, 795, 1605 and 1631 cm^{-1} and bands in the region 1700-2000 cm^{-1} called as "five fingers" are clearly visible. The FTIR spectrum of the sorbent containing PSS-functional groups has new intensive bands at 1376-1350 cm^{-1}, 990-850 cm^{-1}. These bands related to the P-O-R. R-O groups vibrations, and stretching P = S vibrations were observed for PAD400 impregnated with (EtO)2PS2K (I) (Table 1). The spectra of the sorbents after sorption from Ag+ solutions considerably differ from spectra of the sorbents, which indicates formation of metal complexes with dithiophosphoric fragment. In comparison with (i- EtO)2PS2 K, low-frequency shift of the bands (20-30 cm^{-1}) were observed due to formation of the metal-sulfur bonds and lower P=S bond order in 4-membered chelate ring.

Table 2 – Characteristic FTIR bands

Sample	n	D	n	D
$(i\text{- }EtO)_2PS_2K$	687		577, 547	
$(i\text{-}EtO)_2PS_2K$ –PAD-400 (I)	687, 618	0	570, 550	7
Ag^+– $((i\text{- }EtO)_2PS_2)$ –PAD-400 (II)	653	34	551	26

Two endothermic effects at 103, 175 and four exothermic effect at 290, 430, 600 and 810 °C are found on the DTA curves of the PAD-400 sorbent. The total mass loss by the TG curve is equal 98.24%. The DTA curve of the PAD-400 impregnated with $(EtO)_2PS_2K$ sorbent is characterized by two endo-effects at 85, 240 °C and four exo-effects at 280, 520, 735 and 800 °C. The PAD-400 sorbent impregnated with $(EtO)_2PS_2K$ has three endo-effects at 130, 210, 258 °C and three exo-effect at 526, 740, 800 °C after sorption of Ag^+ ions from solution. The TG curve of impregnated samples shows total mass loss in the range of 98.65% at 900 °C temperature.

4. Conclusions

According to FTIR, SEM and DTA, it was found that sorption of silver ions from solutions with impregnated sorbents can occur via formation of the

metal-impregnate surface complexes. The polyfunctional ligands adsorbed on the surface of the polymer matrix, and these ligands interacted with the polymer porous structure fixing in large cavities on the polymer surface. The metal ions bonded with the ligand functional groups forming metal complexes during sorption.

References:

1. Alimarin I. P., Ivanov V. M. Extraction with thio and dithio phosphorus acids//Russian Chemical Reviews. – 1989. – T. 58. – No. 9. – C. 863.
2. Strikovsky A. G., Jerabek K., Cortina J. L., Sastre A. M., Warshawsky A. Solvent impregnated resin (SIR) containing dialkyl dithiophosphoric acid on Amberlite XAD-2: extraction of copper and comparison to the liquid-liquid extraction//Reactive and Functional Polymers. – 1996. – T. 28. – No. 2. – C. 149–158.
3. Ying X., Fang Z. Experimental research on heavy metal wastewater treatment with dipropyl dithiophosphate//Journal of hazardous materials. – 2006. – T. 137. – No. 3. – C. 1636–1642.
4. Jerabek K., Hankova L., Strikovsky A. G., Warshawsky A. Solvent impregnated resins: relation between impregnation process and polymer support morphology I. Di- (2-ethylhexyl) dithiophosphoric acid//Reactive and Functional Polymers. – 1996. – T. 28. – No. 2. – C. 201–207.
5. Rovira M., Hurtado L., Cortina J. L., Arnaldos J., Sastre A. M. Impregnated resins containing di (2-ethylhexyl) thiophosphoric acid for extraction of palladium (II). I. Preparation and study of the retention and distribution of the extractant on the resin//Solvent extraction and ion exchange. – 1998. – T. 16. – No. 2. – C. 545–564.
6. Sharipov K. T., Daminova S. S., Talipova L. L. Crystal and Molecular Structure of Rhodium (III) Diisopropyldithiophosphate//Journal of Structural Chemistry. – 2002. – T. 43. – No. 2. – C. 369–372.

DOI: http://dx.doi.org/10.20534/AJT-16-11.12-66-71

Daminova Shahlo Sharipovna,
Tashkent Chemical Technological Institute,
Department of «Technology of silicate materials and rare precious metals», Scientific Researcher
E-mail: daminova-sh@mail.ru

Talipov Samat,
Institute of Bioorganic Chemistry, Academy of Sciences of Republic Uzbekistan, PhD in Chemistry,
E-mail: samat-talipov@yahoo.com

Kadirova Zukhra Chingizovna,
Tashkent Chemical Technological Institute, Center of Excellence,
Dr. Engineering, PhD in Chemistry,
E-mail: zuhra-kadirova@yahoo.com

Sharipov Khasan Turabovich
Professor, Tashkent Chemical Technological Institute,
Department of "Technology of silicate materials and rare precious metals",
E-mail: sharkhas@yandex.ru

Synthesis and crystal structure of co, cd, bi mixed-ligand complexes of diisopropyldithiophosphate and 2-amino-1-methylbenzimidazole

Abstract: The crystal and molecular structures of the mixed-ligand ternary complexes [Cd (MAB)$_2$ (*iso*-ProPS$_2$)$_2$], [Co (MAB) (*iso*-ProPS$_2$)$_2$], [Bi (MAB) (*iso*-ProPS$_2$)$_3$] were determined. The aminobenzimidazole ligands were monodentate coordinated via *endo*-cyclic N atom. The monodentate coordination in the Cd

complex and the bidentate coordination of the PSS-groups in the Co and Bi complexes were observed. The molecules interaction and packing in crystal structures were considered on the basis of structural data.

Keywords: synthesis, mixed-ligand complexes, the crystalline structure diizopropilditiofosfat, 2-amino-1-methylbenzimidazole.

1. Introduction

Study of dialkyldithiophosphoric acids and their derivatives are very actual due to wide applications in industry, biology and medicine [1, 863]. The ability to form themixed-metal [2, 40] and the ternary mixed-ligand coordination compounds can be explained by the ligand electronic structure [3, 28] and physicochemical properties [4, 674]. The aim of this work is synthesis and X-ray diffraction structural study of [Cd (MAB)$_2$ (*iso*-ProPS$_2$)$_2$], [Co (MAB) (*iso*-ProPS$_2$)$_2$], [Bi (MAB) (*iso*-ProPS$_2$)$_3$] complexes with 2-amino-1-methylbenzimidazole (MAB) and determination of interaction between molecules in crystal.

2. Experimental

Elemental analysis was performed by the atomic absorption spectrophotometer (Aanalyst–800, Perkin Elmer) and the CHNS-analyzer (EA-1108, Carlo-Erba). The ligand coordination was studied by FTIR absorption spectra in the range of 400–4000 cm^{-1} (FTIR 2000, Perkin-Elmer), KBr pellets.

Synthesis of [Cd (MAB)$_2$ (*iso*-Pro$_2$PS$_2$)$_2$]. The MAB solution (0.147 g (1 mmol) in 4 ml of ethanol) was added with stirring to the Cd (*iso*-Pro$_2$PS$_2$)$_2$ solution (0.426 g (1 mmol) in 16 ml of ethanol). The mixture was kept at room temperature for one hour, and the precipitated white crystals were filtered with suction, washed with cold ethanol, dried in air. Found,%: C 39.8 H 4.9 N 7.2 Cd 12.8; Calculated%: C 40.4 H 5.3 N 7.5 Cd 13.5. FTIR spectra, KBr, cm^{-1}: 450, 502, 531, 549, 631 (shoulder), 650 (PS$_2$), 740, 756 (shoulder), 782, 887, 966, 992, 1105, 1141, 1178, 1246, 1298, 1324, 1350, 1372, 1423, 1467, 1510, 1553, 1600, 1637, 2874, 2932, 2976, 3230, 3337, 3420.

Synthesis of [Co (MAB) (*iso*-Pro$_2$PS$_2$)$_2$]. The $CoCl_2 6H_2O$ solution (0,24 g (1 mmol) in 6 mL of the water-ethanol (1: 1) mixture) was added to the MAB solution (0.16 g (1 mmol) in 4 ml of ethanol). Resulting blue solution was added to 1 ml (2 mmol) of aqueous solution of potassium diisopropyldithiophosphate. The blue-green precipitate was vacuum-filtered, washed twice with water and cold ethanol, dried in air. Found%: C 43.07 H 5.85 N 10.72 7.51 Co; Calculated%: C 43.13 H 5.91 N 10.78 7.58 Co. FTIR spectra, KBr, cm^{-1}: 449, 501, 539, 557 (shoulder), 627 (shoulder), 652 (PS$_2$), 740, 756 (broad), 786, 888, 964, 1016, 1103, 1142, 1178, 1242, 1296, 1325, 1373, 1385, 1424, 1467, 1513, 1551, 1597, 1629, 2874, 2932, 2976, 3055, 3338, 3425.

Synthesis of [Bi (MAB) (*iso*-Pro$_2$PS$_2$)$_3$]. The MAB solution (1 mmol in 4 ml of ethanol) added to the Bi (*iso*-Pro$_2$PS$_2$)$_3$ solution (2 mmol in 15 ml of ethanol) by small portions under stirring. The yellow crystals were precipitated from solution after 25 hours at room temperature. The precipitated crystals were filtered with suction, washed with ethanol, dried in air. Found,%: C 31.26 H 5.08 4.27 N 20.93 Bi; Calculated,%: C 31.36 H 5.13 4.22 N 21.01 Bi. FTIR spectra, KBr, cm^{-1}: 429, 501, 527, 553, 613 (broad), 667 (PS$_2$), 741, 884, 963, 1106, 1140, 1177, 1244, 1292, 1315, 1372, 1383, 1417, 1461, 1489, 1544, 1642 (shoulder), 1674, 2868 (shoulder), 2932, 2978, 3059, 3317.

Single crystals suitable for X-ray diffraction were grown by slow evaporation at room temperature in saturated alcohol solutions. The [Cd (MAB)$_2$ (*iso*-Pro$_2$PS$_2$)$_2$] compound was crystallized as colorless, transparent, stable well shaped needle crystals. The [Co (MAB) (*iso*-Pro$_2$PS$_2$)$_2$] single crystals were blue needle-like crystals, and the [Bi (MAB) (*iso*-Pro$_2$PS$_2$)$_3$] single crystals were yellow needles. The crystallographic parameters determined by single-crystal diffractometer (Crysalys Excalibur, Oxford Diffraction) (Table 1). Data processing was performed using SHELXS86 and SHELXL93 program [5, 112]. The structure was solved by direct methods and refined by full-least-squares method in the anisotropic approximation, the hydrogen atoms refined isotropically, and R factor was less than 0.5.

3. Results and discussion

The [Cd (MAB)$_2$ (*iso*-Pro$_2$PS$_2$)$_2$] crystal structure is constructed from mononuclear complex molecules. The crystallographically independent molecules located in the common position (Fig. 1a). The structure of the Cd complex has distorted tetrahedral N2S2-configuration around metal ion, the coordination sphere consists of two S atoms from two monodentate coordinated diisopropyldithiophosphate ions and two nitrogen atoms from two aminobenzimidazole molecules. The bond lengths and angles (Table 2) do not differ from the normal values for Cd diisodithiophosphates [6, 2410]. An intramolecular bond between the sulphur atom and the *exo*-amino group hydrogens (distances: S… NH$_2$ 3.326, S… H — N 3.610 and 3.899 Å; angles:

S-H-N 102.34 and 126.21°) promotes the formation of an electrically stable neutral monomer metal complex stabilized by π-stacking in crystal structure. Packing of molecules in crystal along the direction [10] is shown in Fig. 1a.

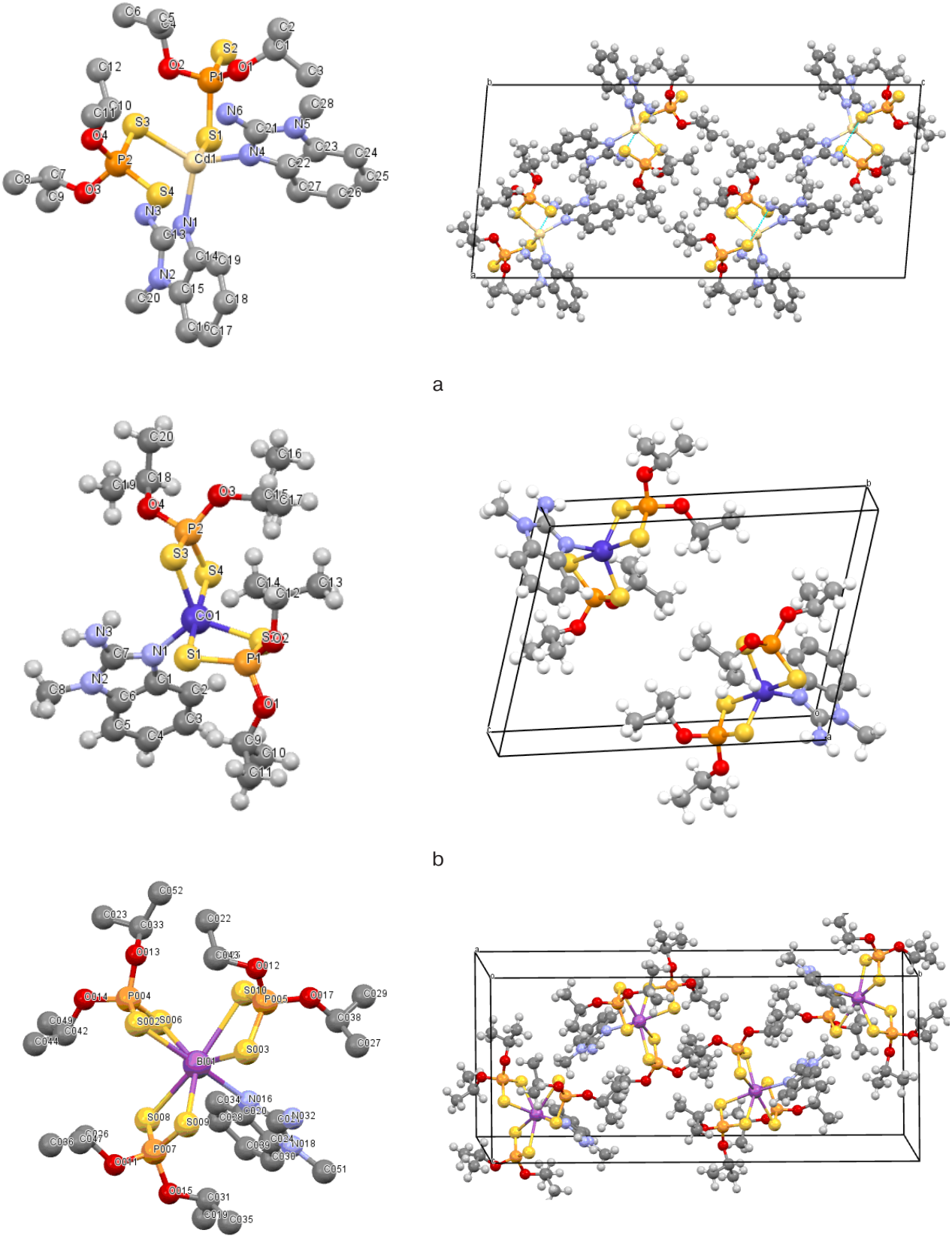

Figure 1. The structure (H atoms are not shown) and the packing of molecules: a) [Cd (MAB)$_2$ (*iso*-Pro$_2$PS$_2$)$_2$]; b) [Co (MAB) (*iso*-Pro$_2$PS$_2$)$_2$], c) [Bi (MAB) (*iso*-Pro$_2$PS$_2$)$_3$]

Table 1. – Main crystallographic parameters and coordination polyhedra in the complexes [M $(MAB)_n$ $(iso\text{-}Pro_2PS_2)_m$] (n, m=1,2; M=Cd, Co, Bi)

Crystal	**[Cd (MAB)$_2$ (*iso*-Pro$_2$PS$_2$)$_2$]**	**[Co (MAB) (*iso*-Pro$_2$PS$_2$)$_2$]**	**[Bi (MAB) (*iso*-Pro$_2$PS$_2$)$_3$]**
Parameters	$P2_1/c$, a=14,032 (5), b=8,962 (5), c=31,502 (5) Å; β=94,798 (5)°, V=3947,65Å^3, Z=4	$P2_1$, a=10.004 (1), b=10.7993 (9), c=15.0131 (14) Å; α=105.702 (8), β=90.254 (8), γ=100.018 (8)°; V=1535.31Å^3, Z=1	$P2_1/c$, a=11.389 (5), b=29.984 (5), c=12.898 (5) Å; β=101.063 (5)°, V=4322.66Å^3, Z=4
M–S, Å	Cd1–S3 2.503(2)	Co1–S1 2.6553(3)	Bi1–S2 2.7198(4)
	Cd1–S1 2.559(2)	Co1–S2 2.3041(3)	Bi1–S3 2.909(1)
		Co1–S3 2.3327(2)	Bi1–S6 2.9545(8)
		Co1–S4 2.5878(2)	Bi1–S8 2.8375(8)
			Bi1–S9 2.798(1)
			Bi1–S10 2.9977(8)
M–N, Å	Cd1–N1 2.255(5)	Co1– N1 2.0167(2)	Bi1–N16 2.6226(4)
	Cd1–N1 2.210(5)		
P–S, Å	P1–S1 2.010(3)	P1– S1 1.9708(2)	P4–S2 2.0083(6)
	P1–S2 1.935(3)	P1– S2 2.0042(2)	P5–S3 1.9937(7)
	P2–S3 2.015(3)	P2– S3 2.0025(2)	P4–S6 1.9827(4)
	P2–S4 1.944(3)	P2– S4 1.9715(2)	P5–S10 1.9777(7)
			P7–S8 1.9821(6)
			P7–S9 1.9994(7)
S–M–S,°	S3–Cd1–S1 108.72 (6)	S1– Co1– S2 80.96 (8)	S2–Bi1–S3 94.35
		S3– Co1– S4 82.90 (9)	S2–Bi1–S6 71.58
		S1– Co1– S4 173.50 (8)	S2–Bi1–S8 92.44
		S1– Co1– S3 92.30 (9)	S2–Bi1–S9 92.64
		S2– Co1– S3 121.29 (8)	S2–Bi1–S10 90.77
		S2– Co1– S4 97.76 (9)	S2–Bi1–S3 94.35
			S3–Bi1–S9 71.02
			S3–Bi1–S10 66.94
			S6–Bi1–S8 76.79
			S6–Bi1–S10 76.67
			S8–Bi1–S9 70.96
N–M–N,°	N4–Cd1–N1 111.64(18)	–	–
S–M–N,°	N4–Cd1–S3 116.96(15)	S2–Co1–N1 122.28(14)	S2–Bi1–N16 169.92(15)
	N1–Cd1–S3 114.41(14)	S3–Co1–N1 115.90(15)	S3–Bi1–N16 94.96(14)
	N4–Cd1–S1 106.87(15)	S4–Co1–N1 96.12(12)	S6–Bi1–N16 98.66(15)
	N1–Cd1–S 195.75(14)	S1–Co1–N1 89.90(14)	S8–Bi1–N16 82.62(14)
			S9–Bi1–N16 94.02(14)
			S10–Bi1–N16 89.34(15)
Bi–S–P,°	P1–S1–Cd1 102.66(9)	Co1–S1–P1 80.47(10)	Bi1–S2–P4 90.40(10)
	P2–S3–Cd1 99.74(8)	Co1–S2–P1 89.23(9)	Bi1–S3–P5 92.41(9)
		Co1–S3–P2 86.38(9)	Bi1–S6–P4 84.35(8)
		Co1–S4–P2 80.29(8)	Bi1–S8–P7 88.84(9)
			Bi1–S9–P7 89.63(8)
			Bi1–S10–P5 90.15(9)
S–P–S,°	S4–P2–S3 115.45(11)	S1–P1–S2 108.73(12)	S2–P4–S6 112.79(8)
	S2–P1–S1 114.51(12)	S3–P2–S4 110.38(10)	S8–P7–S9 110.48(8)
			S3–P5–S10 110.26
M –N –C,°	C21–N4–Cd1 127.3(4)	Co1–N1–C1 127.14(15)	Bi1–N16–C20 124.57(4)
	C22–N4–Cd1 125.9(4)	Co1–N1–C7 128.46(16)	Bi1–N16–C21 127.36(4)
	C13–N1–Cd1 125.7(4)		
	C14–N1–Cd1 128.2(4)		

The [Co (MAB) (*iso*-$Pro_2RS_2)_2$] structure has a five-coordinated distorted tetragonal pyramide polyhedron (Fig. 1b). The distorted N1S4-configuration consists of the two diisopropyldithiophosphates S-S-donor atoms of and the benzimidazole *endo*-cyclic nitrogen. In spite of the Co polyhedron in [Co $(MAB)_2$ $(Ac)_2]\cdot H_2O$ complex [7, 1373], where Co had a tetrahedron configuration with the monodentate coordinated acetate groups, the sulfur atoms lead to 5-coordinated polyhedron in the [Co (MAB) (*iso*-$Pro_2RS_2)_2$] structure, and the SCoS angles within 4-membered chelate rings are deviated in range of 82.90–80.96°. The phosphorus atoms have distorted-tetrahedral configuration (the SPS and OPO angles are equal 110.4, 108.7 ° and 95.71,100.56 °, respectively, the P – S bonds are equal to 1.971 and 2.004 Å), the distance P – O (1.573–1.579 Å) corresponds to single bonds. The Co – N bond is localized via *endo*-cyclic N-atom. The bond length, angles in the benzimidazole ligand are similar to the 2-amino-1-methylbenzimidazole hydrochloride structure [8, 520] and 2-amine-1-methylbenzimidazole dichlorocobalt (II) [7, 1373]. Analysis of the bond lengths and angles of the molecules in the coordination compounds clearly indicates that the MAB molecule has amino-tautomeric form. Amino group is coplanar with a methyl group (the C8– N2– C7– N3 torsion angle is equal to 3.14°), the Co – N bond length (2.017 Å), the Co – S bonds lie in the range of 2.304–2.665 Å, which are comparable to known dithiophosphoric acid complexes containing ligand in a similar orientation [6, 2410].The intra- and intermolecular hydrogen bonds and crystallization water are absence in contrast to similar complex [7, 1373].

The structure of the synthesized mixed-ligand complex [Bi (MAB) (*iso*-$Pro_2RS_2)_3$] characterized by distortion of the pentagonal bipyramidal N1S6-configuration observed in structures of *tris*-diisopropyldithiophosphate of bismuth (III) and gold (III) [9, 369] due to insertion of the 1-methyl-2 aminobenzimidazole molecule. Therefore, bismuth ion is coordinated with six sulfur atoms of bidentate diisopropyldithiophosphate ions and an nitrogen atom of the aminobenzimidazole molecule (Fig.1c). The bond lengths and angles in the complex do not differ from the normal values. The hydrogen bonds are not observed, and the monomer complex particles combined with each other by π-stacking interactions. Packing of complex molecules is shown in Fig. 1c.

4. Conclusions

The [Cd(MAB)2(i-Pro2RS2)2], [Co(MAB)(i-Pro2RS2)2] and [Bi(MAB)(i-Pro2RS2)3] were synthesized and the crystal structures were determined. The structure of the Cd complex has distorted tetrahedral N2S2-configuration. The Co complex molecule has distorted N1S4-tetragonal pyramid coordination structure. The structure of the Bi complex has N1S6-distorted pentagonal bipyramidal molecular geometry configuration. The diisopropyldithiophosphates are bidentate coordinated via S-S-donor atoms in the Co and Bi complexes, and S-monodentate coordinated in the Cd complex. The 2-amine-1-methylbenzimidazole coordinated via endo-cyclic nitrogen. Packing of molecules in crystal characterized by π-stacking interactions without strong intermolecular hydrogen bonds.

References:

1. Alimarin I. P., Ivanov V. M. Extraction with thio and dithio phosphorus acids//Russian Chemical Reviews. – 1989. – T. 58. – №. 9. – C. 863.
2. Rakhmonova DS, Kadirova Z.Ch., Kadirova Sh.A., Parpiev N.A., Dzhorakulova N.H. Synthesis and study of complex compounds of mixed metal acetates of Co (II), Cu (II) with 2-amino-1-methylbenzimidazole//Chemistry and Chemical Technology. – 2015. – No 1. – P. 40-42.
3. Grundemann E., Graubaum H., Martin D., Schiewald E. NMR investigations on benzheteroazoles. 2—NMR investigations of N-acylated 2-aminobenzimidazoles//Magnetic resonance in chemistry. – 1986. – T. 24. – No. 1. – C. 21-30.
4. Daminova S. S., Talipova L. L., Sharipov K. T. The complex compounds of noble metals with diisopropyldithiophosphoric acid //Abstracts of Papers of the American Chemical Society. – 1155 16th ST, NW, Washington, DC 20036 USA : Amer Chemical Soc, – 2002. – T. 224. – C. U674-U674.
5. Sheldrick G. M. A short history of SHELX//Acta Crystallographica Section A: Foundations of Crystallography. – 2008. – T. 64. – No 1. – C. 112-122.
6. Lawton S.L., Kokotailo G.T. Crystal and molecular structures of zinc and cadmium O, O-diisopropylphosphorodithioates//Inorganic Chemistry. – 1969. – T. 8. – №. 11. – C. 2410-2421.
7. Chekhlov A. N. Crystal and molecular structure of bis (2-amino-1-methylbenzimidazole-N) dichlorocobalt (II) //Russian Journal of Inorganic Chemistry. – 2004. – T. 49. – No 9. – C. 1373-1377.

8. Borodkina I. G., Antsnshkina A. S., Sadikov G. G., Mistrnukov A. E., Garnovskii D. A., Uraev A. I., Borodkin G. S., Garnovskaya E. D., Sergienko V. S. & Garnovskii A. D. A model system for the study of competitive coordination in aminoheterocyclic complexes. Molecular and crystal structure of 2-amino-1-methyl-benzoimidazolium chloride hydrate //Russian Journal of Coordination Chemistry. – 2003. – T. 29. – No 7. – C. 519–523.
9. Sharipov K. T., Daminova S. S., Talipova L. L. Crystal and Molecular Structure of Rhodium (III) Diisopropyldithiophosphate //Journal of Structural Chemistry. – 2002. – T. 43. – No 2. – C. 369–372.

DOI: http://dx.doi.org/10.20534/AJT-16-11.12-71-75

Qurbanov Zufar,
assistant,
Tashkent chemical-technological institute
Ikromov Abduvaxob,
professor,
Tashkent chemical-technological institute
E-mail: Ulug85bek77@mail.ru

Synthesis of fatty Acid amide by the sherbule reaction based distilled Fatty Acids

Abstract: Field of application of fatty acid amides because of their reactivity is various. Nitrites, primary amines, valuable flotation agents, additives for fuels based on fatty acid amides have been produced. The amides are obtained based on fatty acids. A fatty acid synthesized by oxidation of paraffins. Until recently, the raw material for the production of paraffin's are hydrocarbon sources, such as oil and natural gas, gas condensate, coal and others. It should be noted that, the content of higher hydrocarbons is low in these sources. Various oxidants are used to produce acids from them. The process is conducted under severe conditions at high temperatures and under high pressure. However, because of decreasing fossil fuel and oil reserves, other raw materials for the production of carboxylic acids have to be investigated from scientists. In this regard, distilled fatty acid (DFA) obtained from soapstock is perspective and the separation of individual components is considered as an actual task.

Keywords: amine, amide, sylvinite, fatty acids, chloride, acid.

The world population is growing rapidly, and the fact that is expected to reach more than 9 billion by 2050, it became evident that the world needs to produce more food to keep up with the growing number of mouths to feed. However, increasing number of people means further urbanization and therefore less farmland to work with, which means that farmers need to increase productivity. It means, by increasing population, the demands for the production of potassium fertilizer also increases. 200,000 tons of export-oriented import substitution potash annually produced in Dehkanabad potash plant [1]. Potash fertilizer is prepared from sylvinite. Uzbekistan occupies one of the leading place in the world by sylvinite stocks. In the stock of Tyubegatana the sylvinite reserve is 215 million tons. Separation of sylvinitefrom ore is carried out by flotation and amines can be used in this purpose. They are used in pharmacy, cosmetics, organic synthesis and in the production of potassium chloride as flotation reagent.

The demand for amines in the "Dehkanabad potash plant" is 250 tons annually. Amines are not produced in Uzbekistan. Therefore, at the present time they buy from foreign countriesfor 3000 USD per ton. Withthe expansion of capacity of the plant the demands for amines also increased.

Higheracid (intermediates of oil and fat industry), fuel alcohols (waste products of biochemical plants), as well as urea and sodium hypochlorite can be used as raw materials for the synthesis of amines [2].

The synthesis of amines is carried out in three stages. In a first step the fatty acid amides are synthesized according to the following reaction:

$$R - COOH + CO(NH_2)_2 = R - CONH_2 + NH_3 + CO_2$$

Reactions carried out at temperatures about 170–180 °C and at atmospheric pressure. In the second stage, primary amines are obtained by Hofmann rearrangement. The process proceeds according to the next reaction:

$R - CONH_2 + NaClO + NaOH + C_2H_5OH_{(solute)} = R - NH_2 + NaCl + CO_2$

The second stage reaction is carried out at a temperature near 80 °C and at atmospheric pressure. In the third step, primary amines in the presence of fusel alcohols areconverted to secondary amines:

$R - NH_2 + R' - OH + K = R - NH - R' + H_2O + K$

In this paper, we havestudied the separation of higher fatty acids and obtaining amides on their basis.

Samples of fatty acids were analyzed by chromatography. At first, fatty acid mixture was treated with diazomethane and transferred their methyl esters. The synthesized fatty acid methyl esters was purified by thin layer chromatography using silica gel adsorbent in the solvent system of hexane/diethyl ether at the ratio of 4:1. The resulting layer of silica gel with methyl ester of fatty acids was treated with iodine vapor. Chloroform was desorbed from silica gel containing methyl ester. After the release of methyl esters from chloroform, samples were placed in a tube and through the adsorbent passed over the solvent hexane [3].

Then, the analysis were carried out on the instrument *Agilent Technologies 6890 N* equipped with a flame ionization detector at a temperature of between 50 °C – 270 °C, in a capillary of 30 m length, filled with the nonpolar phase HP-5. Carrier gas was helium withthe rate of 30 ml/min.

Studied fatty acid composition is shown in Table 1. It can be observed from the table that in the investigated samples of fatty acids mainly contains palmitic ($C_{15}H_{31}COOH$-30,3%), oleic ($C_{17}H_{33}COOH$ – 22,7%) and linoleic ($C_{17}H_{31}COOH$– 42,3%) acids. The study determined on samples of Kattakurgan oil and fat manufacture containing 10 different fatty acids. Exactly, 7 ofsaturatedfattyacids (total – 34.4%) $C_9H_{19}COOH$, $C_{13}H_{27}COOH$, $C_{15}H_{31}COOH$, $C_{16}H_{33}COOH$, $C_{17}H_{35}COOH$, $C_{19}H_{39}COOH$ and 3 unsaturatedfattyacids (total – 65.7%) $C_{16}H_{31}COOH$, $C_{17}H_{33}COOH$ and $C_{17}H_{31}COOH$.

To separation of certain components of fatty acids, distillation temperature were analyzed. Reference data showed that the distillation temperature of palmitic, oleic and linoleic acids are 230.7 °C, 232.0 °C and 230–233 °C at a pressure of 15 mmHg, respectively.

These data show that the temperature in the vacuum distillation of all three fatty acids have substantially similar values. Therefore, the separation into the individual components by a process of distillation of a mixture of fatty acids from DFAin the laboratory revered impractical. The melting point of the fatty acids are very differen: palmitic acid – 62.5–64.0 °C; oleic acid – 13.4–16.8 °C and linoleic acid 5–5.2 °C. This enabled us to separate a technical fatty acid to separated components with small amounts of other fatty acid impurities [4].

Table 1. – The composition of fatty acids,%

Fatty acids	t %
Caproic acid10:0	0.1
Myristic acid 14:0	1.0
Palmitic acid 16:0	30.3
Palmitoleic acid 16:1	0.7
Margarine acid 17:0	0.1
Stearic acid 18:0	2.5
Oleic acid 18:1	22.7
Linoleic acid 18:2	42.3
Arachidic acid 20:0	0.2
Behenicacid 22:0	0.1

Thus, samples of fatty acidsfrom Kattakurgan fat-and-oilmanufacture, are studied. The composition of the fatty acids are determined on the instrument *Agilent Technologies 6890 N*. Individual components, such as palmitic acid, oleicacid and linoleic acid are separated from the mixture offatty acidsbased on melting points, in the technical form including small amount of other fatty acids.

Table 2. – Composition of fusel oil

Composition	%
Isoamylalcohol	65–75
Isobutylalcohol	4–8
Propylalcohol	5–7
Ethanol	1–2
Aldehydes	0,01–0,05
Octyl-nonylalcohols	0,1–0,2
Furfural	0,01–0,02
Fattyacids	0,01–0,05
Water	10–15
Other components	~ 1

Data in the table are averaged accordingly data taken from four different manufactures.

The purpose of research is to provide secondary and tertiary fatty amines. At the first stage we received amides of the DFA on Sherbule reaction.At the second stage, the primary fatty amines are produced by Hoffman rearrangement reaction.At thethird stage, secondary and

tertiary fatty amines by alcoholysis of primary amines with alcohols of fusel oil (wastes of biochemical plants) [5]. In this purpose, the chemical composition of fusel oilssampled from biochemicalmanufactures of Uzbekistan (Yangiyul biochemical plant, Bektemir alcohol plant, Kokand alcohol plant and Andijan biochemical plant) have been studied.

Fusel oil is an oily liquid with a strong unpleasant odor, from light yellow to reddish-brown color with a density of 0.82–0.85 g/cm^3 (at 20 ° C). The composition and properties vary depending on the raw material and the fermentation conditions and selection of fractions at distillation process. The distillation yield of crude alcohol – 0.4–0.8%.

The main components of fusel oil are monohydric saturated alcohols of C_3-C_9, which the main component is isoamyl alcohol. In addition, isobutyl alcohol, propyl alcohol and small amounts of higher alcohols and aliphatic aldehydes, fatty acids, and furfural also can be found from the composition (Table 2).

Fusel oil is fractionated on a continuous pilot plant (Figure 1).

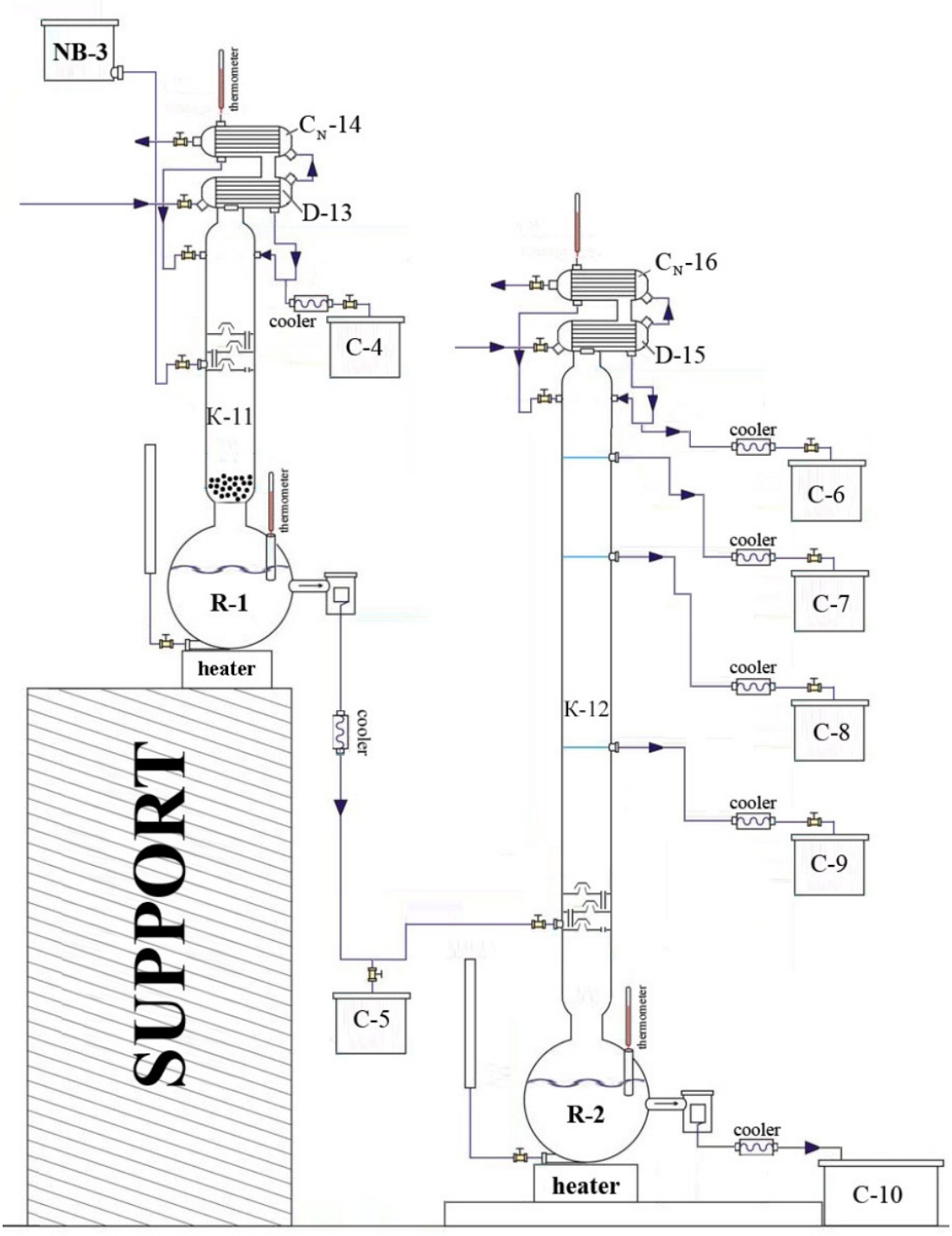

Figure 1. The continuous pilot plant for the fractionation of binary liquid mixtures

Fractionation of substances is conducted depending on boiling points of components containing in the fusel oil. The reflux ratio in the columns is determined by the allocation of the next light volatile fractions. Each separated fraction is fractionated once again in the pilot plant.

Aliphatic amides of cottonseed oil fatty acids synthesized by Sherbule method through the interaction of urea with fatty acids:

$$R-COOH+CO(NH_2)_2=R-CONH_2+CO_2\uparrow+NH_3\uparrow;$$

$$R=C_{12-22}H_{25-45}$$

The synthesized amides were characterized by IR spectrometer "Agilent Technology FTIR-640" (USA) (Figure 2) and gas chromatography-mass spectrometry with gas chromatography complex "Agilent" (Figure 3).

The vibrational transitions for synthesized amides were identified based on the recorded FT-IR spectra in the range of 4000–400 cm^{-1}; the total number of scans is 12.

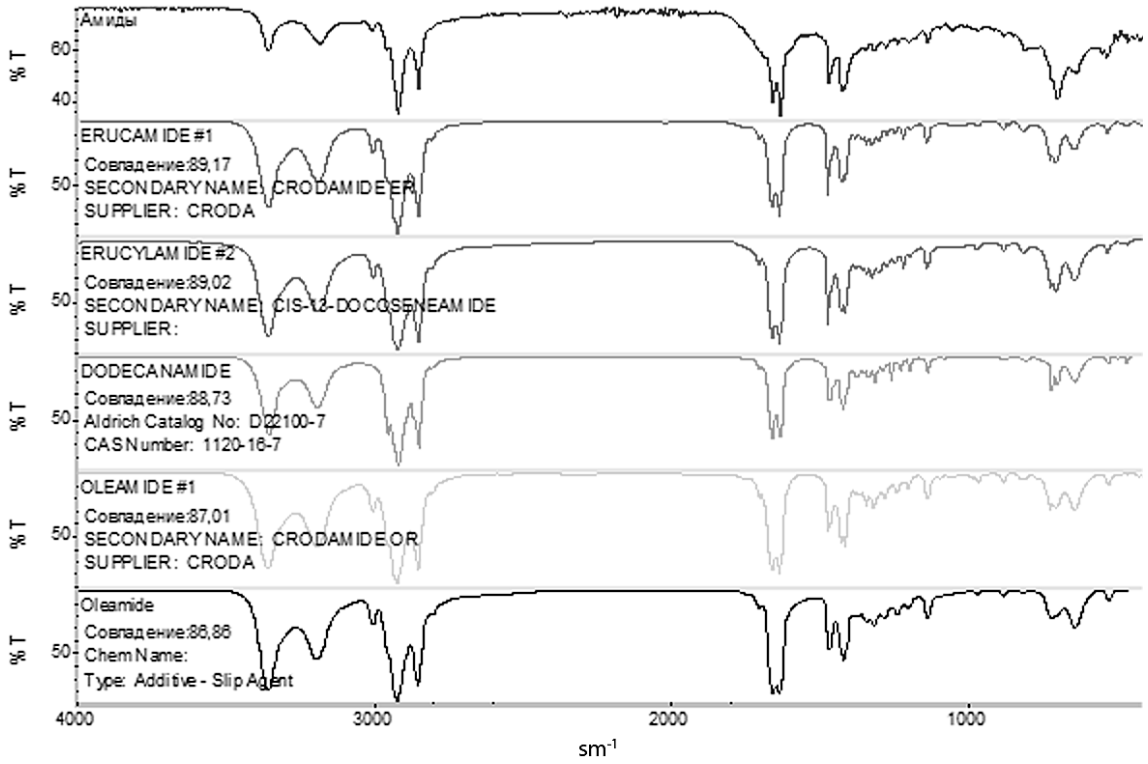

Figure 2. IR spectra of the synthesized fatty acid amides

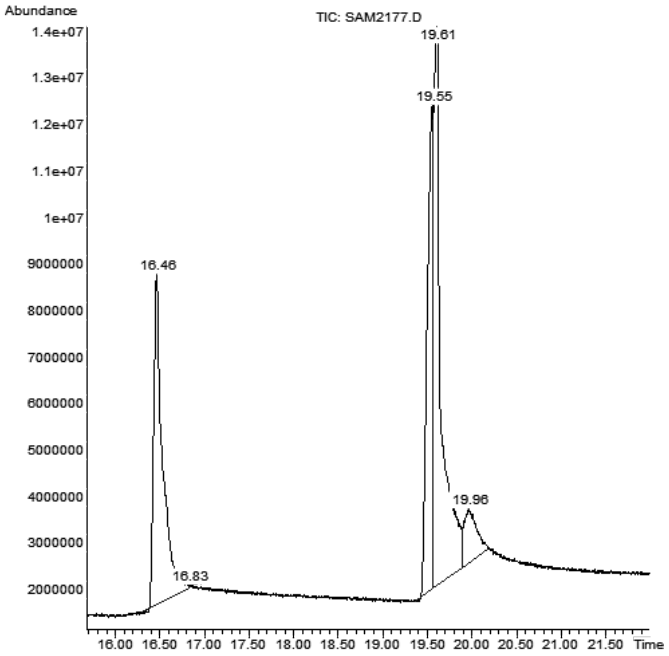

Figure 3. Chromatography/Mass Spectrometry mixtures of aliphatic fatty acid amides

Chromatography/mass spectrometry investigation of the mixture was carried out on a gas-chromatography complex "Agilent 6890B" with mass selective detector "Agilent 5973 inert"; ionization energy of 70 eV; ion source temperature of 230 °C; the temperature of mass filter of 180 °C. Separation was performed on a capillary column HP-5ms, 30m x 0.32mm, stationary phase thickness of 0.50μm (Agilent, USA). Helium was used as carrier gas; carrier gas flow — 1.1 ml/min, input mode — Split 1:20. Separation was carried out in the temperature programming mode: isotherm 170 °C for 4 min, heated to 280 °C at 5 °C/min, isotherm 280 °C for 15 min. Evaporator temperature — 280 °C, sample injection volume of 4μl. Detector interface temperature of 300 °C. Sample preparation. 0.02 g of a mixture of fatty acid amide is dissolved in 5 cm^3isoamyl alcohol (Figure 3).

Studied acid amides can be used as intermediate products for the synthesis of amines by Hoffmann

rearrangement. The secondary and tertiary amines widely used as a flotation agent.Thus, aliphatic amides were synthesized based on the fatty acid mixtures obtained from oil industry wastes. IR spectrometry and gas chromatography/mass spectrometry were conducted in order to analysis of a mixture of aliphatic fatty acid amides.

References:

1. Osichkina R. G., The raw material base of potash and halurgical industry in Uzbekistan, Uzbek chemistry journal, – 2001, – V2.
2. Gitis S. S., Glaz A. N., Ivanov A. V. Workshop on Organic Chemistry of Organic Synthesis, – Moscow, – 1991, – P 303.
3. Weigand K., Experimental methods in organic chemistry, – Moscow. – 1952, – P737.
4. Reutov O. A., Kurs A. L., Butin K. P. Hofman rearrangement.Organic chemistry, Part 4. – Moscow. – 2004. – P. 367–368.
5. Yettiboeva L. A., Gapparov C., Kadirov O.Sh. The chromatographic analysis of fatty acids in the composition of waste of Gulistan fat-and-oil plant, Actual problems of analytical chemistry, IV Republican scientific conference, – 2014, – Volume 1, – P. 303–305.

DOI: http://dx.doi.org/10.20534/AJT-16-11.12-75-77

Mahamathozhaev Dilmurad Rahmatovich,
Tashkent State Technical University,
senior research fellow researcher of the
department «Drilling oil and gas wells
E-mail: sunnatilla29@rambler.ru

Application of mud composition at the opening of unstable clay deposits

Abstract: This paper presents the results of laboratory studies on the development of the composition of inhibiting clay-free drilling fluid and the results of its industrial tests in drilled wells AK "Uzgeoburneftegaz".

Keywords: montmorillonite, scree, landslide, taking the drilling tool, the oil bath that inhibits mud.

In the oil and gas fields in Uzbekistan there are powerful clay deposits consisting of montmorillonite, siltstone, mudstone, and others. Argillaceous rocks. Autopsies clay deposits is often accompanied by talus and landslides wells wall, caused by the interaction of the filtrate used clay mud with passable argillaceous rocks [1, 236–239].

For example, in the area occurred Darahtli № 2 sticking drilling tool due to violation of the integrity of the well bore. To eliminate the sticking of the drilling tool it took 2757 hours. That's the reason stated above in the squares Kokdumalak № 412, 428, Taylok № 9, № 20 North Shurtan, Qamar № 1, Girsan № 29, № 35 and other Chulkuvar occurred sticking drilling tool for the elimination of which spent a huge calendar time and material and technical resources [2, 168–170].

Due to the fact that the cut oil and gas wells, consists of different types of rocks and composition, will act not identical under identical conditions, the mud filtrate. Therefore, the most important factor in maintaining the stability of the borehole is the right choice of the type of drilling mud and its composition, as well as technological parameters [3, 192–198].

The standard formulation of drilling fluids is regulated to maintain filtration indicator while drilling argillaceous rocks less than 10 cm3/30 minutes, which should be provided work reagents stub analyzer in an alkaline medium, ie. E. At a pH greater than 7, especially at elevated temperatures and salinity. But argillaceous rocks have minimum filtration capacity relative to the liquid hydrocarbon — oil (oil fields tires) and water based systems — muds.

At pH = 7 the concentration of hydronium ion (H30 +) and hydroxyl (OH–) is the same. In the case of drilling fluids with pH> 7 the equilibrium dissociation constant is displaced to the right, ie. E. The amount of hydroxyl ions dissociated increases. In this case, the diffusive mass transport begins concentration equalization between mud filtrate and Doi clay-pore, resulting in cell structure from compensation, in general, to weaken bonds between layers and, ultimately, to shattering rock at the borehole wall.

To eliminate this effect the authors of [4, 30–31], was designed drilling fluid formulation with a pH = 6.5 … 7.0 to shift the equilibrium dissociation constant of water left by the reaction:

$H_2O + H_2O + OH– = ON_3 –$ or $2H_2O = H_3O + OH–$

The proposed formulation does not contain chemicals that are in the structure Sodium (caustic soda, soda ash, and others.) Since at higher pH occurs first replacing ion-water type (hydronium) in the clay, and then replacing metal (potassium) of sodium ions. Control of pH and the calcium ions is performed inorganic potassium compounds.

The formulation of drilling mud with a pH of about 7 and an indicator of filtration of up to 20 cm 3/30 min VM-6 was successfully used in the drilling of deep wells, descent and cementing intermediate casing diameter of 219 mm to a depth of 4100 m in the range of occurrence of mudstone.

Given the experience of the application of the composition of the drilling fluid, proposed by the authors [4, 30–31], we have developed a composition of clay-free drilling fluid with inhibitory with pH less than 7 and a low filtration rate for borehole in an unstable clay deposits on the oil and gas fields of JSC "Uzgeoburneftegaz". The results of laboratory tests are shown in Table 1.

Table 1. – The composition and properties of drilling fluids intended for the opening of unstable clay deposits

№	Mud composition	ρ, kg/m³	T_{500}, c	F, cm³/ 30 min	$T_к$, mm	pH	sludge, %
1.	1000 ml of water + 15 g PAA + 300g of NaCl + 50g HCl +30 g graphite + 100 ml of oil	1190	35	4.0	1.0	6.0	6.0
2.	№ 1 + 50% marble powder (Nurata)	1350	45	4.0	1.0	6.0	0
3.	№ 1 + 90% marble powder (Nurata)	1480	75	4.0	1.0	6.0	0
4.	№ 1 + 130% marble powder (Nurata)	1650	120	4.0	1.0	6.0	0
5.	When heated № 5 at 900° C	1650	60	6.0	1.0	6.0	–
6.	№ 6 after cooling to 20 C	1650	125	3.0	1.0	6.0	0

As can be seen from Table 1 based on unhydrolyzed polyacrylamide can prepare a clay-free drilling fluids inhibitor with stable processing characteristics. With the introduction of marble powder can be easily adjusted value of the density of the developed composition of clay-free drilling fluid inhibition. Not unimportant advantage of the proposed composition of the mud is to preserve the original processing properties at high temperatures.

As the data in Table 1 in the preparation of a clay-free drilling fluids inhibiting we abandoned the use of clay, caustic and soda ash and polymer reactants such as 4 K, starch, CMC, VPRG, Uniflok. Also excludes the use of imported organic reagents breakers (CSSC, FXLS, RVSM, etc.), Which are widely used for the passage of clastic sediments to regulate the relative viscosity of drilling mud clay water-based.

On the basis of laboratory tests and received positive results of the composition of inhibiting mud recommended for industrial testing in the wells drilled NHC «Uzbekneftegaz»

Industrial testing of the composition of inhibiting clay-free drilling fluid is produced while drilling the borehole under the technical column on Chunagar Square № 20. First clayless inhibitory prepared fresh mud in a volume of 180 m3, with the following technological parameters: density, 1250–1260 kg/m3; relative viscosity — 35 seconds; Filtering — 3.5–4.0 cm 3/30 min; the pH = 6.0–6.5. After that the replacement of the working circulating clayey mud inhibiting new mud. Drilling of the borehole was carried out using a diamond bit of the Chinese production. In the process of deepening wells circulating drilling fluid is easily separated from major cuttings and colloidal clay particles using vybrosito and sand separator. At the same time technological parameters of the circulating drilling mud remains unchanged, as small clay colloidal particles interacting with flocculant — non-hydrolyzed polyacrylamide aggregated to form a paste-like mass that can be easily removed with the help of treatment plants. Due to this recess during wellbore drilling process parameters circulating solution remained unchanged.

During the ascent and descent of the drilling tool is not seen tightening and planting tools. And this in turn indicates the termination of the hydration and swelling of clay rocks forming the walls of the wells. Prevention, the process of hydration and swelling of argillaceous rocks is provided by the simultaneous action of several inhibiting additives, as well as through the creation of the walls of

the well impermeable thin solid filter cake formed from a non-hydrolyzed polyacrylamide and marble powder. In addition, the use of the proposed composition of the mud help to prevent the formation of glands above the bit and calibrators.

With the application of the proposed composition of inhibiting mud hole to deepen the process was carried out without complications and accidents related to the instability of the borehole wall, and dramatically reduce the time spent on chemical treatment of circulating drilling mud. Rose, mechanical drilling speed in comparison with the use of clay mud, which is widely used in the practice of construction of oil and gas wells. In the process of deepening the wellbore average penetration rate was 8–10 m/h. And this in turn led to a reduction in the wellbore drilling time by a technical column in easily swell and collapsing clay deposits on the Square. Chunagar-20.

Casing safely lowered to the design depth and produced cementing. By obtaining the nominal diameter of the well № 20 Chunagar area, formed a solid impenetrable stone cement behind the casing. Due to what has raised the quality of well casing in the field and, ultimately, led to the improvement of technical and economic indicators of well construction.

Based on the industrial test composition on skv.№ 20 Square. Chunagar and obtained positive results, the proposed composition of inhibiting mud recommended for further use in drilled wells AK «Uzgeoburneftegaz». For example, on the areas of Shurtan-295, New Alan-8, Yangi Karatepa 21, Ilim-12 proposed by the drilling has been successfully used for drilling a borehole in clastic sediments composed of the swell and easily dispersible clay rocks.

As a result of research work on the development of the composition of inhibiting mud and held it for industrial testing in field conditions, the following conclusions:

1. Based on the analysis of geological and technical conditions for drilling oil and gas wells in Uzbekistan found that the most common complications associated with the loss of stability of the borehole, which manifest themselves in the form of landslides and avalanches of argillaceous rocks.

2. It is found that the stability of the well walls folded argillaceous rocks depends on numerous factors independent of each other. To ensure the integrity of the walls of wells during drilling and easily collapsing swellable clay deposits, it is expedient to use special inhibiting muds.

3. The new composition of the clay-free drilling fluid is inhibited to stabilize the well walls in clastic sediments. The distinguishing feature of the composition of the mud developed compared with other types of drilling muds is inhibiting exclude application of caustic soda and soda ash, clay and alkaline polymeric reagents and reactants of imported organic diluents at their preparation and chemical treatment.

4. It was found that the use of inhibiting mud based on non-hydrolyzed polyacrylamide and local inhibiting additives provide improved technical and economic indicators of well construction, due to the prevention of complications and accidents that occur in the process of deepening the wellbore in clastic sediments.

References:

1. Mahamathozhaev DR, FS Kurbanov Huzhamov H. R. Ingibiruyuschy mud to prevent landslides and avalanches wells wall//Collection of scientific works. International scientific-technical conference "Modern problems and ways of development of mineral resources of oil and gas potential" (22 November – 2012 November) – Part 1.
2. Mahamathozhaev D. R. The composition of inhibiting mud for drilling a borehole in clastic sediments//Proceedings of the international conference dedicated to the 85th anniversary of academician Azad Khalil corners Mirzadzhanzade, – Baku, – 21–22 November – 2013.
3. Mahamathozhaev D. R. The drilling fluid for drilling a borehole in clastic sediments//Herald of Tashkent State Technical University. – Tashkent, – 2014. – No 3.
4. Sergeev G. L. Lebzin D. E., Zhigulin V. P. Ambarnova L. drilling fluid technology for drilling in the crumbling shale, mudstone//Drilling and Oil. – M.: Burneft, – 2004. – No 12.

DOI: http://dx.doi.org/10.20534/AJT-16-11.12-78-81

Rahmonov O'ktam Kamolovich,
Head of research and preparation
of scientific and pedagogical staff
of the Tashkent State Technical University
E-mail: uraxmonov@umail.uz

Rakhmonov Toyir Zoyirovich,
"Lukoil Uzbekistan Operating Company"
E-mail: trahmonov@lukoil-international.com

Study of the process of deposition of fine particles in the apparatus with a movable nozzle

Abstract: Based on the analysis and solutions of the equations of motion the formulas allowing to calculate the trajectory of the particles in the carrier gas stream were obtained. Computer and laboratory experiments were condutet and the efficiency of purification of fine particles in the dust collecting apparatus with movable nozzle were depined. The results obtained demonstrate a proper convergence parameters. The investigated dust unit can be used to trap aerosol submicron particles with high efficiency and low energy consumption.

Keywords: Equation movement, fine particles, dust equimont, cleaning efficiency, movable nozzles, gas velocity, intensification process.

Deposition of dust particles on droplets under the forces of inertia are implemented in de-dusting apparatus of wet type. The essence of inertial particle deposition is that when dusty gas flow around a spherical water droplets diameter d_K, current line separated when approaching the drop and closed after its passage. Larger particles under the influence of inertial forces converge with lines and reaching the surface of the droplet deposited on it. Small particles do not have sufficient kinetic energy to overcome resistance to gas and follow the line current, Flex drop and away gas flow. According to the theory of de-dusting [1] likelihood of particle deposition on the drops under the influence of the inertia force increases with increasing mass of particles and increased the speed of its movement towards the drop, and decreases with increasing diameter and resistance drops Wednesday.

According to [2] to increase the speed of the gas and, accordingly, the ratio of kinetic and potential energy (EC/EP) changes the State of the gas-liquid system, accompanied by phase inversion, and eventually the emergence of regimes rising could.

In heavily turbulent flows with heavy traffic flows of packed bodies appear active factors influencing liquid droplets capture small inertial particles. These parameters can significantly alter the terms of a potential flow around the spherical particles of the gas flow. In machines with energy-carrying gas flow in pneumatic transport modes of intense gas-liquid layer influence the turbulence becomes the decisive factor of the deposition of aerosol particles.

Such a mechanism, called inertial-turbulent proposed in [3]. The mechanism opens wide possibilities of theoretical performance analysis of delay aerosols in real liquid systems, which requires however use limiting assumptions do not distort the real picture of the process, which consists in the following: distribution of particles in the volume was adopted evenly distributed, turbulent pulsations taken mono-harmonic, intensity turbulent pulsations is determined by turbulent energy carrier flow, particle, whose coordinates are the coordinates of the drops are considered embedded in the drop.

Movement of sub-micron particles relative to the carrier gas flow is pulsed. The influence of turbulent pulsations on the particles sizes 0.5 ÷ 1 mkm is estimated through the analysis of the equations of motion of the particles.

Differential equations of motion of particles [4] for the longitudinal and transverse speed of gas taking the harmonic dependence of the velocity of turbulent pulsations of time, can be written as follows:

$$\left.\begin{aligned} \ddot{x} + \beta \dot{x} &= \beta\left[U_x + U_{(x)} Sin\ \omega\tau\right] \\ \ddot{y} + \beta \dot{y} &= \beta\left[U_y + U_{(y)} Sin\ \omega\tau\right] \end{aligned}\right\} \quad (1)$$

where β — inertia parameter of particles;

$$\beta = \frac{18\mu}{\rho_r \cdot d_r^2}$$

$U_{(x)}$ — amplitude values of the longitudinal turbulent momentum;

$U_{(y)}$ — amplitude values of the transverse turbulent momentum;

ω — pulse frequency.

On the equations of potential U_x movement are defined by longitudinal and transverse components U_y of the velocity:

$$\left.\begin{aligned} U_x &= U_0\left[1+\frac{1}{2}\left(\frac{R_o}{R}\right)^3\left(1-3\frac{x^2}{R^2}\right)\right] \\ U_y &= -\frac{2}{3}U_0\left(\frac{R_0}{R}\right)^3\frac{xy}{R^2} \\ R &= \left(x^2+y^2\right)^{0,5} \end{aligned}\right\} \quad (2)$$

After mathematical transformations get equation, which allows you to calculate the trajectory of particles in the carrier gas stream:

$$\left.\begin{aligned} x &= A + U_x\tau - \frac{a\omega\beta}{\sqrt{\beta^2+\omega^2}}Sin\left(\omega\tau+\phi_0\right) \\ y &= B + U_y\tau - \frac{b\omega\beta}{\sqrt{\beta^2+\omega^2}}Sin\left(\omega\tau+\phi_0\right) \end{aligned}\right\}, \quad (3)$$

where

$$Sin\phi_0 = \frac{1}{\sqrt{1+\frac{\omega^2}{\beta^2}}}. \quad (4)$$

When you combine the coordinates of a moving particle coordinates drops a particle is considered settled on drop.

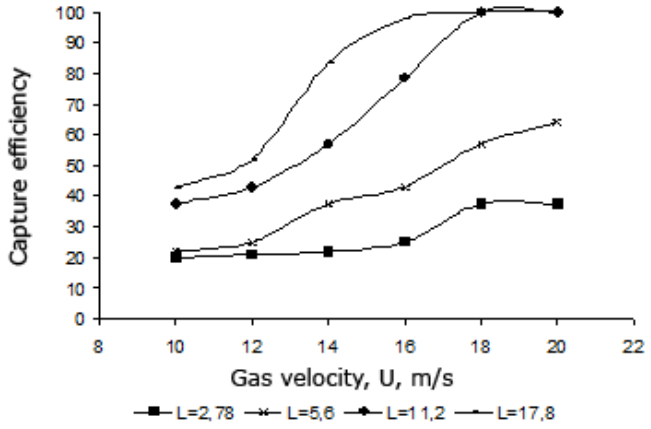

Figure 1. d=2 mkm diameter submicron particle trapping efficiency depencence of gas velocity. Irrigation accurary L×10^{-3}

Computer experiment conducted for the study of the trajectory of the particle size 0,5÷2 mkm. Dust collection efficiency dependence is defined from the gas flow rate and the density of irrigation. In the experiment of a gas-liquid flow rate changed in the range from 10 m/s to 20 m/s and density of irrigation within 0.00278 ÷ 0.0178 m/s.

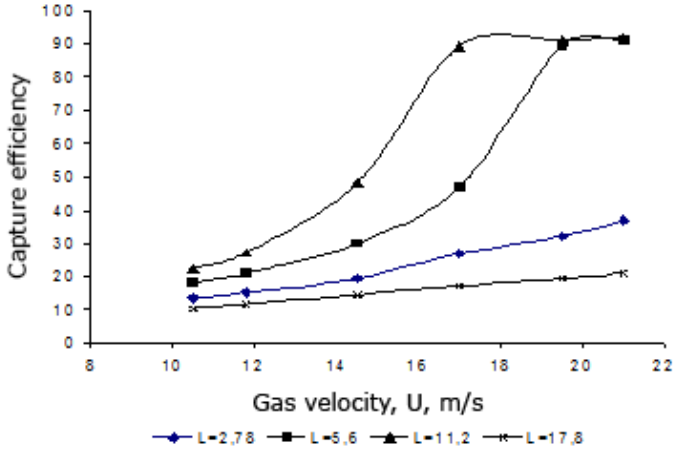

Figure 2. d=0.5 mkm diameter submicron particle trapping efficiency depencence of gas velocity. Irrigation accurary L

Dust collection efficiency dependence of gas flow velocity for particles dr = 2 mkm (fig.1) shows that at speeds above 16 m/s and irrigation density 0.014 ÷ 0.08 m/s effectiveness gives 97 100 ÷%. For particles of size d_r=0,5 mkm (fig. 2) the value of the dust collection efficiency reaches 90% at a speed of 18 m/s gas with a density of irrigation of 0.0178 m/s.

To verify the theoretical results of us studies to identify the extent of the capture of fine aerosols in the dust collecting device with the enclosed attachment.

In the process of research have been measured by definition, fluid and gas flow, gas flow and dispersion of dust of dust.

To determine the dust gas stream external filtering method used on filters AFA.

In so doing, to create iso-kinetic in the selection of sample measurements were done beforehand the speed of movement of the gas piping using a gauge metric tube MIOT. Essence of the method is to achieve equality in line with the flow velocity of the sampling tube and a tract in the sample gas movement.

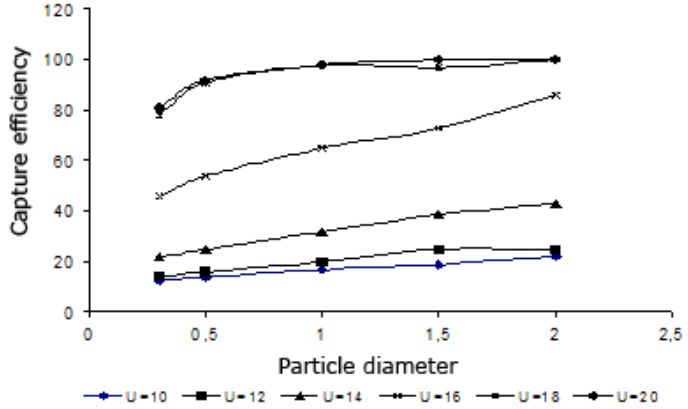

Figure 3. Submicron particle trapping efficiency depencence of fractional composition. Gas velocity U, m/s

Research each filter weighed before and after measurement using the analytical balance. Knowing the difference between scales, cleaning efficiency was determined by the following formula:

$$\eta = \frac{\Delta G_1 - \Delta G_2}{\Delta G_1} \cdot 100\% \qquad (5)$$

To determine particulate emission composition used the method of the internal filter cascade impacting factors, design by NIIOGaz. To identify studies capture sub-micron particles in the device with the enclosed attachment (HV) pilot plant was installed. Installation consists of operations 80 mm diameter HV apparatus, consisting of 200 mm diameter separator, gas blower, running on vacuum. Gas consumption was measured using gas turbine TURGAZ counter-3.

Water consumption by using rotameter. When conducting studies for obtaining fine-dispersed aerosol modeling used arc cutting metals, burning dry leaves and rubber. The results of fine composition shows that the proportion of sub-micron particles in aerosols generated changes within 55 ÷ 72%. For effective cleaning aerosols with such fractional composition of scrubbing machines, used only high pressure Venturi tubes [5], hydraulic resistance which are 20 ÷ 50 kPa.

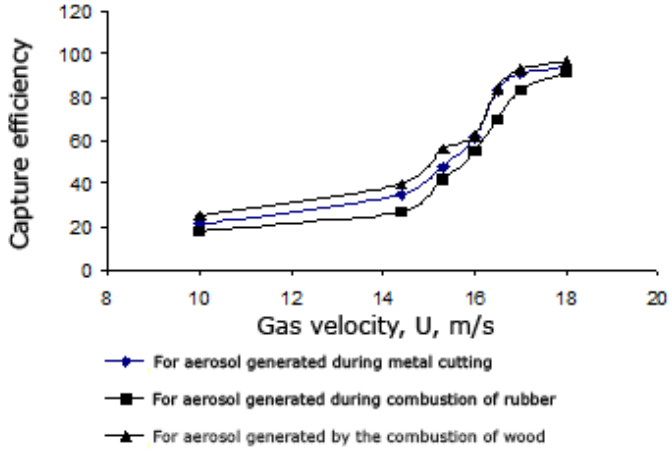

Figure 4. Submicron particle trapping efficiency various finely dispersed aerosols dependence of gas velocity. Irrigation accurary L=40m^3/m^{4}h

Study to determine the effectiveness of the cleaning unit sub-micron particles with a Movable nozzle were conducted in a wide range of gas flow velocity and the flow rate of the fluid. In studies of gas flow rate in the working area changed in the range from 10 m/s to 20 m/s at constant values of the density of irrigation. The dependence of the efficiency capture of sub-micron particles from the gas flow rate obtained in irrigation density 40 m^3/m^2 h, as described in Figure 2.

As you can see from the chart, increase gas flow rate, as can be seen from the theory of dust deposition [1], leads to an increase in the efficiency of dust collecting system. Studies on determination of the efficiency of dust collecting system of gas flow rate, can be divided into two series. At speeds of 10 ÷ 15 m/s cleaning efficiency is growing slowly, and at a speed of 15 m/s and density of 30 irrigation m^3/m^2 h reached 60%. Nozzle elements were used, the size of 6 x 6 mm and weighs 0.6 oz. At speeds over 15 m/s, monitored the UPDF this attachment to the upper restrictive Grill.

In the field of speeds 15÷20 m/s used cylindrical body size 6 x 6 mm nozzle and weight ≈ 1 g, which gave an opportunity to raise the speed of up to 20 m/s. Increase speed of 15 m/s to 20 m/s has been accompanied by a sharp increase in the efficiency of the capture of fine aerosols and collection efficiency reaches 90% value. While hydraulic resistance amounted to 4.4 kPa. Thus, the results obtained show that precipitation apparatus with a Movable nozzle can be used for the capture of submicron aerosol particles with high efficiency and low energy consumption.

References:

1. Rakhmonov T. Z., Levsh V. I., Vagapov I. H. Centrifugal effect in gas-liquid separators/Scientific –technical «Uzbek Journal of oil and gas», – Tashkent, – 1999. – No 4. – P. 25–28.
2. Boyko S. I., Litvinenko A. V., Adzhiev A. Y., Gritsay M. A., Morozov B. M., Prusachenko S. N. Separation systems for units of oil gas treatment//Gas industry. – Moscow, – 2009. – No 7. – P. 32–36.
3. Ujov V. N., Valdberg A. Y., Myagkov B. I., Reshidov I. K. Purification of industrial gases from dust. – M: «Chemistry», – 1981.
4. Symposium on Separation Science and Technology for Energy Applications, Gatlinburg, Tenn., Oct. 18–22, – 2009.//Separ. Sci. and Technol. – V. 45, – No 2. – P. 1167–1181.

DOI: http://dx.doi.org/10.20534/AJT-16-11.12-81-85

Yunusov Furkat Umarovich, PhD,
National University of Uzbekistan, Tashkent, Uzbekistan,
E-mail: yunusov4888@gmail.com
Kabulov Bahodir Jabborovich, Professor,
Tashkent State Technical University, State unitary enterprise
"Science end progress", Tashkent, Uzbekistan,
Akbarov Khamdam Ikramovich, Professor,
National University of Uzbekistan, Uzbekistan, Tashkent,
Makhmudov Ravshankhon Yunuskhonovich, Senior researcher,
Tashkent State Technical University, State unitary enterprise
"Science end progress", Tashkent, Uzbekistan

The study of the structural characteristics of polycaproamide-silica nanocomposite material obtained by the sol-gel method

Abstract: This article provides the structural-morphological studies of the polycaproamide-silica nanocomposite materials, obtained by the sol-gel method based on tetraethoxysilane, polycaproamide and glycerol, by the nitrogen porometry. A significant effect of glycerol on the final structure of the hybrid polycaproamide-silica nanocomposite materials is shown. The values of the surface fractal dimension were defined on the basis of the results.

Keywords: sol-gel, polycaproamide, silica, nanocomposite material, nitrogen porometry, morphology, fractal dimension.

Introduction. The general approach for the synthesis of hybrid polycaproamide-silica nanocomposite materials is the sol-gel method. The mild conditions of conducting the process of hydrolytic polycondensation of silica precursor, as the one alkoxysilanes are most often used, allow the functional monomers, polymers and even biopolymers enter into the reaction system. Such various components of inorganic and organic nature can be mixed in nanometer scales leading to the formation of hybrid polycaproamide-silica nanocomposite materials [1–2].

The sol-gel technology takes a special place on the synthesis of nanocomposite materials and it allows to solve many problems in the creation of such materials by the help of the molecular design. The sol-gel method offers the several advantages, such as the one-step synthesis and the preparation of multicomponent products. The use of the sol-gel technology in the preparation of nanocomposite materials allows to obtain, for example, sorbents having a functionality not only on the surface but also within the matrix. This fact determines the appearance of additional active sites, responsible for the intermolecular interaction in separations, in the sorbent and gives the sorbent new properties [3–4].

A feature of these materials is that on the one hand they can be used as those which are obtained as monolith or microsphere particles. On the other hand, they can serve as starting material for producing porous silica by burning or extraction of the polymer component, or for obtaining porous carbon sorbent by carbonizing the starting material with further leaching of silica [5–6].

Currently the water (hydrolytic) and the waterless (non-hydrolytic) sol-gel processes are used for the production of silica from the alkoxysilanes (tetraethoxy- or — tetramethoxysilanes). The hydrolytic path, become traditional, is based on the hydrolysis reactions catalyzed by acid or base and the condensation of the products of hydrolysis occurring in organic solvents in the presence of water. In the waterless sol-gel process the formation of Si-O-Si siloxane bonds is due to the condensation reactions between substituted and unsubstituted alkoxysilanes with the separation of low molecular weight compounds [7–9].

The objects and the methods of the research. We carried out a one-pot sol-gel process in a reaction system, consisting of tetraethoxysilane (TEOS), polycaproamide (PCA) and alcohols (ethanol and glycerol) dissolved in formic acid, and obtained polycaproamide-silica nanocomposite material.

For that the 5% polycaproamide solution in formic acid was prepared. Further, the calculated amount of ethanol and glycerol, and then tetraethoxysilane were introduced into polycaproamide solution. The solution was subjected to ultrasonic treatment in an ultrasonic bath for 3 minutes for a better homogenization.

Depending on the ratio of the components in the sol-gel reaction, after a time the formation of clear gel was begun. After complete maturation and aging, the gel was dried to the xerogel state. The dried xerogel has been used for the subsequent studies.

The structural analysis was performed by the nitrogen porometry (the specific surface area and pore size analyzer AutosorbI firm «Quantachrome Corp», USA).

Before carrying out the analysis the samples (~ 0,06–0,07 g) were subjected to degassing at 110°C for 4 hours.

The BET equation was used for processing the obtained data [10]:

$$\frac{P/P_o}{V_a\left(1-P/P_o\right)}=\frac{1}{V_mC}+\frac{(C-1)}{V_mC}\cdot\frac{P}{P_o} \qquad (1)$$

where V_a — value adsorption at a relative pressure P/P_o, cm^3/g;

V_m — capacity monolayer cm^3/g;

C — constant depending on the temperature.

S_{sp} — specific surface calculated according to the formula:

$$S_{sp}=V_a\cdot a_m\cdot N\cdot 10^{-20} \qquad (2)$$

where a_m — area occupied by a nitrogen molecule, which is equal to 0.162 nm^2,

N — Avogadro's number, equal $6{,}02\text{x}10^{23}$

Results and discussion. The analysis results listed in Table 1 indicate a significant effect of glycerol on the final structure of polycaproamide-silica hybrid nanocomposite materials. The specific surface S_{sp} of the sample prepared without the addition of glycerol is 4.7 m^2/g, while the addition of glycerol at the ratio of 0.80 mol to the amount of TEOS leads to the increase of the specific surface of the samples 15 times, and at a ratio of 1.30–30 times. Accordingly, the values of pore volumes V_p changes. However, the pore diameter d_p of the sample (1) prepared without the addition of glycerol is greater than in the samples obtained with the addition of glycerol.

It attracts attention the numerical values of the constant C. The numerical values of the constant C for the

sorbent obtained without the addition of glycerol is 17,014, which is peculiar to the sorbents with hydrophobic surface.

The constant determined from the BET equation (1) reflects the degree of interaction between the nitrogen molecules with adsorbent surface and depends on the nature of the surface. The lowest values of the constant ***C*** correspond to the minimum energy of interaction with the non-polar surface. By increasing the energy of the interaction that occurs between the nitrogen molecule and the polar surface, the value of the constant ***C*** increases and the more the polarity, the greater the value of the constant ***C***. The value of found constant ***C*** = 17.01 for a sorbent (Table 1) shows the adsorption on the low-energy surface and indicates the interaction of nitrogen with hydrocarbon chains of PCA.

For the samples obtained in the presence of glycerol, the values of the constant C are greater than 50, which indicate the presence of the polar NH_2 groups (Table 1, sample 2 and 3). From this it follows that the processes taking place by the different mechanisms in the synthesis of the sorbents lead to the formation of interfacial surface containing the functional groups of different nature.

Table 1. – The structural characteristics of polycaproamide-silica nanocomposite materials defined by the nitrogen porometry

Sample	molar ratio of glycerol, mole/mole	Structural characteristics			
		S_{sp}, m^2/g	V_p, cm^3/g	d_p, nm	Constant C
Before calcination					
1	–	4,7069	0,01475	12,5300	17,014
2	0,80	70,8000	0,1539	8,6943	52,379
3	1,30	146,5700	0,2998	8,1831	56,761
After calcination					
1	–	463,25	0,2305	1,99	–
2	0,80	454,45	0,5285	4,65	140,210
3	1,30	562,00	0,7354	5,22	–

This difference is clearly associated with a hydrophilic surface, that is, the presence of polar groups. Thus, it should be noted that after the calcination of the synthesized hybrid polycaproamide-silica nanocomposite materials the silica sorbents are formed both with the high specific surface area and the higher values of the pore volume, whereas from the hybrid material prepared without the addition of glycerol microporous silica with d_p=1.99 nm is formed, while from the hybrid materials synthesized with the addition of glycerol mesoporous silicas with the pore diameters of 4.65 and 5.22 are obtained (Table 1).

The consideration the isotherms of adsorption and desorption of nitrogen for considered polycaproamide-silica hybrid nanocomposite sorbents is showed that they can be attributed to the various types of the sorbents. Since the adsorption isotherm of nitrogen of the hybrid material before calcinations, obtained without the addition of glycerol (Fig. 1), is most likely related to the isotherm of the type III [11], which is typical for non-porous and macroporous sorbents. Indeed, as it can be seen from the figure, both adsorption and desorption isotherms of nitrogen of this sorbent are almost adjacent to the axis of the relative pressure of nitrogen P/P_o.

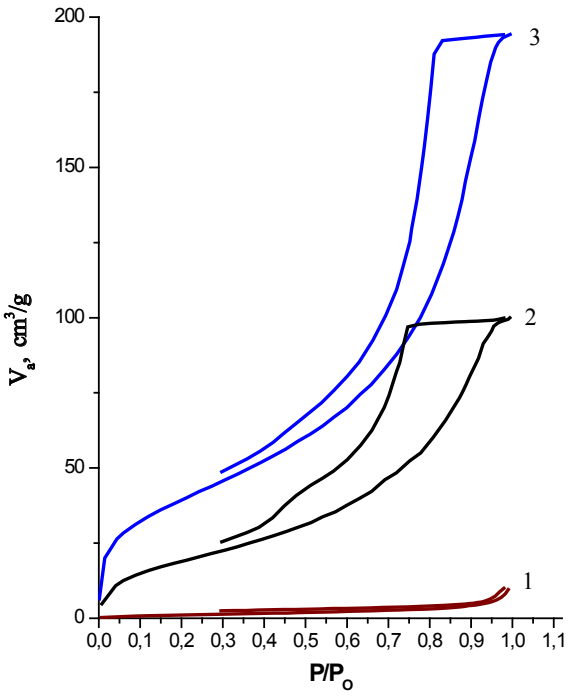

Figure 1. The adsorption and desorption isotherms of nitrogen on non-calcinated polycaproamide-silica nanocomposite materials

1 – in the absence of glycerol; 2 – at a molar ratio of TEOS: Glycerol 1: 0.80; 3 – at a molar ratio of TEOS: Glycerol 1: 1.30

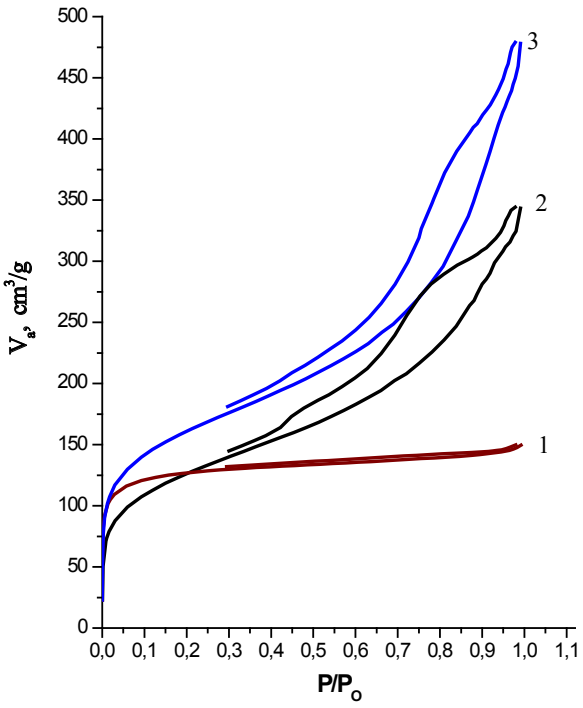

Figure 2. Adsorption and desorption isotherms of nitrogen on calcinated polycaproamide-silica nanocomposite materials

1 – in the absence of glycerol; 2 – at a molar ratio of TEOS: Glycerol 1: 0.80; 3 – at a molar ratio of TEOS: Glycerol 1: 1.30

After calcinations of this sample, the adsorption and desorption isotherms of nitrogen are already related to the isotherm of the type I. In this case, as it can be seen from Figure 2 the Sample 1, there is a horizontal plateau, the beginning of which is coming to an axis of the relative pressure P/P_o is almost at right angles. Adsorption and desorption isotherms of nitrogen at polycaproamide-silica nanocomposite materials obtained with the addition of glycerol with different molar ratio, are type IV, which are characterized by the presence of the hysteresis loop (Fig. 1, 2–3). Moreover, these samples after calcination, the nitrogen adsorption isotherm and desorption retain S-shaped (Fig. 2, 2–3).

Based on the results obtained, by nitrogen porosimetry values defined surface fractal dimension ***D*** (Table. 2).

In Table 2 data indicates that the values of fractal dimension of polycaproamide-silica nanocomposite materials obtained under the same conditions of sol-gel process and the same molar ratio TEOS reagents PCA and ethanol, but with different content of glycerin or its absence, are the numerical values of fractal dimension D in the range of $2 < D < 3$, the relevant surface fractals [12–13].

Table 2. – Surface fractal dimension D for polycaproamide-silica nanocomposite materials

The molar ratio of the starting components				The value of *D*	
TEOS	PCA	Ethanol	Glycerin	Before calcination	After calcination
1	0.50	10.60	–	2.4180	2.9566
1	0.50	10.60	0.80	2.4087	2.6880
1	0.50	10.60	1.30	2.4981	2.6199

Thus, the structural characteristics and morphology of polycaproamide-silica nanocomposite materials indicate complex interactions occurring in the sol-gel process in which a major role, as shown in an article in the development of end-surface properties play glycerol additive. Moreover, the more added the glycerol, especially branched formed surface of the final product.

References:

1. Danks A. E., Hall S. R. and Schnepp Z. The evolution of 'sol–gel' chemistry as a technique for materials synthesis.//Mater. Horiz. – 2016. – No 3, – P. 91–112.
2. Nakanishi K. and Tanaka N. Sol-gel with phase separation. Hierarchically porous materials optimized for high – performance liquid chromatography. Separations.//Acc.Chem.Res. – 2007. – No 9 (40). – P. 863–873.
3. Ismail Ab Rahman1 and Vejayakumaran Padavettan. Synthesis of Silica Nanoparticles by Sol-Gel: Size-Dependent Properties, Surface Modification, and Applications in Silica-Polymer Nanocomposites.//Journal of Nanomaterials. – 2012. – P.1–15.
4. Lee J., Han S., and Hyeon T. Synthesis of new nanoporous carbon materials using nanostructured silica materials as templates.//J. Mater.Chem. – 2004. – No 4 (14). – P. 478–486.
5. Brian L. Cushing, Vladimir L. Kolesnichenko, and Charles J. O'Connor. Recent Advances in the Liquid-Phase Syntheses of Inorganic Nanoparticles.//Chemical Reviews. – 2004. – Vol. 104, No 9 – P. 3893–3946.

6. Jung-Pil Lee, Sinho Choi and Soojin Park. Preparation of silica nanospheres and porous polymer membranes with controlled morphologies via nanophase separation.//Nanoscale Research Letters. – 2012. – 7:440 – P. 1–7.
7. Hay J. N. and Raval H. M. Synthesis of organic-inorganic hybrids via the non-hydrolytic sol-gel process.//Chem. Mater. – 2001. – No 10 (13). – P. 3396–3403.
8. Niederberger M. and Garnweitner G. Organic reaction pathways in the nonaqueous synthesis of metal oxide nanoparticles.//Chem.Eur. J. – 2006. – No 12 – P. 7282–7302.
9. Cora Lind, Stacy D. Gates, Nathalie M. Pedoussaut and Tamam I. Baiz. Novel Materials through Non-Hydrolytic Sol-Gel Processing: Negative Thermal Expansion Oxides and Beyond.//Materials. – 2010. – No 3 – P.2567–2587.
10. Dollimore D., Spooner P., Turner A. The BET method of analysis of gas adsorption data and its relevance to the calculation of surface areas.//Surface Technology. – 1976, – Vol. 4, – No 2, – P. 121–160.
11. Gregg S. J. and Sing K. S. W. Adsorption, Surface Area and Porosity, – 2 d ed.//Academic Press, – London, – 1982, – P. 303.
12. Kukovecz Á. Z. Kónya I. Pálinkó D. Mönter W. Reschetilowski and I. Kiricsi. Surface Fractal Properties of Morphologically Different Sol–Gel Derived Silicates.//Chem. Mater., – 2001, – 13 (2), – P 345–349.
13. Ahmad A. L., Mustafa N. N. N. Pore surface fractal analysis of palladium-alumina ceramic membrane using Frenkel–Halsey–Hill (FHH) model.//Journal of Colloid and Interface Science – 2006. – 301. – P.575–584.

DOI: http://dx.doi.org/10.20534/AJT-16-11.12-85-88

Yarkulov Akhror Yuldashevich,
teacher department of «Physical chemistry»
of the National University of Uzbekistan named of Mirzo Ulugbek
E-mail: yaaxror@ rambler.ru.

Umarov Bakhrom Smanovich,
senior teacher of "Department of physical chemistry"
of the National University of Uzbekistan named of Mirzo Ulugbek.,
E-mail: ubaxrom@mail.ru.

Akbarov Khamdam Ikramovich,
doctor of sciences, professor, department of "Physical chemistry"
of the National University of Uzbekistan named of Mirzo Ulugbek
E-mail: akbarov-Kh@rambler.ru

Thermodinamical properties of mechanical mixtures and nanocompositions diacetatcellulose-silica

Abstract: With using of microbalance Mak-Ben sorbtion of water steams by nanocompositions and mechanical mixtures of diacetatcellulose (DAC)–silica has been investigated. On the base of isotherms of sorbtion of water steams values of the middle free energy of mixing and Gibbs energy have been calculated. By theory of polymolecular adsorption (theory of Braynayr-Emmet-Teller) BET "water" surface and parameters of capillary-porous structure of investigated samples were determined. On the base of results of comparison of thermodinamical parameters conclusions were made about particulates of interactions of mechanical mixtures and nanocompositions DAC-silica.

Keywords: nanocomposition, sorbtion, isotherma, Gibbs energy, theory BET, capillary-porous structure, theory of De Bur-Zviker.

Nanocomposites are materials including in their composition particles both organical (molecules or macromolecules) and inorganical compounds dispergated to nanodemension level and forming between themselves stable chemical bonds. Such materials are used as energetical nanomaterials, at production of sensor, special types of ceramics, thin-films structures and optical surfaces and are characterized by properties charply

different from properties of materials obtained with using of individual components including in their composition.The larges adventages in obtain of nanocompozits were reached at using sol-gel technology.

Sol-gel technology of obtain of compositional nanomaterials is based on carring out of hydrolysis of molecular chemical substances-precurces forming at this nano-dimention particles dispergaited in solvent "sol". Then policondensation of sol particles is carried out at which nano-particles have formed clasters forming matrix named "gel" and containing in porous molecules of solvent. Following evaporation of solvent has allowed to obtain ligh solid body with development inner surface named "aerogel" or "kserogel". Sol-gel synthesis is carried out at relatively low temperatures and has allowed to obtain materials homogeneous by their structure properties and also has gave an possibility to introduce in their composition of particles of different nature. The grate part of inner volume of gels (aerogels) is atribited to meso-porouses (diametr from 1 to 100nm) which are especially attractive for dispergation in them nanodimension particles and obtain of composit nanomaterial.

Sience about nanocomposits — class of nanocompositional materials distinguishing beature of which is nanodimension degree of their structural components (particles of metal and metalloids, their oxides, halhogenids and so on) has been arised in last years on the inaction of different filds of nowladges. In litrature for designation materials containing from organical phase (polymer) and nanodispesrional mineral phase termin "hybrid nanocomposits" is used and sometime-"metalomatrixal composits", "monophasal hybrids".

If compositional part or such polymer-inorganical materials are polymers of biological origin then the termin "nanobiocomposits " is used [1–3].

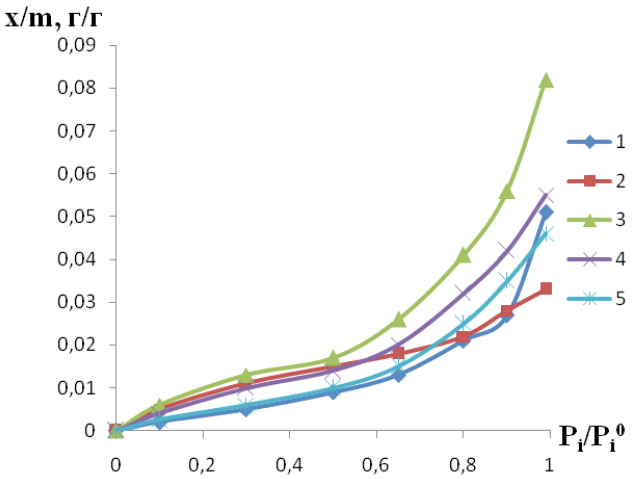

Figure1. Isotherms of sorption of water steams by initial components and their mechanical mixtures at 298K: 1. DAC; 2. Silica; 3. DAC-silica 50:50; 4. DAC-silica 40:60; 5. DAC-silica 60:40

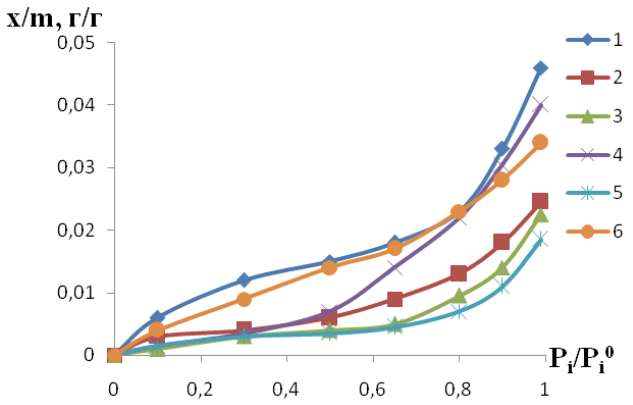

Figure 2. Isotherms of sorption of water steams at 298K by nanocompositions:1. DAC-silica (40:60); 2. DAC-silica (40:60)+limonic acid (LA); 3. DAC-silica (50:50) 4. DAC-silica (50:50)+LA; 5. DAC-silica (60:40) 6. DAC-silica (60:40)+LA

The aim of this work was sorptional and thermodinamical investigations of nanocompositions and mechanical mixtures of diacetylcellulose (DAC)-silica [4].

On fig.1,,2 isotherms of sorption of water steams by initial DAC, silica, their mechanical mixtures and nanocompositions DAC-silica at ratio of components 40:60; 50:50 and 60:40 are presented.

It is shown that introduction in composition of amorphous silica of hydrophilic polymers has carried out to following effects: in first character of isotherms of sorption has changed: at transition from polymer to polymer-inorganical systems they have S-shape character. In second on isotherms of sorption for samples with increasing of silica content the sorption ability sharply increased what can be connected with capillary condensation of water in porous structure of silica. Increasing of polymer concentration has carried out to it's degenerations and in last at equaled consentration of components in mixtures and nanocompositions it is possible to note a full coincidence of sorption isotherms.

For quantitave value of thermodinamical stability of system DAC-silica also were calculated the free energies of mixing polymer-solvent Δg^m on the base of calculations of chemical potentials of solvent $\Delta\mu_1$ and polymer $\Delta\mu_2$ and by concentration dependence (table 1) values of Gibbs energy ΔG_i were determined for initial polymers and ther mixtures of different compositions.

Table 1. – Values of the middle free energy of mixing polymer-solvent and the Gibbs energy for initial samples DAC, silica, their mixtures and nanocompositions calculated by isotherms of sorptions of water steams

№	Samples	$-\Delta g^m_{max}$, Dj/g		$-\Delta G_i$, Dj/g	
		Mechanical mixture	Nanocom-positions	Mechanical mixtures	Nanocom-positions
1	DAC (powder)	2,89	–	3,10	–
2	SiO_2 (powder)	4,73	–	4,95	–
3	DAC-silica 40:60	6,67	6,45	7,40	6,60
4	DAC-silica 40:60+LA	–	4,87	–	5,10
5	DAC-silica 50:50	5,02	2,44	5,30	2,50
6	DAC-silica 50:50+LA	–	2,87	–	3,00
7	DAC-silica 60:40	3,57	1,40	3,75	1,50
8	DAC-silica 60:40+LA	–	3,78	–	3,90

Obtained values of the Gibbs energy are in range of negative values what has whitnessed about spontaneity of carring out of process of solution of mixture components and nanocompositions in water and good affinity of investigated mixtures to solvent. Thermodinamical affinity to water was the most for mechanical mixtures and nanocompositions: composition DAC-silica 40:60 and their nanocompositions in presence of limonic acid have occupied the midlle state and for them affinity to water is decreased with increasing of DAC content in system.

In table 2 and 3 results of calculations by method Braunauer-Emmet-Teller (BET) of values of nanomalecular layer, general volume of porouses, middle radius of porouses and specifical surface of initial polymers, their mechanical mixtures and nanohybrid compositions DAC-silica (40:60, 50:50, 60:40) have been determined.

Table 2. – Parameters of capillyar-porous structure of initial samples of DAC, silica and their mechanical mixtures calculated by sorption of water steams

№	Sample	x_m, g/g	S_{sp}, m^2/g	W_0, sm^3/g	r_{mid}, Å
1	DAC (pouder)	0,0078	27,68	0,051	36,85
2	SiO_2 (pouder)	0,0102	36,03	0,033	18,31
3	DAC-silica (40:60)	0,0119	42,08	0,082	38,97
4	DAC-silica (50:50)	0,0104	36,75	0,055	29,93
5	DAC-silica (60:40)	0,0060	21,19	0,046	43,42

Table 3. – Parameters of capillyar-porous structure of nanocompositions DAC-silica calculated by sorption of water steams

№	Sample	x_m, g/g	S_{sp}, m^2/g	W_0, sm^3/g	r_{mid}, Å
1	DAC-silica (40:60)	0,014	48,16	0,044	18,3
2	DAC-silica (40:60)+LA	0,0086	30,23	0,035	23,15
3	DAC-silica (50:50)	0,004	13,84	0,0225	32,514
4	DAC-silica (50:50)+LA	0,0034	12,05	0,04	66,4
5	DAC-silica (60:40)	0,0026	9,14	0,0185	40,5
6	DAC-silica (60:40)+LA	0,0085	29,88	0,034	22,27

Calculations have shown that at comparison of mechanical mixtures with nanohybrid compositions the values of monolayer capacity and specifical surface for all mechanical mixtures are higher than for nanohybrid compositions. With increasing of DAC content values of these parameters decreased.

Value r_{midle} has a highest value for nanogybrid composition DAC-silica at their ratio 50:50 in the presence of acid (LA) what obviously is connected with fact that LA carrying-out role of structural agent. Absence of correlation between W_0 and S_{sp} can be explaine by differences in distribution of porouses by radiuses.

Adsorption theory De Bur and Zwiker claborated for describtion of processes of interaction of polar sorbates with polar sorbents can be used in case of compositional systems DCA-silica-water. It also can be used to processes bonding of water both by adsorption and absorption mechanisms. Results of experimental control of equation De Bur and Zwuker are carried out in work [5]. Linearization isotherm of sorption of water has

allowed to determine value "real" sorption didn't complicating by capillary condensation and clasterization of water. From fig.3. it is shown that in range of relative pressure 0,65 for mechanical mixtures DAC-silica isotherms are linear. For nanocompositions DAC-silica (40:60); DAC-silica (40:60)+LA in all range of the relative pressure isotherms are linear.

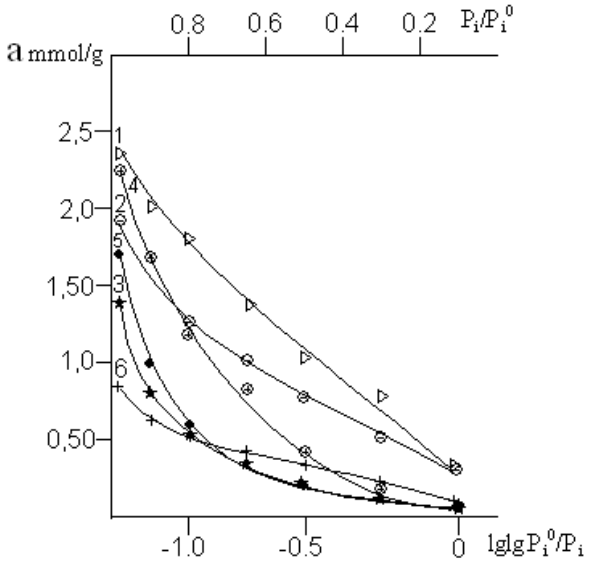

Figure 3. Isotherms of sorption of water steams by mechanical mixtures DAC-silica in coordinates of equation De Bur Zviker at 298 K: 1) DAC; 2) Silica; 3) DAC-silica (40:60); 4) DAC-silica (50:50); 5) DAC-silica (60:40)

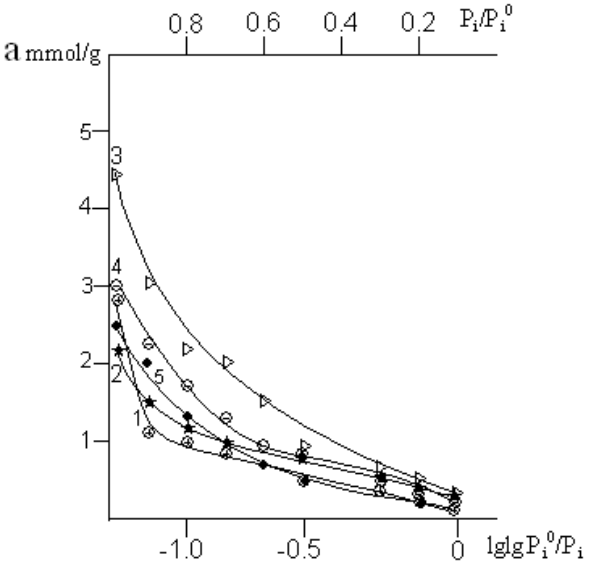

Figure 4. Isotherms of sorption of water steams by nanocompositions DAC-silica in coordinates of equation De Bur-Zviker at 298 K: 1) DAC-silica (40:60); 2) DAC-silica (40:60)+LA.; 3) DAC-silica (50:50); 4) DAC-silica (50:50)+LA; 5) DAC-silica (60:40); 6) DAC-silica (60:40)+LA

On the base of carrying out investigations the following conclusions were made:

Sorption of water steams by initial DAC, silica, their mechanical mixtures and nanocompositions of different compositions has been investigated;

Thermodinamical parameters of interaction such as the middle free energy of mixing and Gibbs energy in systems polymer-water have been determined;

With using of theory Branauer-Emmet-Teller the values of "water surface" of investigated samples were determined; such parameters as nanomolecular layer, radius of porouses and total volume of porouses were calculated;

By theory De Bur-Zwiker values of "real" sorption didn't complicated by capillary condensation and clasterization of water for different investigated samples were determined.

References:

1. Suzdalev I. P. Multcomponent nanomaterials. Advenseses of chemistry – 2009. – 78 (3), P. 266–301.
2. Pomogaylo A. D. Hybrid polymer-inorganical nanocomposits. Advenseses chemistry. – 2000. – 69 (1), – P. 60–89.
3. Davlatova A. R., Akbarov Kh. J., Kabulov B. D. Sol-gel synthesis of nanomaterials on the base of silica and perspectives of their using. Composition materials, – 2015, – No 4, – P. 37–38.
4. Kabulov B.D, Negmatov S. S., Yunusov F. U., Vildanova A. R., Shpigun D. A., Akbarov Kh.I, Ahunjanov K. A. Sol-gel process in obtain organo-inorganical hybrid functionalized nanocompositional material – sorbent for chromatography//International symposium "Chemistry for biology, medicine, ecology and agriculture. ISCHEM; – 2015, – Sankt-Peterburg, – P. 107.
5. Yarkulov A.Yu., Umarov B. S., Yunusov M. Y., Yunusov F. U.,. Akbarov Kh.I, Thermodinamical and sorbtion properties of nanohybrid compositional materials on the base tetraetoxysilan and diacetatcellulose. DAN RUz – 2014, – No 1, – P. 57–60.
6. Akbarov Kh. I. Theoratical analysis of interaction in system cellulose-water. Vestnic NUUZ. – No 5. – 2005. – P. 3–7.
7. Akbarov Kh. I. Thermodinamical analysis of water state in different celluloses. Chemistry of natural compounds. – No 5. – 2004. – P. 425.

Section 9. Electrical engineering

DOI: http://dx.doi.org/10.20534/AJT-16-11.12-89-94

Baghdasaryan Marinka,
National Polytechnic University Of Armeni,
Professor, Doctor of Department of Electrical Engieenering,
E-mail: m.baghdasaryan@seua.am

Avetisyan Artem,
National Polytechnic University of Armeni,
Ph. D., Research Associate,
E-mail: artemavetisyan83@gmail.com

Alaverdyan Sonik,
National Polytechnic University Of Armeni,
Ph. D., assistant of Department of Electrical Engieenering,
E-mail: sona.alaverdyan@yandex.ru

Developing the mathematical model for investigating the ore mill electric drive system

Abstract: The necessity of comprehensive consideration of the operation modes of the ore mill drive synchronous motor is substantiated by means of studying the change of its internal θ angle. A mathematical model for investigating the dynamic phenomena of the ore mill drive system is proposed, allowing to study the dynamics of operation modes of drive motors of different mills, under the conditions of the change in the supply voltage and the load moment.

Keywords: mathematical model, synchronous motor, operation modes, ore mill.

Introduction. Ore grinding is the main process of ore beneficiating enterprises, some construction and chemicals productions and has an important role in raising the labour efficiency in those production enterprises. The implementation of that technological process by high technical and economic criteria can be ensured by providing a stable and reliable operation of powerful electric drive systems used in them. Considering the abovementioned, and also the fact that the solution of the problems aimed at raising the efficiency of the ore-grinding process can be an important incentive for raising the productivity of mine-beneficiating and construction enterprises, the development of the method for investigating the electromechanical system used in that process is urgent.

Statement of the problem. The works aimed at investigating the electric drive system ensuring the ore grinding can be classified into two groups. In some of them, the study and improvement of the electric drive system operation is considered exclusively from the standpoint of the mill operation modes [1–2], while in the others — by the characteristics of electric drive motors consisting of the electromechanical system, control equipment, and the mechanisms transmitting the power from the motor to the mill [3–4].

The analysis of the well-known works devoted to the investigation and improvement of the operation modes of the electric drive system ensuring the ore grinding shows that unique methods for investigating the operation modes have been developed by different authors and significant theoretical experimental investigations have been carried out.

At the same time, it should be mentioned that the well-known experimental and theoretical materials do not take into account the characteristics peculiar to the electromechanical system mill — motor, in particular, the dynamic behavior of the load, the possibilities of falling out of the synchronous mode during operation, the

random nature of the process. Besides, it is impossible to apply the traditional methods for investigating the operation modes of the electric drive system connected with the change in the technical and economic requirements of the ore-grinding process. That is why it is expedient to consider the problem of investigating and improving the operation modes of the electric drive system providing the ore grinding from a new standpoint. This can be implemented by applying well-known materials, revealing new opportunities, and developing a research model of the operation mode, which is the goal of this work. The peculiarity of the ore-mill electric drive is conditioned by the existence of relationship between the electromechanical phenomena of the drive and the technological process of ore grinding.

Regardless of the form of the electric drive used, the qualitative and quantitative characteristics of the finished product (ground ore) characterizing the operation of the system are conditioned by the operation states of the ore mill, the motor, control devices and the mechanisms transmitting the power from the motor to the mill. It can also be confirmed by the complete active power formed on the rotational axis of the mill drum [5]. The complete active power consumed by the mill drive motor is used for putting the active load of the mill into motion and a number of losses and is determined by expression (1) [6]:

$$P = \frac{P_o + P_P}{h_D h_M}, \qquad (1)$$

where η_D is the motor efficiency; η_M – the efficiency of the drive mechanism transmission, allowing to consider the drive mechanism losses in the crown gear, in the clutch; P_o — the useful power; P_{Π} — the loss power.

Taking into account (1) and the formula of determining the motor power, we will obtain:

$$mIU\cos\phi = \frac{P_o + P_P}{h_D h_M}, \qquad (2)$$

where m is the number of phases; I – the stator current; U – the supply voltage of the network; $\cos\phi$ – the power coefficient.

Taking into account (2) and using the circular diagram of the synchronous motor, graphical dependencies between the electrical parameters of the motor and the filling degree of the ground material (K_h) (Fig. 1) have been confirmed. The $\cos\phi = f(K_h)$, $\sin\phi = f(K_h)$, $I = f(K_h)$ dependencies have been obtained by measuring the electrical parameters of the DC-260–38–36 motor used for the core mill drive by special sensors. From Fig. 1 it follows that the most sensitive is the curve $\sin\phi$.

Considering the dependence $\cos\phi = f(K_h)$ and the dependence obtained for the angle θ

$$\theta = arctg\frac{I\cos\phi}{U/x_q + I\cos\phi},$$

the change in the angle θ conditioned by the change of the mill filling degree can be estimated.

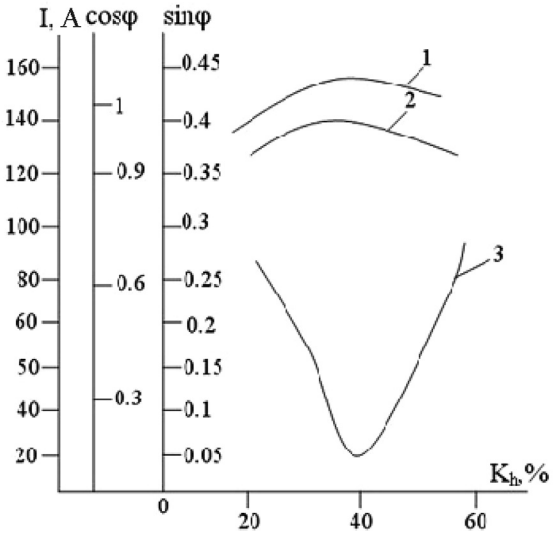

Fig. 1. The dependencies of the electrical parameters of the mill drive electric motor on the filling degree of the intra-mill load (K_h). 1 — the dependence of the stator current on the filling degree of the load; 2 — $\cos\phi = f(K_h)$; 3 — $\sin\phi = f(K_h)$

Many works investigating the $\theta = f(t)$ dependence of the synchronous motor are known [7], but they limit themselves only by confirming the dependence $\theta = f(t)$ of the synchronous machine to study its fluctuations, and the change of the angle θ by $\Delta\theta$ is considered in relation to its constant value θ_0: $\theta = \theta_0 + \Delta\theta$.

Respectively, the following dependence is used for the M_E electromagnetic moment, which is a function from the angle θ

$$M_E = M_{Eo} + \Delta M_E.$$

Such investigations cannot estimate the motor operation mode dynamics ensuring the mill electric drive under the conditions of the qualitative and quantitative characteristics of the supplied ore and the voltage change.

Developing an investigation model for the ore mill electric drive system. For developing the investigation models for the operation modes of the ore mill electric drive system motor, the ratio characterizing the dependence of the mechanical characteristics of the motor and the mill is used:

$$M_D = M - M_c, \qquad (3)$$

where M is the synchronous motor moment; M_c – the moment of resistance of the ore mill; M_D – the dynamic moment of the drive system, depending on the system's moment of inertia [8] and is determined in the following way:

$$M_D = T_m \frac{ds}{dt}, \quad (4)$$

where T_m is the constant of inertia; s -the slide.

The synchronous motor moment is determined [9]:

$$M = \frac{mUE_f \sin\theta}{x_d \omega} + \frac{mU^2 \sin 2\theta}{\omega}\left(\frac{1}{x_q} - \frac{1}{x_d}\right), \quad (5)$$

where m is the number of phases, U – the phase voltage applied to the stator winding; E_f – the excitation electromotive force; θ – the phase shift angle between the main electromotive force and the network voltage vectors; x_d – the inductive resistance of the stator phase according to the longitudinal axis; x_q – the inductive resistance of the stator phase according to the cross section axis; ω – the angular velocity of the motor. M_c is the moment of resistance of the ore mill and is determined in the following way:

$$M_c = m_c g R_{01} \sin\alpha, \quad (6)$$

And if we bring it to the motor, we will obtain:

$$M_c = m_c g R_{01} \frac{\omega_c}{\eta_M \omega} \sin\alpha, \quad (7)$$

where ω_c is the angular velocity of the mill rotation; g – the free fall acceleration, η_M – the efficiency of transmission from the motor shaft to the mill drum; α – the detour angle of the material in the mill; R_{01} – the 00_1 distance (Fig. 2); m_c – the mass of the material ground in the mill.

The 00_1 distance is determined [9] by:

$$R_{01} = \frac{2R\sin^3\frac{\lambda}{2}}{3\left(\frac{\lambda}{2} - \sin\frac{\lambda}{2}\cos\frac{\lambda}{2}\right)}, \quad (8)$$

where λ is the central angle of the sector corresponding to the filling degree of the material in the mill (Fig. 2); R – the radius of the mill drum.

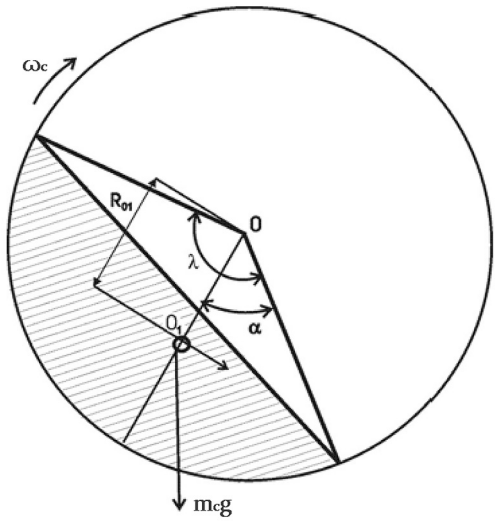

Fig. 2. A scheme for determining the moment of resistance of the ore mill

The mass of the material ground in the mill is determined [9] by:

$$m_c = \frac{\gamma L R^2}{2}(\lambda - \sin\lambda), \quad (9)$$

where γ is the volumetric density of the ground material; L – the length of the mill drum.

Placing equations (4), (5) and (7) in (3), we will obtain [10]:

$$T_m \frac{ds}{dt} = \left(\frac{mUE_f \sin\theta}{x_d} + mU^2 \sin 2\theta\left(\frac{1}{x_q} - \frac{1}{x_d}\right)\right)\frac{1}{\omega} - \\ - m_c g R_{01} \frac{\omega_c}{\eta_M \omega} \sin\alpha$$

Expressing the ω by the slide s and the angular velocity of synchronous rotation ω_c, we will obtain:

$$T_m \frac{ds}{dt} = \left(\frac{mUE_f \sin\theta}{x_d} + mU^2 \sin 2\theta\left(\frac{1}{x_q} - \frac{1}{x_d}\right)\right) \times \\ \times \frac{1+s}{\omega} - m_c g R_{01} \frac{\omega_c (1+s)}{\eta_M \omega} \sin\alpha, \quad (10)$$

from which:

$$T_m \frac{ds}{dt} = \left(\frac{mUE_f \sin\theta}{x_d} + mU^2 \sin 2\theta\left(\frac{1}{x_q} - \frac{1}{x_d}\right)\right)\frac{s}{\omega} - \\ - m_c g R_{01} \frac{\omega_c s}{\eta_M \omega} \sin\alpha + \\ + \left(\frac{mUE_f \sin\theta}{x_d} + mU^2 \sin 2\theta\left(\frac{1}{x_q} - \frac{1}{x_d}\right)\right)\frac{1}{\omega} \quad (11) \\ - m_c g R_{01} \frac{\omega_c}{\eta_M \omega} \sin\alpha.$$

Considering that $s = \frac{d\theta}{dt}$ and performing some modifications, we will obtain:

$$T_m \frac{d^2\theta}{dt^2} = \left(\left(\frac{mUE_f \sin\theta}{x_d} + mU^2 \sin 2\theta\left(\frac{1}{x_q} - \frac{1}{x_d}\right)\right)\frac{1}{\omega} - \right. \\ \left. - m_c g R_{01} \frac{\omega_c}{\eta_M \omega} \sin\alpha\right)\frac{d\theta}{dt} + \quad (12) \\ + \left(\frac{mUE_f \sin\theta}{x_d} + mU^2 \sin 2\theta\left(\frac{1}{x_q} - \frac{1}{x_d}\right)\right)\frac{1}{\omega} - \\ - m_c g R_{01} \frac{\omega_c}{\eta_M \omega} \sin\alpha.$$

To investigate the state of the system in different operation modes by (12), the MatLab software package has been used. To construct the model, expression (12) is introduced by basic units:

$$\frac{d^2\theta}{dt^2}=\frac{1}{T_{m\mu}B}\cdot\left[\left(\left(\frac{mUE_f\sin\theta}{x_d}+mU^2\sin 2\theta\left(\frac{1}{x_q}-\frac{1}{x_d}\right)\right)\frac{1}{\omega}-m_c gR_{01}\frac{\omega_c}{\eta_M\omega}\sin\alpha\right)\frac{d\theta}{dt}+\right.$$

$$\left.+\left(\frac{mUE_f\sin\theta}{x_d}+mU^2\sin 2\theta\left(\frac{1}{x_q}-\frac{1}{x_d}\right)\right)\frac{1}{\omega}-m_c gR_{01}\frac{\omega_c}{\eta_M\omega}\sin\alpha\right],$$

where $T_{m\mu}=\frac{GD^2n^3p}{3450\sqrt{3}\cdot 10^{-3}\cdot UI}$, $B=\frac{\sqrt{3}UIp}{\omega}$, and here GD^2 is the rotor's acceleration torque; n – the frequency of synchronous rotation; p-the number of synchronous motor stator pair of poles; I – the stator current.

The model for estimating the electric drive motor operation in different operation modes is shown in Fig. 3.

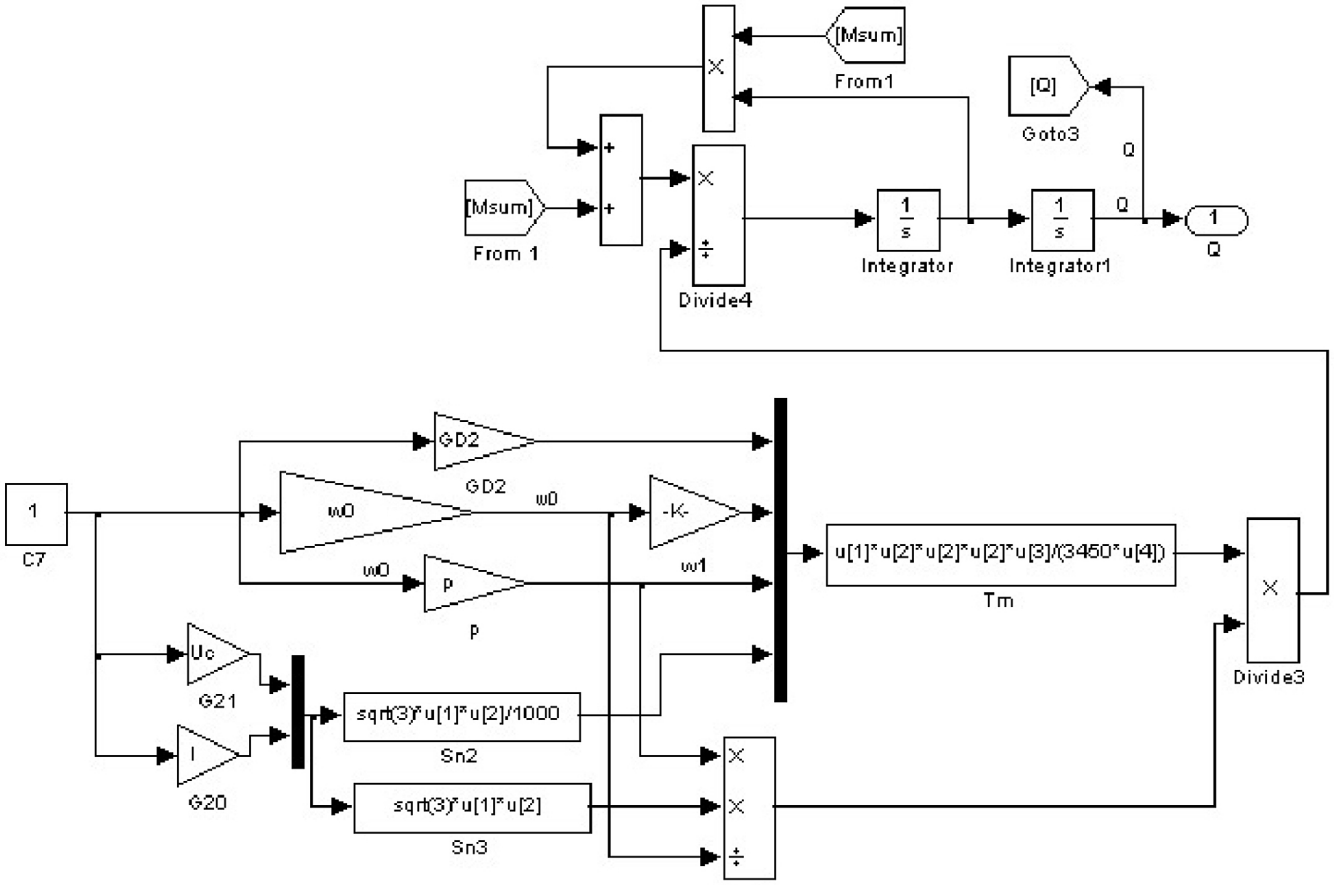

Fig. 3. The block-diagram of the model for estimating the operation of the electric drive motor of ore mill

The calculation block of the "From1" components of the model introduced in Fig. 3 is presented in Fig. 4.

By the results "From1" of testing the developed model, the changes of the θ angle have been constructed at different values of the mill load mass ($m_c^{/}<m_c^{//}$) (Fig.5) and at different values of efficiency of the rotation moment transmitting from motor shaft to the mill drum ($\eta^{/}<\eta^{//}$) (Fig. 6). As it can be seen from the characteristics, both in case of an increase in the load mass and a decrease in the transmission efficiency, the amplitude values of the angle θ turn out more conditioned by the growth of the resistance moment.

Conclusion

A model for investigating the dynamic phenomena of the ore mill synchronous drive system is developed enabling to study the dynamics of drive motors operation modes of different mills under the conditions of changing supply voltage and load moment. The application of the proposed model can be the basis for increasing the electric drive system reliability and improvement of the start-up modes.

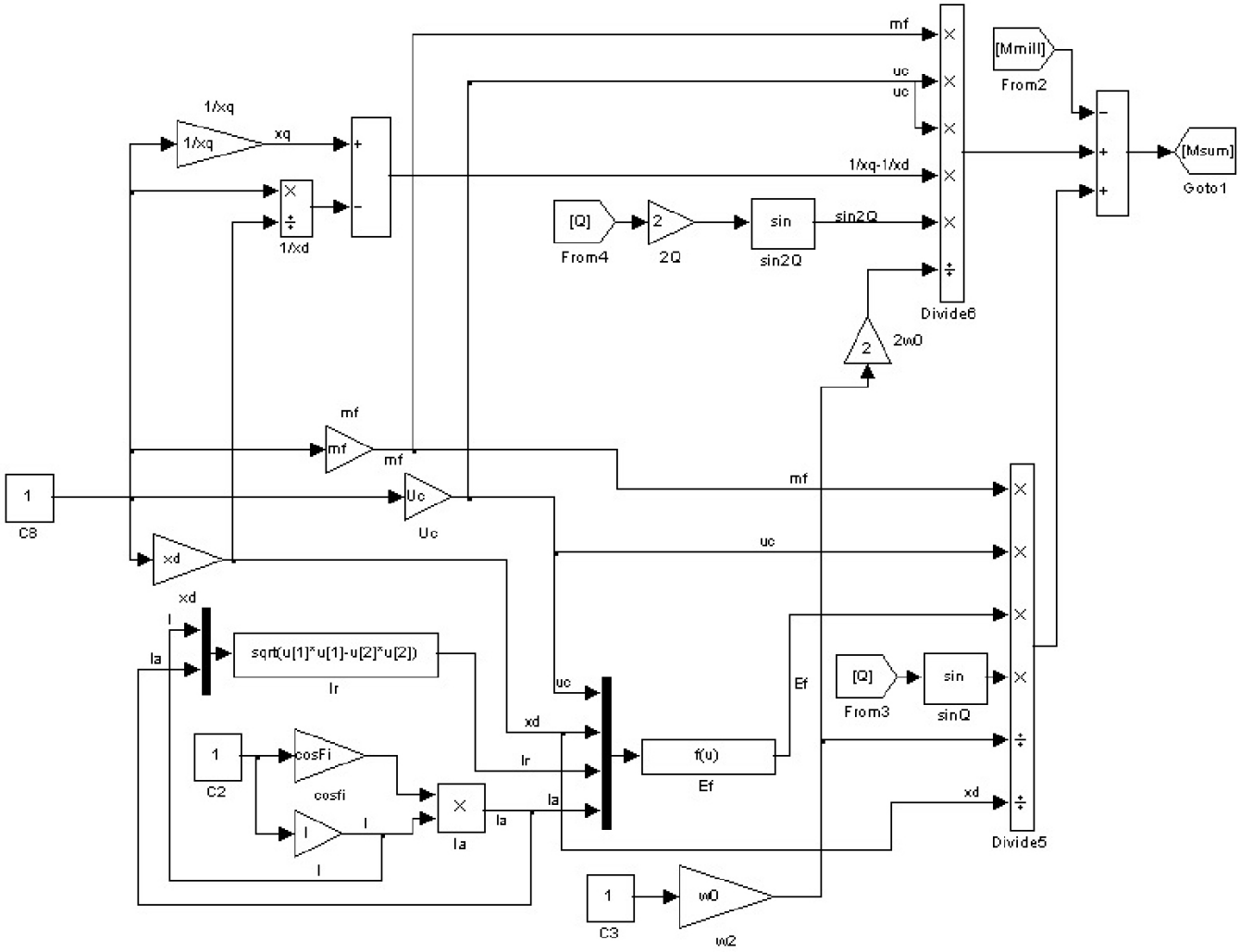

a)

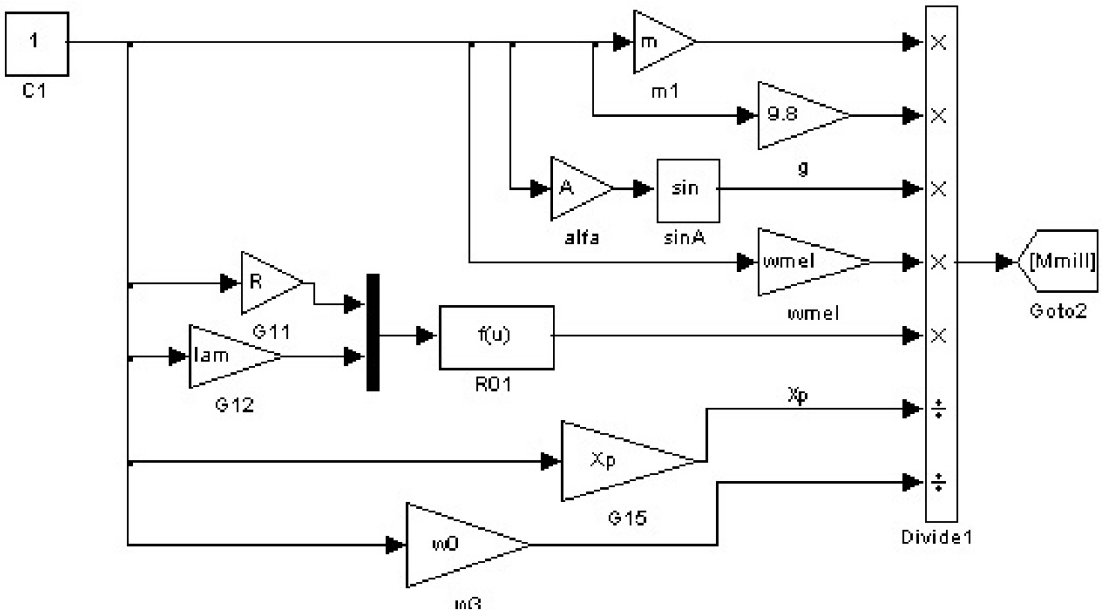

b)

Fig. 4. Calculation schemas a) Calculation schema of “From1” component; b) Calculation schema of the “From2” component included in “From1” component

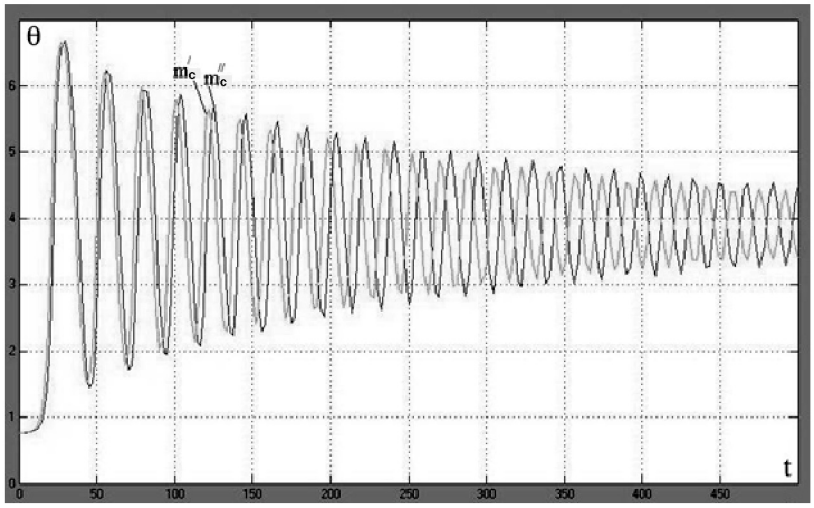

Fig. 5. Dependence of the change of angle θ on time at different load masses $\left(m_c^{'} < m_c^{''}\right)$

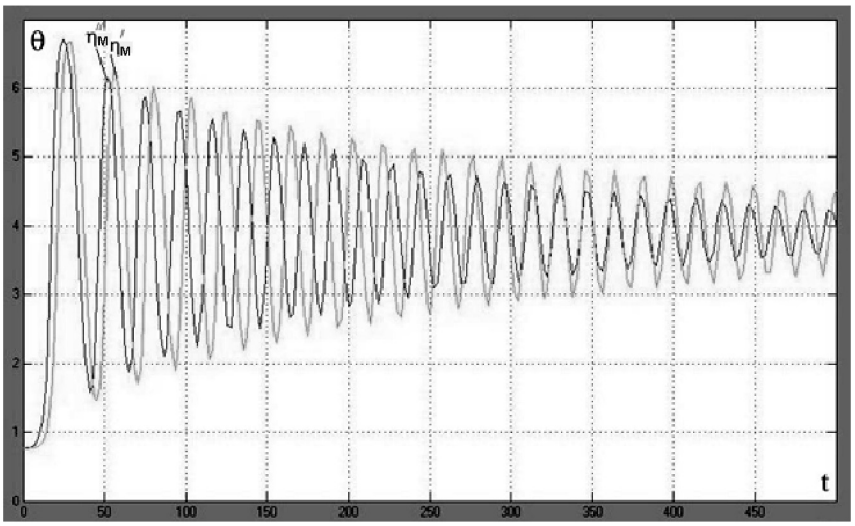

Fig. 6. Dependence of the change of angle θ on time at different efficiencies of transmission ($\eta^{'} < \eta^{''}$)

References:

1. Pending patent 2304438 (RF). Automated control device for the ore crushing process./B. B. Bnin, V. M. Kurkin, V. A. Borovkov, A. G. Marodadki, V. M. Leushin. – Publ. in Proceedings. – 2003. – N14. (in Russian).
2. Schnatz R., Int. J. Miner. Optimization of continuous ball mills used for finish-grinding of cement by varying the L/D ratio, ball charge filling ratio, ball size and residence time//Process. – 2004. – N1. – P. S. 55; – S. 63.
3. Kuvaev Ya. G. Automated expert energy-saving control system with exclusive cycle of wet ball grinding.//Naukovo, Practical journal. – 2006. – No 3, URL: htt://www.nas.gov.ua/scinn/pages/uu03060.html#

Contents